MODELING OF UNSATURATED AND STRUCTURED SOILS

by

Ioannis Chatzigiannelis

Diploma (1999) National Technical University of Athens

SUBMITTED TO THE DEPARTMENT OF
CIVIL AND ENVIRONMENTAL ENGINEERING
IN PARTIAL FULFILLMENT OF THE REQUIREMENTS FOR THE DEGREE OF

MASTER OF SCIENCE IN CIVIL AND ENVIRONMENTAL ENGINEERING

at the

MASSACHUSETTS INSTITUTE of TECHNOLOGY

June 2001

Signature of Author.....
Department of Civil and Environmental Engineering
June, 2001

Certified by.....
Andrew J. Whittle
Professor of Civil and Environmental Engineering
Thesis Supervisor

Accepted by.....
Oral Buyukozturk
Chairman, Departmental Committee of Graduate Students

MODELING OF UNSATURATED AND STRUCTURED SOILS

by

Ioannis Chatzigiannelis

Submitted to the Department of Civil and Environmental Engineering
On May 18, 2001, on partial fulfillment of the requirements for the degree of

Master of Science in Civil and Environmental Engineering

ABSTRACT

The Hato Rey weathered alluvium (in San Juan) has an extraordinary structure and behavior, which extends beyond the notion of classical soil mechanics. As a first attempt to model its behavior, modeling of two distinct types of soils, partially saturated and structured soils within the framework of hardening elastoplasticity is investigated.

For partially saturated soils two independent stress state variables (net stress and matric suction) are used to describe soil behavior. Modified Cam Clay effective stress model is extended to the unsaturated domain (forming Barcelona Basic Model, Alonso *et al.*, 1990) by introducing to two yield mechanisms that produce irreversible deformations (loading-collapse and wetting).

Behavior of various types of structured soil is unified using a scalar parameter (degree of bonding) as to measure the effects of structure. Description within the framework of elastoplasticity is implemented using the Modified Cam Clay as model representing the fully destructured state. The yield surface corresponding to in situ conditions has the same shape as the reference model but is enlarged due to the presence of cementation bonds. Upon loading degree of bonding degrades using an exponential damage law and the yield surface converges to the reference state.

In both cases the model extensions' capabilities and limitations are tested in typical single element tests.

Thesis Supervisor: Andrew J. Whittle, Professor of Civil and Environmental Engineering

Acknowledgements

Professor Whittle has been a mentor for me in the course of these two years, always leading my research to new paths and providing answers to many of my questions. His vast knowledge in soil modeling is, I believe, imprinted in this thesis. Moreover his trust in me has made me feel comfortable while working here.

I would like also to thank Prof. Ulm for his interest in my research (esp. Chapter 3) and for lecturing his course in such fascinating way. His enthusiasm will be a striking memory for me from MIT.

Part of this thesis would not have been able to be written without the help and contribution of Guoping Zhang (especially in Chapter 2), whom I thank deeply.

I would also like to thank two other Professors I had the honor to work with:
Prof. Gazetas for urging me to pursue graduate studies in the US and Prof. Kausel for entrusting me to teach the recitation of his structural dynamics course.

Also, my memories from the two years I spent in MIT are full of images with the friends I acquired. Special thanks to my "geotech" friends: Maria-Katerina, Michalis, George, Dominic, Vlado, Matt, Kartal, Bea, Jean-Louie, Christina, Pong, Yun and also to Achilleas, Ricardo, Fotis, Noelle (and the list goes on…)

"For me, modeling is about beauty"

Claudia Schiffer

Table of Contents

Table of Figures

Notation

In this Thesis the following conventions (unless explicitly stated) hold:

Scalars (zeroth order tensors):	a, A	(*plain italic*)
First order tensors and vectors:	$\boldsymbol{a}$	(***bold italic***)
Second order tensors:	$\mathbf{a}$	(**bold lowercase**)
Fourth order tensors and matrices:	$\mathbf{A}$	(**BOLD UPPERCASE**)

In some cases the index notation of tensors is used for the purpose of clarity. In that cases and since tensors refer to quantities in 3-dimensional space, indexes run from 1 to 3.

The following symbols denote tensorial operations:

1. The scalar product of tensors (symbol "·") implies contraction of the middle index, e.g. $\boldsymbol{a}\cdot\mathbf{b} = a_i \cdot b_{ij} = c_j = \boldsymbol{c}$. It can be seen that the scalar product of two tensors of order m and n is a tensor of order $(m + n - 2)$
2. The double contraciton of tensors (symbol ":") induces contraction of the two middle indexes, e.g. $\mathbf{A} : \mathbf{b} = A_{ijkl} : b_{kl} = c_{ij} = \mathbf{c}$. The resulting tensors of a double contraction of tensors of order m, n is a tensor of order $(m + n - 4)$
3. The tensor product of tensors (symbol "⊗") of order m, n creates a new tensor of order $m + n$ (e.g. $\mathbf{a} \otimes \mathbf{b} = a_{ij}\, b_{kl} = C_{ijkl} = \mathbf{C}$)

The invariants of a tensor can be expressed using the tensorial operations. Therefore, the two more commonly used stress invariants are expressed as:

$$I_1 = \boldsymbol{\sigma} : \mathbf{1}$$

$$J_2 = \frac{1}{2}\, \mathbf{s} : \mathbf{s}$$

List of symbols

a_0	SCC parameter: rate of degradation of degree of bonding
A	Tensor linking elastic strain with changes in suction
b	Biot coefficient in poromechanics
b	SCC parameter: degree of bonding
c	Cohesion
$\mathbf{c}$	Second order tensor
c_v	Coefficient of consolidation
d (prefix)	Increment, e.g. $d\boldsymbol{\varepsilon}$ strain increment tensor or differential, e.g. df differential of yield function
$\mathbf{D}$	Elasticity stiffness tensor
dev	Deviator of a tensor
e	Void ratio
$\mathbf{e}$	(infinitesimal) strain tensor deviator
$\boldsymbol{E}$	Transformed (infinitesimal) strain vector
f	Yield function
g	Plastic potential
G	Shear modulus
G_s	Specific gravity of soil particles
h, H	Elastoplastic modulus
$\mathbf{I}$	Fourth order unit tensor
I_p	Plasticity index
J_2	Second invariant of tensor (usually stress)
k	BBM parameter controlling the increase in apparent cohesion
K	Bulk modulus
K_0	Lateral earth pressure coefficient
k_v	Hydraulic conductivity
$\mathbf{L}$	Tensor relating changes in hardening variables with plastic multipliers
M	Critical State Line slope
M	Phase mass
N	Compression curve intercept
$p = \frac{1}{3}\sigma_{kk}$	Mean stress
$p = \frac{1}{3}\sigma_{kk} - u_a$	Net mean stress (in partially saturated soils)
p_c	BBM parameter, reference stress

p_0	Preconsolidation pressure
p_0^*	Preconsolidation pressure for saturated conditions
P	Volumetric component of $\boldsymbol{P}$
$\boldsymbol{P}$	Gradient of the plastic potential
$\boldsymbol{P}'$	Deviatoric component of $\boldsymbol{P}$
$q = \sqrt{3J_2}$	Equivalent shear stress
Q	Volumetric component of $\boldsymbol{Q}$
$\boldsymbol{Q}$	Gradient of the yield function
$\boldsymbol{Q}'$	Deviatoric component of $\boldsymbol{Q}$
r	BBM parameter controlling the limiting value for compression ratio
$s = u_a - u_w$	Matric suction
s_0	Maximum past suction
S_u	Undrained shear strength
$\mathbf{s}$	Stress tensor deviator
S	Degree of saturation
$\boldsymbol{S}$	Transformed stress vector
u	Pore pressure
$v = 1 + e$	Specific volume
V	Volume
w	Water content
w	SCC parameter for type of bond degradation
w_L	Liquid limit
α	BBM parameter in the flow rule, SCC parameter for the tensile strength
β	BBM parameter controlling the change in compression ratio
δ_{ij}	Kronecker delta
$\boldsymbol{\varepsilon}$	(infinitesimal) strain tensor
κ	Swelling ratio
$\boldsymbol{\kappa}$	Tensor of hardening variables (order can vary)
λ	Lame's constant
λ	Compression ratio
$d\lambda$	Plastic multiplier
μ	Shear modulus
ν	Poisson's ratio
π	Osmotic suction

$\boldsymbol{\sigma}$	Stress tensor
$\boldsymbol{\sigma}' = \boldsymbol{\sigma} - u_w\mathbf{1}$	Effective stress tensor
τ	Shear stress
ϕ	Friction angle
ϕ^b	Friction angle for associated with friction
χ	Bishop parameter
ψ	Total suction

Superscripts

e	Elastic
p	Plastic
-1	Inverse of tensor

Subscripts

a	Air
at	Atmospheric
f	Failure
i, j	Direction (x, y, z) or index (1, 2, 3)
ep	Elastoplastic
q	Deviatoric
s	Suction or Solids
t	Tangential or tensile
v	Void
vol	Volumetric
w	Water
,	Denotes partial differentiation

Other

$\mathbf{1} = \delta_{ij}$	Second order unit tensor

Chapter 1: Introduction

Most existing soil models refer to time-independent behavior of fully saturated reconstituted soils (usually under monotonic loading) which can be thought to exhibit normalized behavior. These soils, although rarely found in practice, offer a conceptually sound framework for understanding and simplifying soil behavior. As experience and experimental evidence is accumulated, advances in soil modeling are possible to encompass progressively more complex behavior. Such progress in soil modeling has been helped by the advances in three major fields:

Mechanics of materials: Soils cease to exhibit linear elastic behavior at a very small threshold strains, therefore non-linear elasticity and plasticity are essential in soil modeling. Plasticity is a relatively new theory since it was developed in the middle of the previous century (in the works of Hill, 1950 and Prager & Hodge, 1951). Initially developed to describe successfully the inelastic behavior of metals, plasticity was soon adopted in soil mechanics, introducing concepts as yielding and yield function, flow rule etc.. However, real soil behavior rarely obeys simple plasticity models (e.g. von Mises), nor satisfies associative plasticity. Moreover the onset of inelastic deformation occurs at very small strains, forcing refinements in the elastic-plastic theory, such as bounding surface plasticity (Dafalias & Herrman, 1982), sub-loading surface models (e.g. Hashiguchi, 1977), endochronic models (e.g. Bazant, 1971) and other techniques. Equally important in the application of plasticity for soils, is the existence of a critical state conditions for shearing to large shear strains. Critical state soil mechanics (e.g. Schofield & Wroth, 1968) provides the framework for modeling this behavior.

Laboratory techniques: A theory in the science of materials can only be validated (or disproved) in conjunction with reliable experimental data. Such precise measurements became feasible in the last 15 years through detailed measurements of small strain non-linearity in the range of (10^{-4}% - 10^{-5}%) (e.g. Lo Presti, 1994; Jardine *et al.*, 1999). Great improvements have also been made in sampling procedures and in-situ monitoring which provide information about the natural state of soils. Laboratory tests serve as guides for the development of a model, since elastoplastic models require selection of several components (such as yield function, plastic potential and flow rule) that should agree with experimental measurements. Moreover, new theories required tests beyond the usual practice, thus pushing the advance of new experimental devices and techniques.

Advances in Computers: The majority of soil models present the constitutive equations in incremental form, whose analytical integration is often impossible or inefficient. Only with the advent of computers has the numerical solution of such equations become possible. Moreover the application of constitutive models in engineering problems requires the use of finite elements procedures, since it often encompasses complex boundary conditions, rendering the use of computers essential.

This thesis is a primer on the modeling of the Hato Rey weathered alluvium (Zhang, 2001), whose structure and behavior are highly complex and extend beyond existing frameworks of soil behavior*. The main part of the thesis refers to two distinct types of soils, namely partially saturated soils and structured soils. Partially saturated soils are characterized by pore water deficiency and usual concepts such as the principle of effective stresses do not hold (e.g. Fredlund & Rahardjo, 1993). Structure refers to the arrangement of soil particles and the cementation between them (e.g. Burland, 1990), and structured soils often exhibit distinct behavior from reconstituted soils. The first step is to describe the general characteristics of soil behavior as idealized in the literature. The main objective is to highlight the specific features of each soil type, in contrast to

* see Chapter 2 for details

framework of normalized soil behavior and to identify modifications needed to established effective stress models for clays and sands. Based of simplifications in observed behavior, an existing reference model (Modified Cam Clay) can be modified to describe both partially saturated and structured behavior

Organization of the thesis

The structure of this thesis is as follows:

Chapter 2 gives a summary of the geotechnical properties of the Hato Rey alluvium including a brief commentary on its geologic origin, index properties and mineralogy, and available information on the compressibility characteristics, shear strength and hydraulic conductivity. On-going research by Zhang (2001) has revealed a complex multi-scale structure of the soil which can explain its observed engineering properties.

Chapter 3 deals with the behavior of soils in partially saturated states. After a quick review of the phase relations for a three-phase model it is shown that two independent stress state variables can be introduced to describe the state of unsaturated soils. One of the easiest and most studied model for unsaturated soils, the Barcelona Basic Model (Alonso *et al.* 1990) is presented and described in detail. The chapter identifies the model parameters, their physical meaning and experimental procedures for their measurement. The model's predictive capabilities are illustrated by simulations of single-element soil tests.

Chapter 4 addresses the problem of structured and cemented soils. The general characteristics of the mechanical properties are described in a unified way for many structured soils (following the similar work by Leroueil & Vaughan, 1990). It is concluded that the concept of degree of bonding can be used along with the framework of elastoplasticity to describe the transition from intact to fully destructured soil states. A

simple extension to a reference effective stress model is introduced (based on proposals by Gens & Nova, 1993). This Structured Cam Clay model introduces the degree of bonding through a scalar parameter, whose hardening rule is governed by a damage type mechanism. The degree of bonding can only soften with accumulated plastic straining causing the initial (large) yield surface to approach the reference yield surface. Simulations for single element tests show that the SCC framework can describe qualitatively the behavior of structured soils on certain loading paths

Chapter 5 gives a summary of the experiences in implementing the BBM and SCC models. The chapter also discusses further extensions of these models that will be necessary to simulate the behavior of a structured, partially saturated such as the old alluvium in Rio Piedras.

Chapter 2: The Hato Rey formation

This chapter describes the composition, structure, mechanical and flow properties of the Hato Rey ('*old alluvium*') formation in Rio Piedras, Puerto Rico. The data presented here are the results of research and extensive laboratory testing carried out at MIT during the course of the past 3 years (Zhang, 2001).

The new light rail transit system (Tren Urbano) includes a 1.5km underground section through the town of Rio Piedras. The tunnels are constructed within deep deposits of old alluvium (Hato Rey formation). The soil is best termed a *transported residual soil* and its geological origins and engineering properties were first investigated by Deere (1955) and Kaye (1959). Borehole data suggest that the soil deposits are highly heterogeneous. More detailed geological studies in conjunction with the Tren Urbano project have led to a subdivision of the vertical profile into 3 main layers, namely an Upper Clay (UC), a transitional Middle Zone (MZ) and Lower Sand (LS) (WCC, 1998) (see Figure 2.1). These subdivisions were based on standard USCS classification and ASTM standards for determining particle size distribution and plasticity.

During construction, ground movements caused by tunneling activities greatly exceeded the anticipated values, which led to countermeasures (consolidation and compensation grouting) and an extensive laboratory testing program of the old alluvium. The laboratory results (which are briefly summarized here) showed that the old alluvium possesses unexpected properties and therefore behavior. Indeed, this old alluvium does not fit into any of the recognizable classes of soils (covered in USCS classification schemes) or of residual soils (e.g. Vaughan *et al.*, 1988; Pandian *et al.*, 1993). From the areal distribution and lack of fossils it is concluded that the deposits were derived from igneous and

metamorphic rocks in the central upland areas. These materials were then transported and deposited by fluvial processes as a piedmont alluvial fan, formed during the early Pleistocene. The deposits have undergone extensive post-depositional erosion and weathering leaving only quartzitic sand grains and secondary structures "in the forms of joints, concretions and occasional cementation" (Deere, 1955). The latter description refers to complex processes of chemical breakdown and reprecipitation.

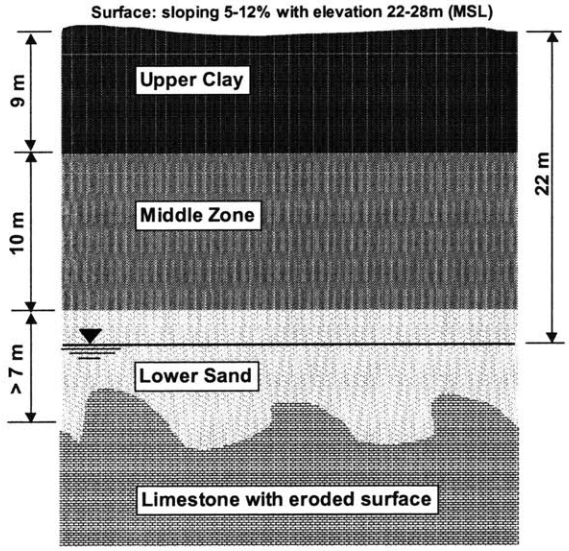

Figure 2. 1: Typical profile of old alluvium (Hato Rey formation) in Rio Piedras, San Juan.

Experiments conducted on intact block samples of the old alluvium provided preliminary data about its structure, chemical composition, index properties and mechanical characteristics, but also highlighted major limitations in the current understanding and characterization of cemented soils. The Upper Clay is a medium stiff, brittle, red or reddish brown clay. This layer, has an average thickness of 8-9m and consists mostly of red, or mottled red and white, silty clays with complex patterns of white veins. The Middle Zone (10m thick) is a very stiff, brittle, light brown to yellowish sandy clay, silt or clayey sand with abrasive sand grains (mostly quartz). It is denser than the upper clay and contains more quartz sand. Lower sand contains clean white quartzitic sand and silty sand. This layer is less weathered than the two upper layers.

2.1 Classification

Classification of residual soils using conventional procedures often poses difficulties (as reported by many authors, e.g. Townsend, 1985; Vaughan *et al.*, 1988; Finke *et al.*, 1999), which may contribute to the high variability in vertical stratification reported from the site investigation. The particle size distribution for the old alluvium is summarized in Figure 2.2. Natural MZ material is more coarse-grained (40% of particles larger than 0.06mm compared to 10% for the UC), while UC contains a much higher clay fraction (50% of particles less than 0.002mm compared to 20% for the MZ). The particle size distribution changes drastically with various means of drying and mechanical disaggregation. Specifically, air drying and mechanical disaggregation in a blender produce much higher apparent clay fractions for both the UC and MZ. On the other hand oven drying causes minimal change in size distribution.

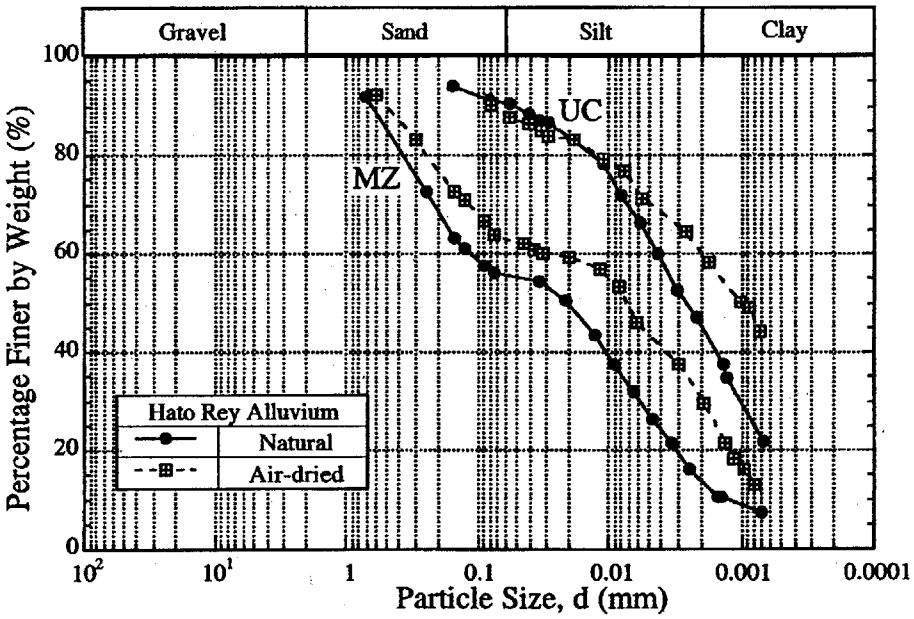

Figure 2. 2: Particle size distributions for old alluvium. Effect of air-drying (after Zhang, 2001)

The effects of drying and mechanical disaggregation are also very pronounced in the Atterberg limits of the materials, presented in Figure 2.3. The MZ specimens have a

lower liquid limit, w_L, and plasticity index, I_p, compared to the UC samples. The MZ data plot above the A-line and would therefore be classified as either MH or CH according to USCS definitions. Invariably, the more energy is put into breaking down the soil structure, the higher the resulting plasticity. The liquid limit increase by 15% and 10% in the MZ and UC materials respectively. The plasticity index increases by 15% and 12% for these two materials. Air-drying and oven-drying increase the plasticity indexes for both soils, whereas, the liquid limits increase slightly for MZ and decrease for UC compared to the intact material. In essence the effect or air drying is a sharp increase in the ratio I_p/w_L which indicated that the soil becomes tougher. This last result is in marked contrast with index properties of other tropical residual soils reported in the literature (e.g. Townsend, 1985; TRS, 1997; see Figure 2.4). In summary, the intrinsic Atterberg limits (M3, U3) reflect the mineralogy, while in the intact state the soil structure hinders the plastic behavior of the soil.

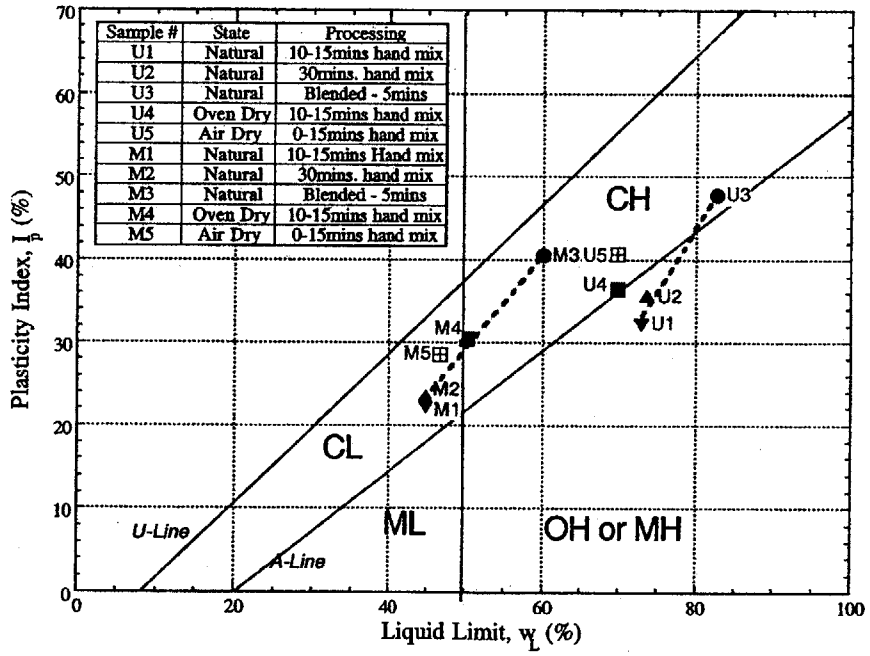

Figure 2. 3: Plasticity characteristics of old alluvium. Effect of drying and mechanical blending (after Zhang, 2001)

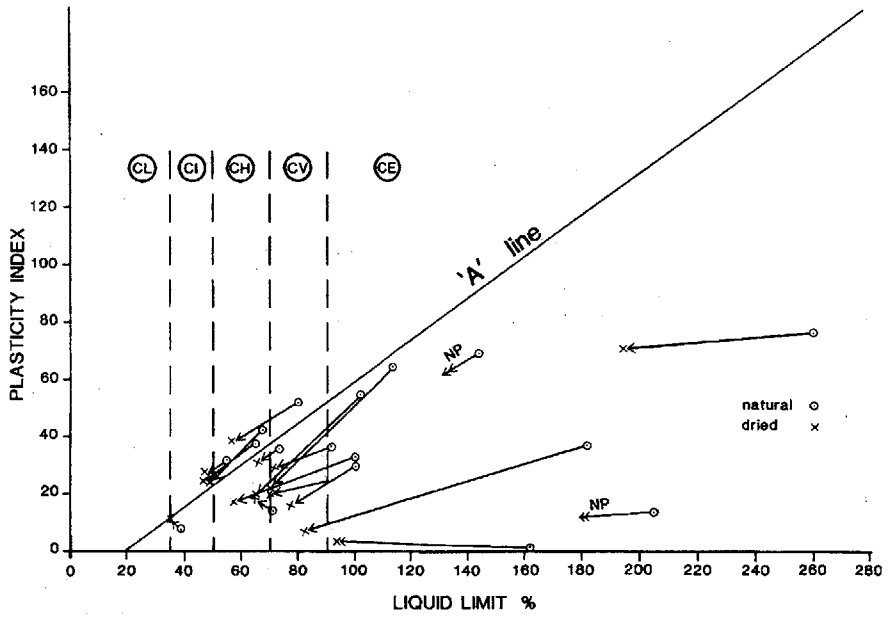

Figure 2. 4: Effects of drying on plasticity characteristics of tropical residual soils (after TRS, 1997)

2.2 Chemical composition and micro-structure

An extensive series of tests have been carried out to determine the chemical, mineralogical and particle distribution of the old alluvium. The tests included X-ray fluorescence (XRF), thermal analysis for quantitative analysis of minerals spectroscopy for analyzing the chemical composition, X-ray diffraction (XRD) for identifying clay minerals, scanning electron microscopy (SEM) for studying the physical characteristics, $CaCO_3$ content, salt concentration, and pH.

The mineral types identified in the soil are presented below and their quantities in the layers UC and MZ are summarized in Table 2.1.

1. Oxides: Iron oxides found in the soil samples (by XRD and thermal analysis) are identified as *goethite* and *hematite*. Goethite is a very fine particled substance that grows as particles are cemented together. Goethite is also identified as the cementing

agent for the clay particles. Hematite consists of very fine positively charged particles, which are attracted to the negatively charged clay surface. These iron oxides fall into the clay fraction and are also responsible for the colorization of the soil; hematite is bright red and geothite yellowish or brown. Tests involved also removal of iron oxides by chemical means (Dithionite-Citrate-Bicarbonate, DCB). The resulting material has increased fine clay fraction and drastically different Cation Exchange Capacity (CEC). Other oxides traced in the soil where *brookite* (titanium oxide) and *hausimannite* (manganese oxide).

Mineral	Method	Upper Clay [%]	Middle Zone [%]
Clays (total)		*52*	*47*
Kaolinite	Thermal analysis	34	25
Smectites	XRF	18	13
Illite		0	3
Pyrophyllite		0	3
Montmorillonite		0	3
Quartz	XRD	22	31
Orthoclase Feldspar	XRF	9	14
Muscovite		*trace*	*trace*
Goethite	Thermal analysis	8	3
Hematite	XRF	4	0
Brookite	XRF	1	1
Total		**95**	**95**

Table 2. 1: Summary of mineralogy for the old alluvium (after Zhang, 2001)

2. Clay minerals: XRD tests identified *kaolinite* and *smectite* as the main clay minerals. Upper clay contains a high percentage of kaolinite. The presence of smectites denotes a swelling potential of the soil when wetted. However, in the intact soil condition they

are coated with goethite and therefore they are inactive. In the Middle Zone *illite*, *pyrophillite* and *montmorillonite* are also present in smaller amounts.

3. Rock minerals: Several rock minerals are also identified in the old alluvium. *Quartz*, *orthoclase K-feldspar* and *muscovite* are present in the soil, with quartz being present in larger quantities as indicated by XRD tests. Due to their resistance in weathering these are probably remnants from the parent rock material. Middle Zone has larger amounts of these minerals, which implies a smaller degree of weathering.

2.3 Behavior in 1-D Compression Tests

Drained compression behavior in incremental oedometer tests on intact specimens of UC and MZ materials is shown in Figure 2.5. The samples were partially saturated at the start of the test, but were inundated with water at $\sigma'_v \leq 100$kPa. The MZ material has a much lower initial void ratio and undergoes much smaller compression than the UC. The first loading curved for both materials appear similar to typical sedimented clays, exhibiting an increase in compression index with confining pressure. In both cases a vertical quasi pre-consolidation pressure can be estimated using conventional methods. This suggests that the intact soils are highly overconsolidated (Vargas, 1953), but the principal mechanism of pre-consolidation pressure is associated to the breakdown of the cementation or particle structure.

One very distinct and unusual feature of the compression behavior of the old alluvium is the large rebound that is observed during unloading. Amazingly, the MZ sample shows almost a complete restoration of the initial void ratio after unloading at 30MPa (Figure 2.5). This is directly associated with the breaking of cementation bonds in the soil structure and can be explained either by the cementation acting to prevent swelling of clay particles (within the particle aggregates), or by masking the true cation exchange

capacity (Yong & Warkentin, 1996). Therefore, the amount of swelling reflects directly the breakdown of the cementation.

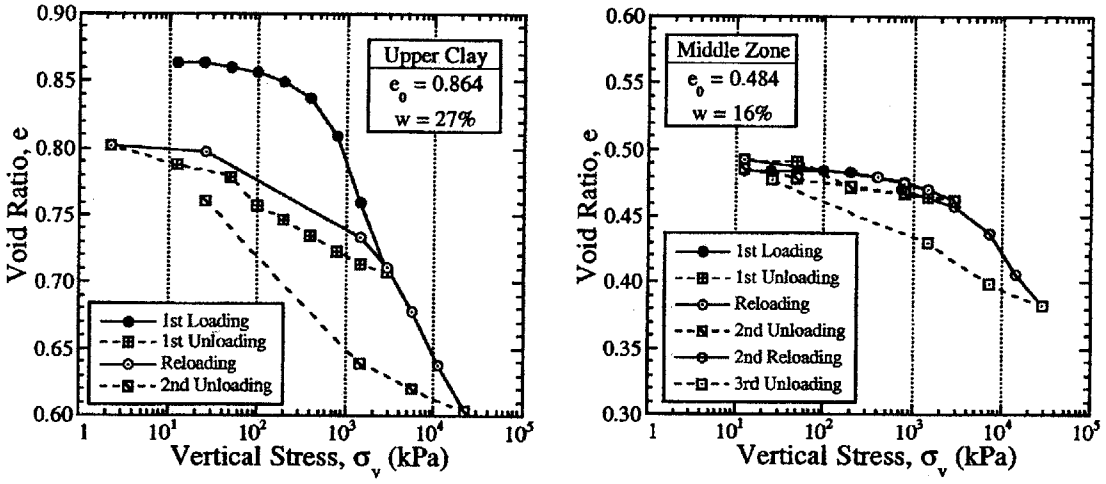

Figure 2. 5: Compression behavior of intact old alluvium

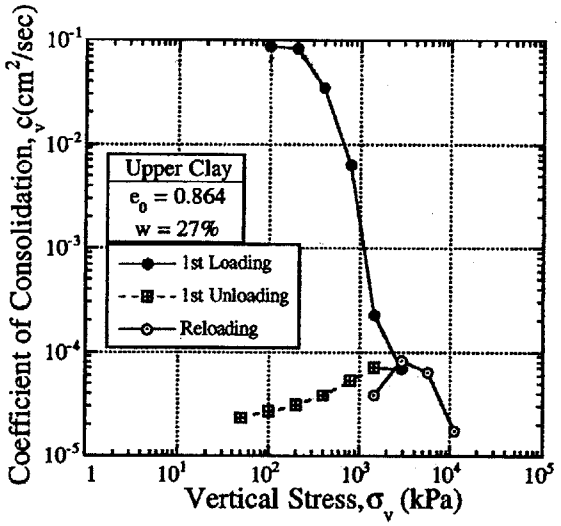

Figure 2. 6: Variation of consolidation properties during 1-D compression oedometer tests (after Zhang, 2001)

Changes in structure are also indicated by changes in coefficient of consolidation, c_v, with loading. The parameter c_v is interpreted from the displacement-time response measured

during each step of incremental oedometer test using conventional procedures. Figure 2.6 shows that the coefficient of consolidation decreases by more than three orders of magnitude during first loading of the UC! This result suggests a large reduction in the overall hydraulic conductivity of the specimen, and is almost certainly linked to volume changes within the aggregates. It is most remarkable that the coefficient of consolidation continues to decrease even during unloading (Figure 2.6). Similar results have been reported in the literature for compression of volcanic ash soils (e.g. Wesley, 1999).

2.4 Soil Structure

The old alluvium has a remarkable structure as revealed in images obtained by Zhang (2001) using Environmental Scanning Electron Microscope (ESEM) (Figure 2.7). The elementary clay particles are kaolinite and smectite. These clay flakes are glued together forming a single aggregate of size 10-20μm that is coated by geothite. Inside the single aggregate, the clay particles are not dispersed, but rather are aggregated with face to face parallel configuration. The single aggregate is stable due to coating and in the intact state the clay minerals are thus indiscernible. Single aggregates then form rosette-shaped group of aggregates (size: 50-100μm), during crystal growth of clay minerals. The aggregates are again connected by goethite. Finally rosettes (aggregates groups) are connected by bridges of iron oxides forming a matrix of aggregate groups with large voids (see Figure 2.8).

The mechanical behavior and flow properties of the old alluvium can thus be explained taking into account the soil structure. In the intact condition the soil consists of fairly large aggregate groups connected with iron oxides. This structure is relatively stiff as part of load is carried by the bridges between the aggregates groups with small deformations occurring. The large voids of the structure allow free flow of water through the soil mass. Moreover the clay particles are covered by a thin coat of goethite that does not allow

water to come in contact with smectites (that would cause swelling of the clay particles). Thus the stability of the soil in water can be explained.

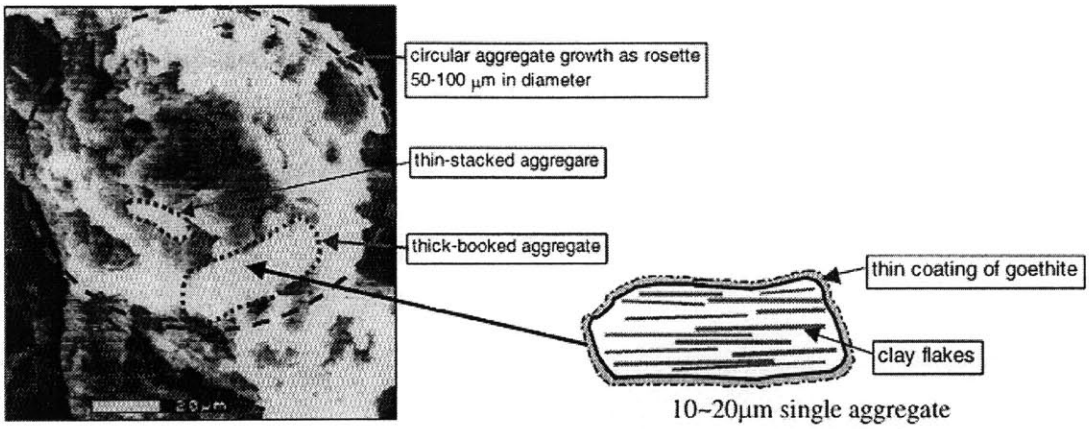

Figure 2. 7: ESEM photograph depicting the soil structure (after Zhang, 2001)

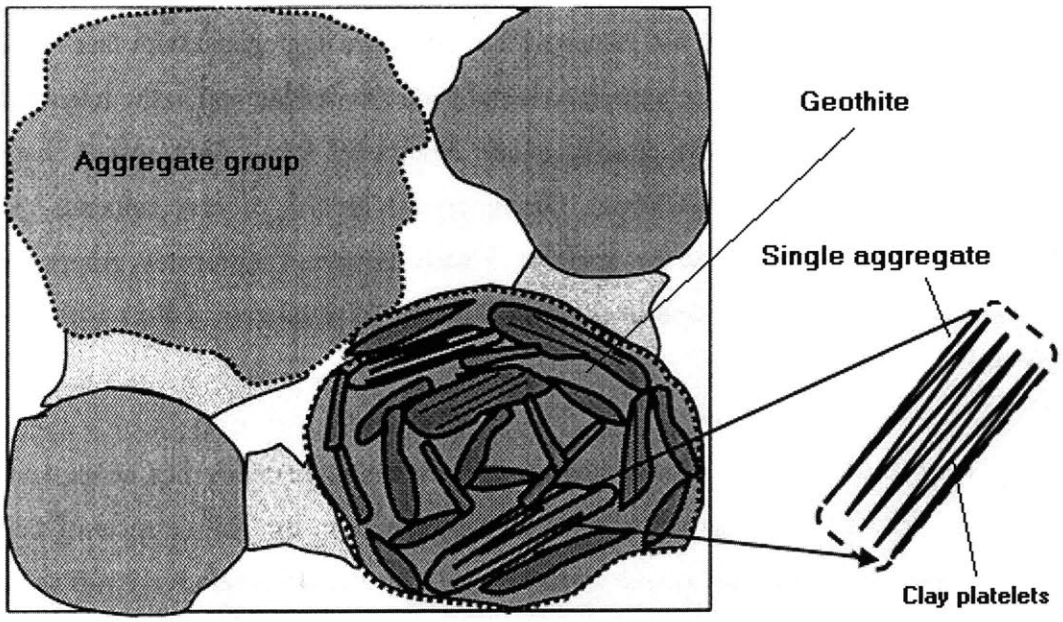

Figure 2. 8: Schematic structure of old alluvium (Zhang, 2001)

There are two levels of destructuration in this conceptual model: first the bonds between the rosettes are broken and the soil has sand like behavior, since in essence it behaves as a

granular material with relatively weak aggregate groups. The clay particles remain covered by the coat of goethite and are still unreactive when inundated. When the cementing agent is removed (either by further loading or by chemical reactions) and the aggregates break down, the clay particles become exposed. If water is available the clay particles swell, filling the voids and thus hydraulic conductivity and coefficient of consolidation become very low. The destructured state is highly compressible (as is expected of clay minerals with parallel configuration) and much of the true cohesion is now lost.

2.5 Guidelines for modeling

It is obvious that modeling the behavior of the old alluvium goes far beyond the current capabilities of existing soil models. Knowledge of the microstructure and mineralogy are essential for modeling the behavior of the old alluvium. As cementing bonds are broken between the aggregate groups, the swelling of clay minerals at the microscopic level influences the macroscopic behavior. Several models have been presented in the literature on interpreting clay swelling (e.g. Gens & Alonso, 1992; Dormieux *et al.*, 1995; Pothier *et al.*, 1997; Murad & Cushman, 1997). Much of the work on materials with swelling clays has been done in relation with the behavior of unsaturated soils with expansive behavior. The Gens and Alonso model was developed for unsaturated soils (Barcelona Basic Model (BBM), Alonso *et al.*, 1990) and was then modified to include swelling at the micro-level. Therefore, as a first step, modeling of unsaturated soil behavior is reviewed in Chapter 3, and the BBM is presented.

Equally important is the modeling of soil structure. The model should be therefore able to describe the effects of cementation bonds in the soil and the transition as the cementation is lost either by loading or by chemical reasons. In the last 15 years there is a growing body of literature on the behavior (e.g. Burland, 1990; Leroueil & Vaughan, 1990; Kavvadas *et al.* 1993) and constitutive modeling (e.g. Gens & Nova, 1993; Rouiania &

Muir Wood, 2000; Kavvadas & Amorosi, 2000) of cemented soils. Modeling of cemented materials is usually done in relation to the fully destructured state. A brief review of the principles of constitutive modeling of cemented soils using the framework of elastoplasticity is presented in Chapter 4, and an application to a simple effective stress model is demonstrated.

Chapter 3: Modeling of the behavior of Partially Saturated Soils

3.1 Unsaturated soil behavior

This chapter considers the application of elasto-plasticity for modeling the mechanical behavior of *partially saturated* soils. Partially saturated soils can be characterized by their pore water deficiency. Unsaturated soils are different both in nature and engineering properties from saturated soils, and therefore their behavior does not adhere to classical, saturated soil mechanics.

Soils are porous materials that have at least two phases. In *fully saturated* conditions, the interparticle voids are completely filled with fluid (usually water), which applies positive pore pressure to the solids. On the contrary in partially saturated soils air is also present in the voids and the pore-water pressure is usually negative. Such conditions arise in cases where the pore fluid is limited; such cases include soils above the water table and soils in arid and semi-arid regions. Excavation, remolding and recompacting processes also result in a partially saturated soil. Moreover, unsaturated condition are present in most swelling clays and residual soils; two types of soils that exhibit unusual and sometimes problematic behavior (Alonso *et al.*, 1990). It is therefore not surprising that conditions of partial saturation are usually associated with special soil behavior.

The field of soil mechanics has historically focused on soil behavior in either fully saturated or dry conditions, which can be considered as two-phase material. Following Terzaghi (1926), deformation and shear strength of saturated soils are functions of the effective stresses acting on the soil skeleton. This is the basis for effective stress

modeling of saturated soil behavior. Additional state variables are needed to describe the behavior of a three phase partially saturated soil (solid, fluid, air).

Partially saturated soils can be conveniently described within the framework of poromechanics (e.g. Coussy, 1995; also Fredlund & Rahardjo, 1993). The three phases are distinguished as air, water and soil solids*. The volume occupied by the pore fluid and air is the total volume of voids. The air phase can be continuous or occluded. The degree of saturation is defined as the percentage of void space that is occupied by water.

$$S(\%) = \frac{V_w}{V_v}(100\%) \tag{3- 1}$$

where V_w is the volume occupied by the water phase and V_v is the total volume of voids (see Figure 3.1).

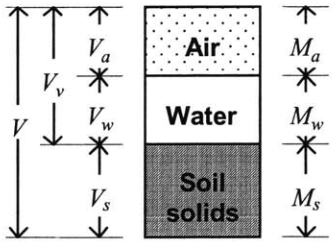

Figure 3. 1: Volume-mass relations

Experimentally the degree of saturation can be obtained from the basic volume-mass relationship for soils:

$$S\,e = w\,G_s \tag{3- 2}$$

since void ratio, e, and water content, w, and the specific gravity of the solid particles, G_s, are easily measured quantities.

* a more rigorous approach would include contractile skin as a fourth phase, approach which is seldom followed (Fredlund & Morgensten, 1977).

For saturated conditions the volume of water is the same as the volume of voids and the degree of saturation is, $S = 100\%$. The other limit, $S = 0$, represents dry soil. For $S < 1$ there are partially saturated conditions and S is a measure of how close is the material to saturation. For a soil with a continuous air phase usually $S < 80\%$, occluded air bubbles usually exist for $S > 90\%$, while for $80\% < S < 90\%$ there is a transition between those two conditions (Fredlund & Rahardjo, 1993). According to this perspective, effective stresses modeling of saturated soils represents the limiting case of a two-phase material, with incompressible fluid phase and solid particles.

In partially saturated soils the *total suction*, ψ, represents the free energy of the soil water. The formal definition of total suction was given in 1965 in a review panel of research workers on *Moisture Equilibria and Moisture Changes in Soils Beneath Covered Areas* (Aitchison *et al.*, 1965) as:

> "Total suction or free energy of the soil water: In suction terms, it is the equivalent suction derived from the measurement of the partial pressure of the water vapor in equilibrium with a solution identical in composition with the soil water, relative to the partial pressure of water vapor in equilibrium with free water."

Total suction consists of two components, namely *matric* suction, s, and *osmotic* suction, π (see Figure 3.2).

$$\psi = s + \pi = (u_a - u_w) + \pi \tag{3-3}$$

where u_a is the pore-air pressure and u_w is the pore-water pressure. Matric suction is the difference between the air pressure and the pore-water pressure that exists due to capillary effects between soil particles. The value of matric suction in a partially saturated soil is associated with the curvature of the menisci (at air-water interface). Osmotic (or solute) suction corresponds to the osmotic pressure of the soil water, and hence depends on the salt concentration in the free pore water.

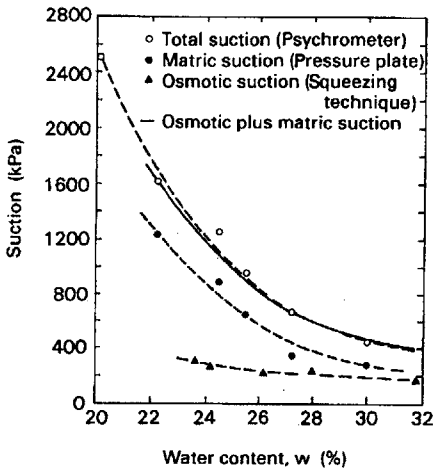

Figure 3. 2: Total, matric and osmotic suction measurements on compacted Regina clay (after Krahn & Fredlund, 1972)

3.1.1 Stress state variables

The mechanical behavior of soils can be described in terms of the state of stress in the soil. These are called stress state variables and are independent of the physical soil properties. The number of state variables required to fully describe the state of a soil depends primarily on the number of phases involved.

For saturated porous media, the mechanical behavior is very neatly described using the *effective stress* (e.g. Biot, 1941; Coussy, 1995)

$$\sigma' = \sigma - b\, u_w \tag{3-4}$$

as a stress state variable*, where σ is the total normal stress, u_w is the pore-water pressure and b is the Biot coefficient. The Biot coefficient is associated with the bulk

* Using tensors, the effective stress tensor is defined as $\boldsymbol{\sigma}' = \boldsymbol{\sigma} - b\, u_w \mathbf{1}$, where $\boldsymbol{\sigma}$ is the stress tensor and $\mathbf{1} = \delta_{ij}$ is the second order unit tensor.

moduli of the soil skeleton, K, and of the solid phase (i.e. solid particles), K_s, as follows (Biot relation).

$$b = 1 - \frac{K}{K_s} \tag{3- 5}$$

For incompressible fluid and solid particles the Biot coefficient is, $b = 1$, and the effective stress reduces to the familiar expression:

$$\sigma' = \sigma - u_w \tag{3- 6}$$

In real soils the Biot coefficient is very close to unity, ranging from 0.998 in dense sand to 0.999+ in NC clays (Mitchell, 1993). As a result, Terzaghi's assumption of effective stress (eqn. 3-6), serves as an excellent approximation and has been extensively used in soil mechanics.

In partially saturated soils, the air phase is also present. The mechanical behavior is controlled by three stress fields, namely total stress $\boldsymbol{\sigma}$, pore-air pressure $u_a\mathbf{1}$ and pore-water pressure $u_w\mathbf{1}$.

It would be advantageous to extend the principle of effective stress to partially saturated soils. Numerous effective stress equations have been proposed by various authors (e.g. Croney *et al.*, 1958; Bishop, 1960; Aitchison, 1961; Jennings, 1961). All equations incorporate a soil parameter* in order to form a single-valued effective stress variable. However, experiments have demonstrated that apart from difficulties in determining the material parameters, the effective stress equation is not single-valued, but there is dependency on the stress path followed (e.g. Morgensten, 1979; Toll, 1990). Re-examination of the single effective stress equations has led many researchers to suggest the use of independent stress variables.

* e.g. the equation proposed by Bishop (1960) reads $\sigma' = \sigma - u_a + \chi\,(u_a - u_w)$, where χ is a material parameter

Fredlund and Morgensten (1977) suggested that for incompressible soil particles any two stress variables among the set of three independent stress tensors is capable of explaining the constitutive behavior of unsaturated soils, (and can describe a smooth transition to saturated conditions):

$$\boldsymbol{\sigma} - u_a\mathbf{1}, \qquad \boldsymbol{\sigma} - u_w\mathbf{1}, \qquad (u_a - u_w)\mathbf{1} \tag{3- 7}$$

The choice actually depends on the reference pressure. It is common practice to select air pressure as a reference pressure*, and the net stress, $\boldsymbol{\sigma} - u_a\mathbf{1}$, and matric suction, $s\mathbf{1} = (u_a - u_w)\mathbf{1}$, as stress state variables. It can be seen that for saturated conditions the stress state variables reduce to the effective stress tensor and the zero tensor respectively. Fredlund and Morgensten justify the use of this set of parameters theoretically by considering the equilibrium equations of a four-phase material (including contractile skin as the fourth phase), and experimentally by a series of null tests† (Fredlund & Morgensten, 1977).

However, this choice is neither universally accepted, nor is it without some deficiencies. The main disadvantage is the that suction term corresponds to matric suction and usually does not take into account osmotic suction. There are indications (Blight, 1983) that solute suction does not contribute significantly to shear strength. On the contrary, several authors (e.g. Jimenez Salas *et al.*, 1973; Morgensten & Balasubramanian, 1980; Richards *et al.*, 1984) report that changes in osmotic suction induce volumetric strains in partially saturated soils. According to Nelson and Miller (1992) the significance of osmotic suction is undermined by the fact that changes in osmotic suction occur only when there is a change in salt concentration. It should be noted also that when flow through unsaturated soils is considered, total suction should be taken into account.

* For instance Geiser *et al.* (1999) chooses u_w as reference pressure and $\boldsymbol{\sigma} - u_w\,\mathbf{1}$ and $s\mathbf{1}$ are used as stress state variables

† Tests where individual components of the stress state variables are modified, but the stress state variables themselves are kept constant. If the selection of stress state variables is valid, then no volumetric change or distortion should be recorded.

It is obvious that, when the stress state variables mentioned above are selected, matric suction and its measurement is of utmost importance. Matric suction can be related to the water content (soil-water characteristic curve) or to the degree of saturation. Such relations are path specific and it is known that hysteresis loops are present in wetting-drying cycles (see Figure 3.3). For dry soils where the water content approaches zero, suction has a limiting value of several hundreds MPa. Experimentally matric suction is measured using tensiometers (Fredlund & Rahardjo, 1993), which provide the negative pore-water pressure. Normal tensiometers measure up to 90kPa. However, recent research at MIT and Imperial College has made it possible to measure suction up to several hundreds of kPa's (Sjoblom, 2000).

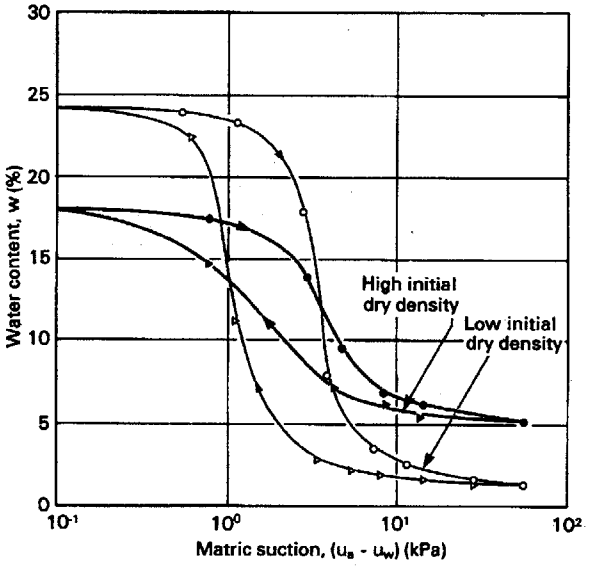

Figure 3. 3: Typical hysteresis loop in drying-wetting cycles in suction-water content diagram of a compacted silty sand (after Croney & Coleman, 1954)

In the remaining part of this chapter the following triaxial stress space variables are defined and their use is adopted:

$$p = \tfrac{1}{3}(\sigma_1 + 2\sigma_3) - u_a, \text{ net mean stress} \qquad (3\text{-}8)$$

$s = u_a - u_w$, matric suction (3- 9)

$q = \sigma_1 - \sigma_3$, shear stress (3- 10)

3.1.2 Volume changes in unsaturated soils

The effects of partial saturation on the volumetric behavior of soils can be studied by comparing 1-D compression tests on saturated and partially saturated samples with suction-controlled tests. The stress space in such tests is now reduced to two ($\sigma_v - u_a$, s or p, s). Typical stress paths comprise of increasing net pressure (vertical in oedometer and isotropic in consolidation tests) with constant water content or decreasing suction (wetting) at different pressure levels.

The main trends in such tests are identified as:

1. Increase in suction leads to stiffening of the soil (with respect to externally applied loads) (e.g. Aitchison & Woodburn, 1969) and an increase in the apparent preconsolidation stress (Dudley, 1970). The idealized behavior for compression tests at different values of constant suction is shown in Figure 3.4.

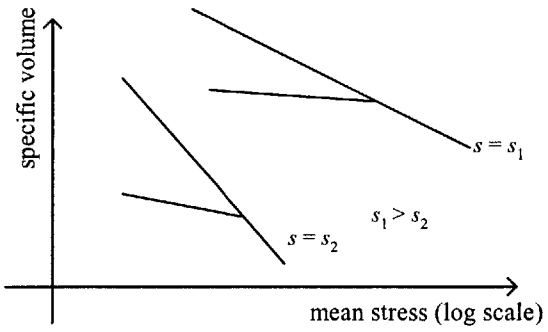

Figure 3. 4: Idealized behavior for isotropic loading for different levels of (constant) suction. Stiffness is increased with increasing suction

2. The volumetric response depends not only on the initial and final states, but also on the particular path that was followed. This applies for paths that involve increase in total stress or increase in suction. On the contrary, it has been often reported (e.g. Matyas & Radhakrishna, 1968; Barden *et al.*, 1969; Lloret & Alonso, 1985; Josa, *et al.*, 1987) that loading paths with non-increasing suction are essentially path independent. Therefore volumetric behavior can be described by state surfaces relating suction, stress variables and void ratio.

3. Swelling or collapse of unsaturated soils is governed mainly by two factors, namely the microfabric and the total stress at which the wetting occurs. In expansive soils elementary clay particles in more or less parallel configuration are dominant. A soil structure with a matrix made from elementary assemblages of clay aggregates has a behavior in wetting that ranges from swelling at low confining pressures to collapse when total mean stress is high (e.g. Maswoswe, 1985; Justo *et al.*, 1984). This is exemplified in Figure 3.5. Note that the amount of collapse increases with increasing stress, as reported by many authors (e.g. Barden *et al.*, 1969; Dudley, 1970).

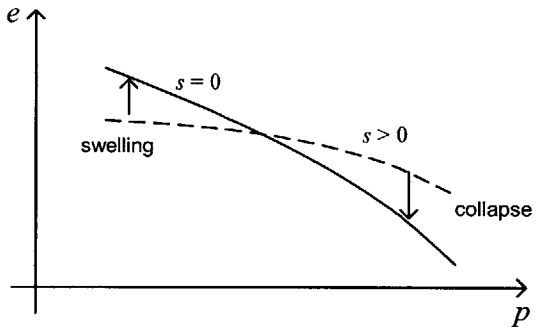

Figure 3. 5: Swell and collapse depend on confining stress (low and high respectively)

4. At constant external load, variations in suction (drying) induce irreversible volumetric strains (e.g. Yong *et al.* 1970; Josa *et al.*1987) (see Figure 3.6). Drying-wetting cycles induce accumulated plastic strains (Escario & Saed, 1986).

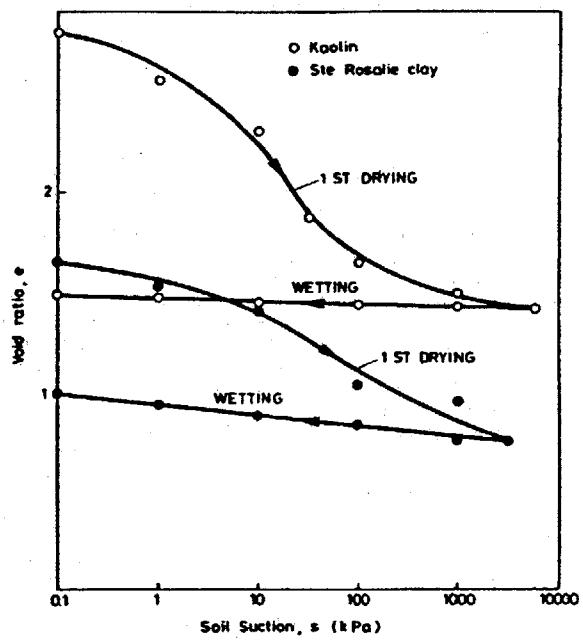

Figure 3. 6: Irreversible changes in void ratio induced by a drying, wetting cycle (after Yong *et al.*, 1970)

So it is seen that irreversible volumetric deformations in partially saturated soils can arise from loading, drying or combination of both.

3.1.3 Shear strength of unsaturated soils

Experimental results (Blight, 1983) suggest that osmotic suction does not have a significant effect on shear strength and shear stiffness. Experimental results have therefore concentrated on the effects of matric suction.

The shear strength of saturated soils is most commonly represented by the Mohr-Coulomb criterion assuming normal effective stresses on the failure plane:

$$\tau_{ff} = c' + \sigma'_{ff} \tan\phi' \qquad (3\text{-}11)$$

Fredlund *et al.* (1978) proposed the extension of the Mohr-Coulomb criterion to partially saturated soils using two stress state variables (eqn. 3-7):

$$\tau_{ff} = c' + (\sigma_{ff} - u_{af}) \tan\phi' + (u_{af} - u_{wf}) \tan\phi^b \qquad (3\text{-}12)$$

where u_{af}, u_{wf} are the air and water pressures at failure and the second friction angle, ϕ^b, represents the increase in shear strength due to matric suction. Fredlund & Rahardjo (1993) report values for ϕ^b, for various soils ranging from very small values to values of the order of the friction angle, ϕ'. Equation 3-12 implies that all envelopes of equal matric suction have the same slope angle, ϕ', and an increased apparent cohesion, c:

$$c = c' + (u_{af} - u_{wf}) \tan\phi^b \qquad (3\text{-}13)$$

Constant friction angle for certain range of suction has been reported by Bishop *et al.* (1960), Fredlund *et al.* (1978), Ho & Fredlund (1982), Escario (1980) (see Figure 3.7) and others. Departures from this pattern have been reported by Escario & Saez (1986) and Delage *et al.*(1987).

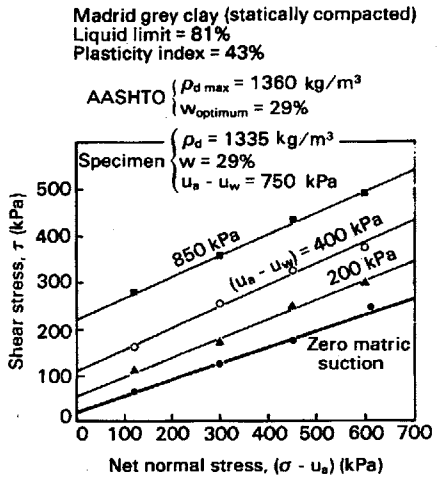

Figure 3. 7: Increase in shear strength due to an increase in matric suction (after Escario, 1980)

3.1.4 Key features of unsaturated soil behavior:

- Suction increases the apparent preconsolidation stress and the stiffness in yield.
- Volumetric deformation is essentially path independent only for stress paths that involve loading and/or wetting.
- As suction increases apparent cohesion increases as well.
- Drying induces irreversible volumetric deformation, while subsequent wetting is almost elastic.

A detailed summary of the mechanical properties of unsaturated soils can be found in Alonso *et al.* (1987).

3.2 Modeling of partially saturated soil behavior

As was described in the previous section, irreversible phenomena may originate from changes in suction and/or from loading. Modeling the unsaturated behavior within the framework of elastoplasticity a yield function is introduced, and plastic strains are induced upon plastic loading (bridging the irreversible deformations irrespective of origin). Alonso *et al.* (1990) describe one of the first systematic attempts to model the behavior of partially saturated soils using the framework of elastoplasticity. The resulting Barcelona Basic Model (BBM) is a simple extension to the well known Modified Cam Clay effective stress model (e.g. Roscoe & Burland, 1968) that is used extensively for saturated soils. Their model subsequently evolved in a series of papers (Gens & Alonso, 1992; Alonso *et al.*, 1994; Alonso *et al.*, 1999) and was extended to account for soils susceptible to swelling (Barcelona Extended Model, BEM).

Wheeler and Sivakumar (1995) and Wheeler (1996) propose a slightly different version of the Barcelona Basic Model (see section 3.2.2) by proposing a more general expression

for compression ratio in the unsaturated domain. This requires more data from laboratory suction controlled tests for parameter estimation. Moreover Wheeler (1996) included specific water volume as an additional state variable. Such a modification is necessary when predictions of changes in water content are needed.

Other models for partially saturated soils that have been published in the literature include:

a) Kohgo *et al.* (1991) which presents an effective stress formulation using an equivalent pore pressure depending on the value of suction.
b) Geiser *et al.* (1997a), (1997b) used the Disturbed State Concept to describe the effects of partial saturation. As fully adjusted state the state of full saturation is chosen.
c) Geiser *et al.* (1999) develops an elastoplastic model using the 'effective' stress and the matric suction as state variables.

It is noted that apart from Kohgo *et al.* (1991) which implements a single effective stress variable, all other modeling attempts consider two independent stress state variables, one of which is the matric suction.

This section summarizes the original formulation of the Barcelona Basic Model (Alonso *et al.*, 1990) and illustrates typical predictions of the model. The formulation is derived in triaxial stress space and net mean stress, p, matric suction, s, and shear stress, q are used as stress state variables (eqns. 3-8,9,10)

3.2.1 Elasticity

The elastic deformation of BBM preserves the unload-reload used by the Modified Cam Clay:

$$d\varepsilon_{vol} = \frac{dp}{K} = \frac{\kappa}{v}\frac{dp}{p} \qquad (3\text{-}14)$$

where K is the (tangent) bulk modulus, κ is the swelling ratio and $v = (1 + e)$, is the specific volume, p, is the net mean stress as was defined in eqn.3-8.

This implies that the elastic part of deformation caused by changes in stresses is not influenced by the level of suction. For shear deformations a constant shear modulus, G, is assumed. For the modeling of the reversible (elastic) deformations inside the yield surface due to changes in suction, Cam Clay elasticity can be modified accordingly. An equivalent swelling ratio, κ_s is defined and determined through tests that include drying paths.

$$d\varepsilon_{vol}^{e} = \frac{ds}{K_s} = \frac{\kappa_s}{v}\frac{ds}{s + p_{at}} \tag{3- 15}$$

where K_s is the bulk modulus corresponding to changes in suction, s is the matric suction and p_{at} is the atmospheric pressure (used to avoid a zero denominator when matric suction becomes zero). Changes in suction do not induce any shear deformation.

3.2.2 Compression Loading

The cornerstone of the BBM formulation is the volumetric compression behavior for partially saturated soils at different levels of matric suction. The analogy to saturated soil behavior is preserved, by assuming a linear relation between volumetric strain (or void ratio) and mean net stress in a semilog plot (see Figure 3.8):

$$v = N(s) - \lambda(s) \ln\frac{p}{p_c} \tag{3- 16}$$

where v is the specific volume, N is the reference specific volume at reference pressure p_c, and λ is the compression ratio. Both λ and N functions of the matric of suction and according to section 3.1.2, at larger suction levels the response is stiffer so $\lambda(s)$ is an increasing function of s.

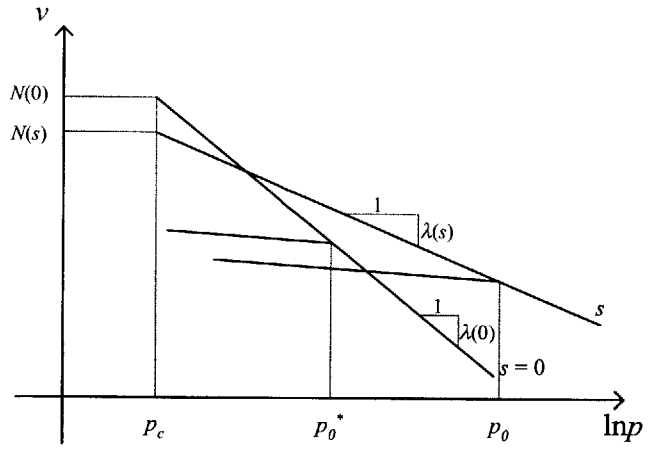

Figure 3. 8: Compression curves for saturated and unsaturated soil

In Figure 3.8 the idealized compression curves for two levels of matric suction ($s = 0$ and $s > 0$) are shown. The apparent preconsolidation net stress for the partially saturated case is p_0. The relation with the preconsolidation net stress at saturation p_0^* provides a guide for the shape if the yield surface in the s-dimension. For p_0, p_0^* lying on the same yield function equation 3-16 at $s = 0$ and $s > 0$ can be related by matching the changes in specific volume with elastic changes predicted by equations 3-15, 3-15. The final result is

$$N(\mathrm{s}) - \lambda(s)\ln\frac{p_0}{p_c} + \kappa\ln\frac{p_0}{p_0^*} + \kappa_s\ln\frac{s+p_{at}}{p_{at}} = N(0) - \lambda(0)\ln\frac{p_0^*}{p_c} \qquad (3\text{-}17)$$

Assuming that there exists a level of pressure that saturation can be approached through a wetting path that involves only swelling*,

$$N(0) - N(s) = \kappa_s\ln\frac{s+p_{at}}{p_{at}} \qquad (3\text{-}18)$$

then the Loading-Collapse (LC) yield surface can be found as follows:

* Wheeler & Sivakumar (1995) and Wheeler (1996) present a slightly different version of BBM. No variation of $N(s)$ and $\lambda(s)$ is assumed, but values are instead determined by compression experiments at different matric suction levels

$$\frac{p_0}{p_c} = \left(\frac{p_o^*}{p_c} \right)^{\frac{\lambda(0)-\kappa}{\lambda(s)-\kappa}} \tag{3- 19}$$

The variation of compression ratio, λ, with suction is described from empirical data:

$$\lambda(s) = \lambda(0)\left[(1-r)e^{-\beta s} + r\right] \tag{3- 20}$$

where equation 3-20 introduces two material constants, namely r and β, that control the limiting value of compression ratio and its rate of increase, respectively. Combining the two preceding equations extends the behavior of the soil in isotropic loading into the unsaturated domain (LC yield surface in Figure 3.9).

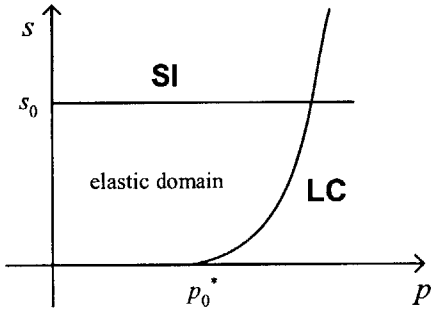

Figure 3. 9: Elastic domain in *p-s* space bounded by the yield curves (Loading-Collapse (LC) and Suction Increase (SI))

Within the framework of elastoplasticity p_0^* is an internal variable. Its hardening rule is found by complete analogy with the classical density hardening of the preconsolidation pressure in saturated conditions:

$$\frac{dp_0^*}{p_0^*} = \frac{v}{\lambda(0)-\kappa} d\varepsilon_{vol,LC}^{p} \tag{3- 21}$$

where $d\varepsilon_{vol,LC}^{p}$ denotes the plastic volumetric strain increment corresponding to the LC yield mechanism.

3.2.3 Changes in matric suction

Equally important for the successful modeling of unsaturated soil behavior is the volumetric behavior in wetting-drying cycles. However since experimental data are scarce, a simple suction threshold ($s = s_0$) is assumed to bound the elastic domain (see Figure 3.9). Increasing the suction beyond this threshold is assumed to cause irreversible deformation. The compression behavior due to increased matric suction is written:

$$d\varepsilon_{vol} = \frac{\lambda_s}{v}\frac{ds}{s + p_{at}} \tag{3- 22}$$

where λ_s is the apparent suction-compressibility parameter.

Combining with eq. 3-16 the hardening rule for the evolution of the internal variable, s_0, is obtained:

$$\frac{ds_0}{s_0 + p_{at}} = \frac{v}{\lambda_s - \kappa_s} d\varepsilon^p_{vol,SI} \tag{3- 23}$$

where $d\varepsilon^p_{vol,SI}$ is the plastic volumetric strain increment caused by the SI yielding mechanism. Equations 3-21, 3-23 imply independent hardening of the two yield surfaces. However, there is experimental data (Josa *et al.*, 1987) about definite coupling between the two yield curves, therefore the hardening rules can be modified to depend on total volumetric plastic strain ($d\varepsilon^p = d\varepsilon^p_{vol,LC} + d\varepsilon^p_{vol,SI}$) and not on plastic volumetric strains that are attributed separately to changes in net stress and suction.

3.2.4 Shear strength

Section 3.2.2 showed that increases in matric suction lead to an increase in shear strength and apparent cohesion. If the increase in apparent cohesion is linear with suction (as

suggested in eqn. 3-13) then the tensile strength can be related to suction through a single parameter, namely k:

$$p_s = k\,s \tag{3-24}$$

The shear strength of partially saturated soils is described in the BBM formulation by assuming that the yield function in (p, q, s = const.) space has the same geometry as the MCC model and is fully determined by the preconsolidation pressure, p_0, and tensile strength, p_s. The yield function in triaxial space (for an assumed constant value of suction) is the MCC ellipse scaled to the preconsolidation pressure, p_0, and tensile strength, p_s (see Figure 3.10). The critical state line in each s = const. plane has slope M.

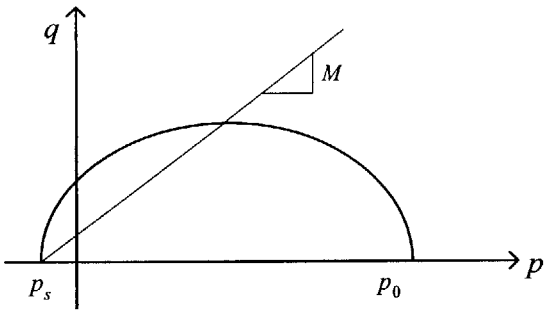

Figure 3. 10: Yield line in the *p-q* space for certain amount of suction

The complete yield function can then be visualized in the 3-dimensional p-q-s space (Figure 3.11).

Non-associated flow is assumed such that the SI yield surface generates only volumetric plastic strains:

$$\frac{\partial g_{SI}}{\partial p} = 1; \quad \frac{\partial g_{SI}}{\partial q} = 0 \tag{3-25}$$

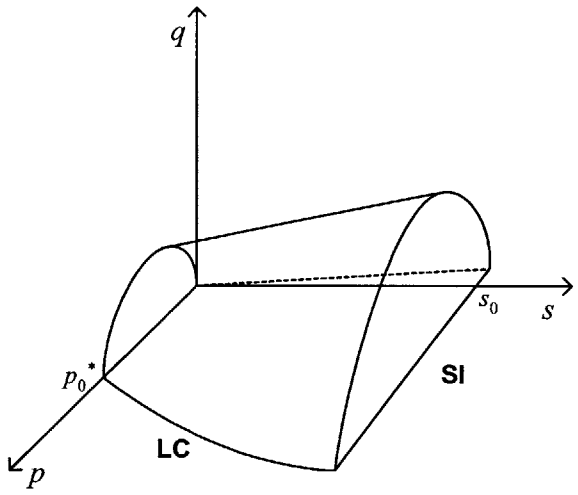

Figure 3. 11: Yield surfaces in *p-q-s* space

For LC yield, the flow rule of MCC is slightly modified according to suggestions by Ohmaki (1982) in order to improve predictions for K_0 values.

$$\frac{\partial g_{LC}}{\partial p} = M^2(2p - p_0 + p_s); \quad \frac{\partial g_{LC}}{\partial q} = 2q\,\alpha \tag{3-26}$$

where $\alpha = \dfrac{M(M-9)(M-3)}{9(6-M)} \dfrac{1}{1-\dfrac{\kappa}{\lambda(0)}}$.

Complete details of the model are presented in **Appendix B**.

3.2.5 Numerical implementation of BBM

The Barcelona Basic Model was implemented in the MATLAB script *smodel*, which was suitably modified to include multiple yield function plasticity and matric suction as an extra stress state variable.

The formulation of BBM introduces six material parameters (p_c, r, β, λ_s, κ_s, k) in addition to those used by MCC ($\lambda(0)$, κ, M, G). The backbone of the model is the variation of compression ratio with matric suction (eqn. 3-20). Four material parameters are associated with this (p_c, r, β, $\lambda(0)$ and the internal variable p_0^*), and can be determined from isotropic loading tests at different constant suction values (along with M, κ). The measured parameters ($\lambda(s)$, p_0) are relatively well defined and can be used to estimate the input parameters p_c, r and β. Parameters λ_s, κ_s, and internal variable s_0 must be measured in tests with wetting-drying cycles. Note that parameter λ_s and the hardening variable do not need to be determined if problems that will not include drying are in mind. The remaining parameters (M, G, k) refer to the behavior of soil in shear and their determination will require shear strength tests. It is concluded that although routine testing cannot give access to the values of all the parameters, most parameters are well defined and have physical significance.

Model's predictive capabilities are illustrated through a series of representative element tests. Material input parameters are those introduced by Alonso *et al.* (1990) and correspond to a moderately compressible clay/silt with $\phi' = 25.4^\circ$.

Compression ratio, $\lambda(0)$	0.2	'suction' swelling ratio, κ_s	0.008
Swelling ratio, κ	0.02	Critical State Line slope, M	1.0
Limiting compression ratio, r	0.75	Shear modulus, G	10MPa
Rate of change in λ, β	12.5MPa^{-1}	Increase of apparent tensile strength, k	0.6
Reference pressure, p_c	0.10MPa		
'suction' compression ratio, λ_s	0.08	Initial void ratio, e_0	0.9

Table 4. 1: Material parameters used in the simulations with BBM

The values for the hardening variables (preconsolidation pressure and maximum past pressure) were varied according to the specific simulation.

1. Loading paths with wetting:

The first series of simulations subject the soil to different isotropic loading and wetting paths. In the *p-s* space, loading paths are carried out with constant suction, while wetting paths occur at constant mean stress. Figure 3.12 illustrates the compression behavior associated with Loading-Collapse (LC) mechanisms. The results show that the total change in void ratio does not depend on the loading path (as is dictated by the existence of *p-q-s-e* state surfaces), as long as monotonic loading and wetting are applied.

Figure 3.12b also demonstrates that volumetric response due to decreases in matric suction are related to the confining pressure . Thus in part A-B decrease in suction caused some (small) elastic swelling, while the same amount of suction decrease causes collapse at high confining pressure (part F-C) as was commented in section 3.1.2.

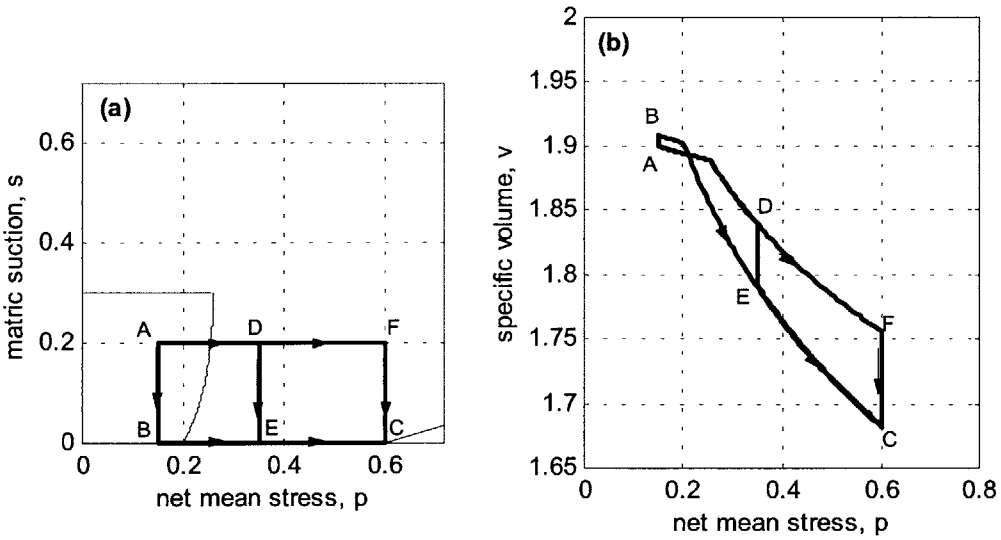

Figure 3. 12: Loading and wetting at different net mean pressure

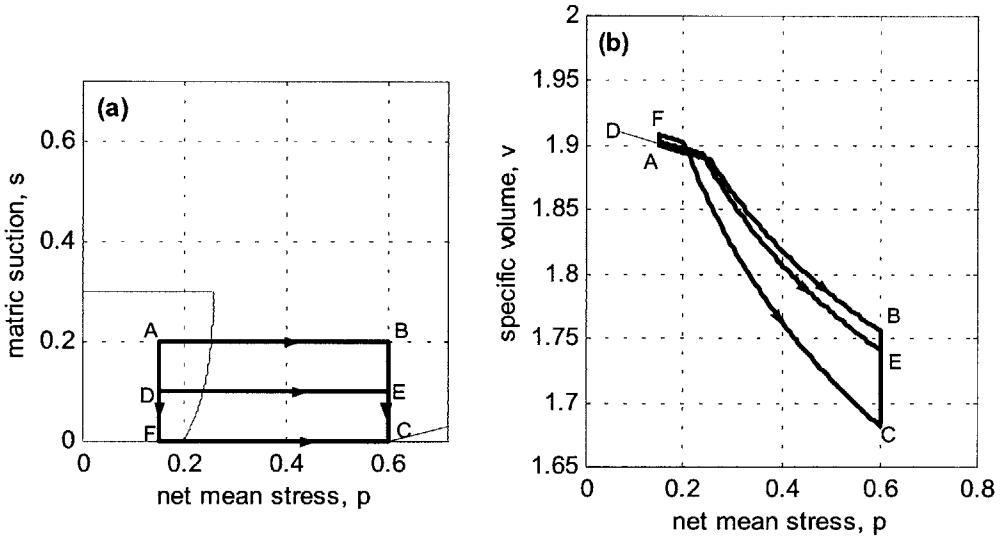

Figure 3. 13: Wetting and loading at different suction levels

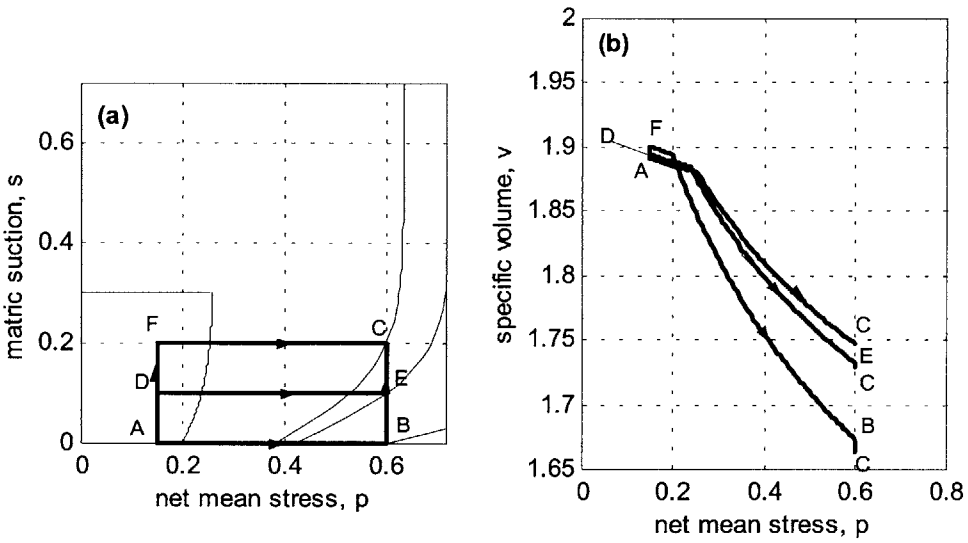

Figure 3. 14: Drying and loading at different suction levels

2. Loading paths with drying:

The next series of simulations involve loading at different suction levels, combined with drying. In contrast to the previous loading with loading and wetting paths, when drying occurs the changes in volume are load path dependent, consistent with experimental data. For example, Figure 3.14 shows that the LC yield curve is activated at different net stresses and the amount of elastic contraction caused by final drying is also different.

3. Wetting-Drying cycles:

A series of simulations consider an initial stress state A (Figure 3.15) at a small maximum past suction. As suction is increased (drying, A-C) at constant mean net stress the suction increase (SI) yield mechanism is activated and plastic strains develop. Since the two yield mechanisms are coupled, there is also increase in preconsolidation pressure involved. Therefore in the subsequent loading path yielding occurs at greater net mean stress (Figure 3.15b). Note that for repeated drying-wetting cycles, experimental data show that plastic strains accumulate, an aspect that cannot be reproduced by a purely elastoplastic yield surface.

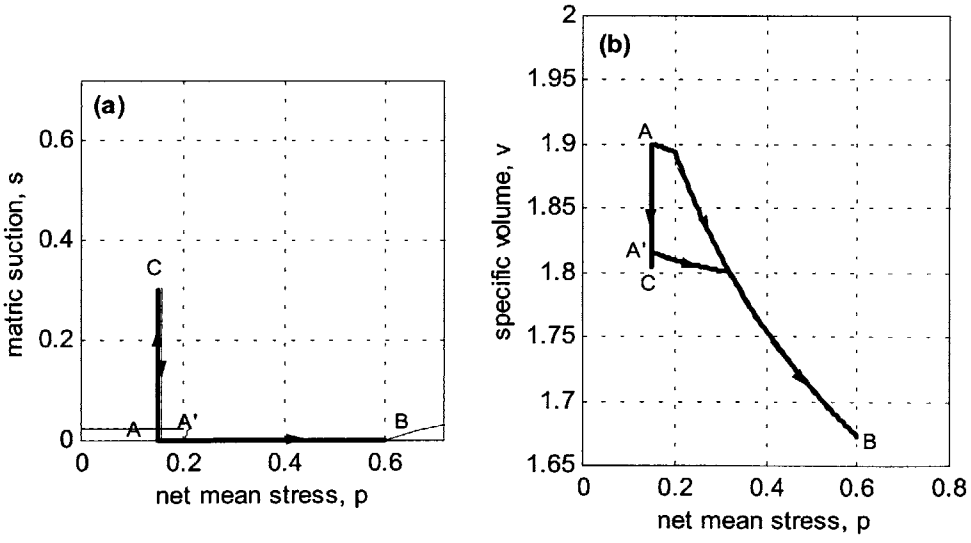

Figure 3. 15: Drying-wetting cycle and subsequent loading

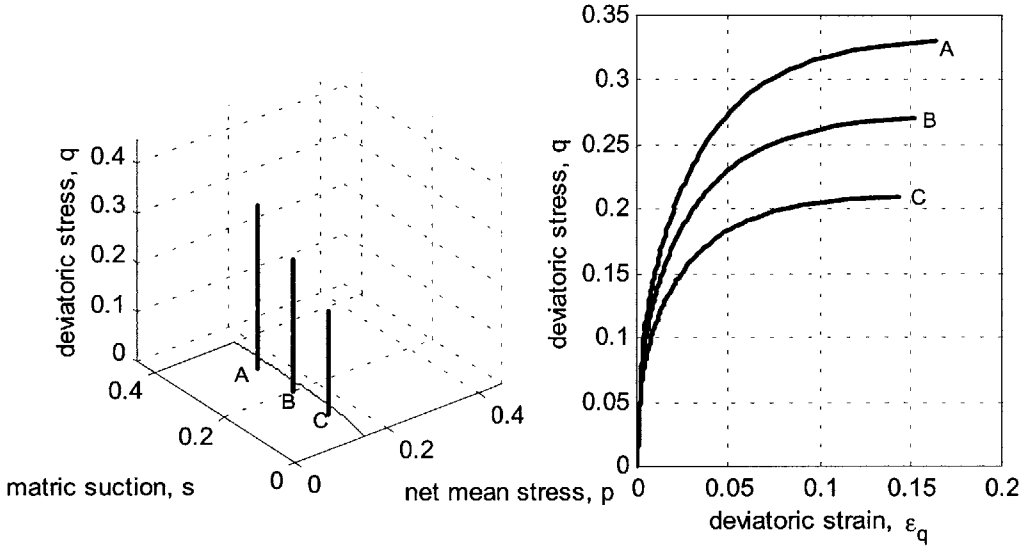

Figure 3. 16: Drained shear test at different suction levels

4. Drained shear tests:

In this series of tests, the soil was subjected to drained shear until failure was reached, at three different suction levels and relatively small OCR. Failure was reached at progressively higher shear stress, as suction increased, which agrees with trends in experiments run on unsaturated soils (section 3.1.3).

The BBM introduces a rational extension to a reference effective stress model (MCC) for modeling partially saturated soils. The extension is based on observations on real unsaturated soil behavior, and mathematical tools to quantify the desired behavior with the concept of elastoplasticity are derived. Recently, a more theoretical background was given by Dangla *et al.* (1997), and the BBM was placed within the framework of poro-plasticity and thermodynamics of porous media. Certain trends (with some notable exceptions, such as hysteresis and accumulation of plastic strains in drying-wetting cycles) can be reproduced qualitatively using a unified approach. Swelling to collapse

behavior with increasing confining stress is reproduced, but only moderate amounts of swelling can be predicted.

Most importantly BBM provides a platform on which further refinement can be made. More specifically, the dependence of the compression ratio on the level of matric suction can be checked as more laboratory data become available and improved. An equally important modification is the dependence of suction (which is a stress state variable) with an easily measured quantity, such as the water content or the degree of saturation. Finally the dependence of shear strength on suction has to be refined, since up to now only latent enlargement via enlargement of the MCC elastic domain is introduced.

Chapter 4: Modeling of Structured Soils

4.1 Structure in natural soils and weak rocks

Most research in soil mechanics in the past decades (in characterization of mechanical properties and their constitutive modeling) involved almost exclusively reconstituted soils. Critical state mechanics (e.g. Roscoe & Burland, 1968) is now very well established and seems to be suitable framework for the behavior of saturated clays and sands with no bonding at contacts. In reconstituted soils quite advanced elastoplastic constitutive laws have been able to describe measured behavior (e.g. Pestana, 1994). Such laws provide the mechanical characteristics in terms of the current state of the material (effective stresses and void ratio) and its stress history (usually conveyed in the maximum pre-consolidation pressure).

However, it has been also recognized that natural soils have components of stiffness and strength, which cannot be accounted for by the principles of 'classical' soil mechanics alone, but instead stem from the influence of *soil structure* (e.g. Burland, 1990; Leroueil & Vaughan, 1990). Such behavior has been recognized in a variety of soils such as soft sensitive clays (e.g. Tavenas & Leroueil, 1990), stiff clays (e.g. Burland *et al.*, 1996), sands (e.g. Mitchell & Solymar, 1984), residual soils (e.g. Vaughan, 1988), as well as in weak and weathered rocks (e.g. Elliot & Brown, 1985). The behavior of structured materials falls in the intermediate region between rocks and soils and the understanding of their behavior has fallen behind that acquired for rocks and unstructured soils.

The term soil structure is used to account for the 'fabric' (referring to the arrangements of particles) and interparticle bonding. This rather generic term refers to the mechanical

characteristics of this class of materials and does not reveal the nature of structure. In fact soil structure can arise from numerous causes. Bonds at interparticle contacts can form from solution and deposition of silica at particle contacts in sands (Mitchell & Solymar, 1984), from cold welding at interparticle contacts under high pressure, from deposition of carbonates (e.g. Kelly *et al.*, 1974; Anagnostopoulos *et al.*, 1991), hydroxides and organic matter from solution. Moreover soil structure can arise from recrystallization of minerals during weathering (e.g. Vargas, 1953), and from modification of the adsorbed water layer and interparticle attractive forces in clayey soils (*thixotropy*; e.g. Mitchell, 1993).

Although the effects of structure on material behavior can be viewed in a unified way (by essentially providing bonding between particles or aggregates of particles), it is important to identify the differences that the various types of bonding induce to the soil substance (McGown & Collins, 1975). Therefore, two main categories can be distinguished:

First, there are many soils that consist actually of smaller elementary particles (e.g. sand grains, clay aggregates) which are held together by a cementing agent at the (existing) interparticle contacts. Degree of bonding can vary but does not alter the original soil particles and their properties (intrinsic properties Burland, 1990). For such structured soils the breakage of bonds leads to a behavior that is instantly recognizable as the uncemented soil.

The second category includes soils that have acquired structure through dissolution and re-precipitation processes. Such soils are usually weathered rocks and residual soils which have undergone changes in their chemical composition in the structuring process. It is obvious that for these types of structured soils no known intrinsic behavior can be assumed. Moreover, the breakage of bonds may lead to drastically different behavior from the intact configuration (as is characteristically the case in quick clays and some

residual soils*). It is therefore possible that the generic approach to structured soils, as is usually followed, may not apply for such specific classes of structured soils.

The actual history of structural generation is usually difficult to track, and the causes that gave rise to structure may not be obvious. It is then desirable to develop a framework that is indifferent to the specific details of the soil structure. Indeed, the study of structured soils has advanced a lot by the landmark paper by Leroueil & Vaughan (1990), which has described the effects of structure in a unified way, regardless of the specific origin and type of structure. Since then, other researchers (Kavvadas *et al.*, 1993a; Kavvadas & Anagnostopoulos, 1998; Cotecchia & Chandler ,1997 and 1999) have followed the same direction, identifying common behavior features in cemented soils, weak rocks and natural clays, independent of the special characteristics of these (very different) materials.

The effects of the structure on the mechanical characteristics of soils depend on the magnitude of the cementation bonds (expressed by the bond strength) and the time of bond development during the geologic history of the deposit. The description of structured soils is often made in comparison with a condition of the soil with absence of structure. Accordingly a measure of the soil structure is the sensitivity index which refers to the ratio of a material property(e.g. swelling index (Burland, 1990), shear strength (Cotecchia & Chandler, 1997)) at the intact in situ state and the state with zero structure (fully destructured).

The state of soil without structure usually occurs after large straining of the material resulting in loss of structure (*destructured* soil) or may refer to a soil which never exhibited structured behavior (*non-structured* soil). Thus the intrinsic properties of soils (inherent and independent of the natural state) provide a frame of reference for assessing the in situ state of a natural soil and the influence of structure on its properties. This

* The loss of structure gives rise to the swelling in the microlevel

general principle forms the basis for most of the existing efforts to model structured soils (see section 4.2).

4.1.1 Effects of structure in mechanical behavior

In this section, common trends of structured soils that have been published in the literature will be presented, ultimately seeking a general description of structured soil behavior, to serve as a basis for modeling.

A simple demonstration of the effects of structure can be seen when considering the compression curves of a soil. The Virgin Compression Line (VCL) represents the possible states (void ratio and confining stress) of stable equilibrium and forms a state boundary for re-sedimented soils (also called Intrinsic Compression Line (ICL)). For soils that are destructured and in the absence of creep phenomena this line represents the only possible states that a soil can have immediately after deposition. However the development of bonds at inter-particle contacts allows the soil to sustain greater pressure without any change in porosity due to the stiffening of the soil skeleton (i.e. part of the load is carried by the bonds). The soil can then be found in stable equilibrium states on the wet side of the VCL, (Figure 4.1, right hand side).

In a real soil deposit, states of the soil immediately after deposition and bond generation form the *Sedimentation Compression Line* (SCL) (Burland, 1990). The relative positions of SCL and VCL depend on the bond strength and mode of bond formation. If the bonds are developed relatively uniformly and independent of the depth (i.e. confining pressure) the SCL differs from the VCL by a constant amount of pressure (line (a) in Figure 4.1). On the contrary when bond development occurs progressively with depth (i.e., depends on the time of deposition), and bond strength is proportional to the confining pressure and the SCL can become parallel to the VCL (line (b) in Figure 4.1), a fact that has been

reported in many experimental results(see Figure 4.2). It should be noted that not all natural soils lie on the SCL since post-depositional effects may alter the state of the soil.

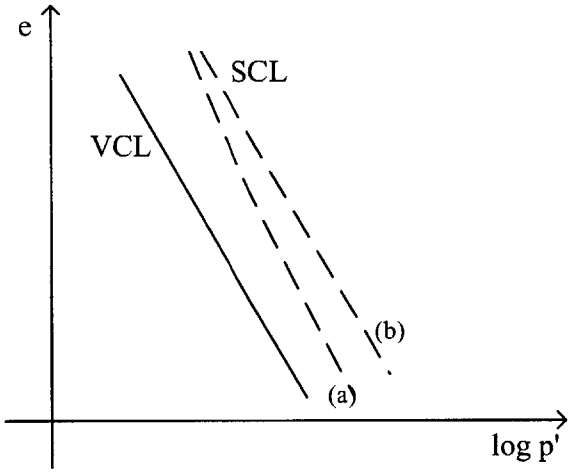

Figure 4. 1: Virgin Compression and Sedimentation Compression Lines

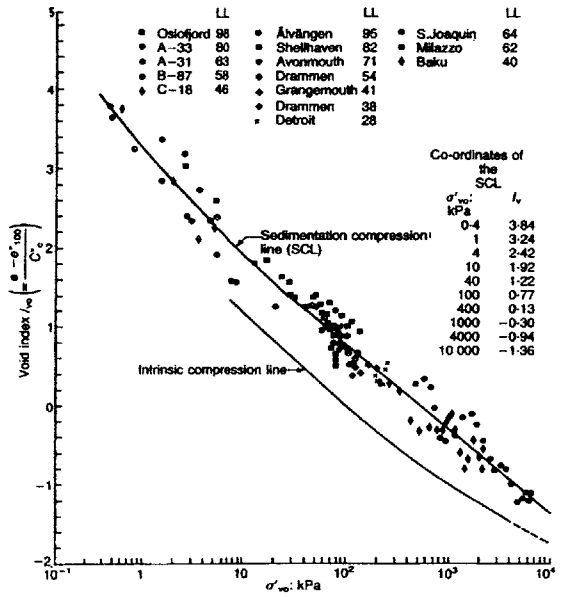

Figure 4. 2: Sedimentation Compression Curves for various natural NC clays. Void index is used to normalize the behavior of clays at different void ratios (after Burland, 1990).

Equally distinct is the behavior of structured soils in one-dimensional compression tests (see e.g. Figure 4.3). The stress-strain curve is usually *S*-shaped, revealing a very marked yield point. Compared to soil without structure, the initial behavior is very stiff as the presence of cementation bonds leads to stiffer response. Moreover the preconsolidation pressure σ'_p has a sharp increase, which again is attributed to the bond carrying part of the load before the first yield occurs. Note that the preconsolidation pressure is usually a direct measure of the size of the yield surface in soil modeling. Therefore it is usually assumed that the elastic domain of structured soils in their intact state is substantially larger then the one corresponding to the reconstituted material (see Figure 4.4 for idealized behavior in 1-D compression).

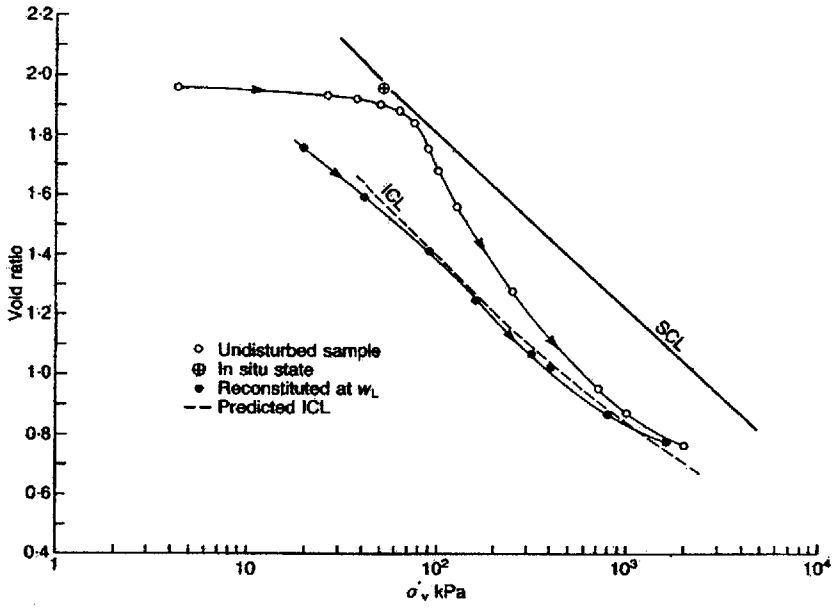

Figure 4. 3: Oedometer tests on undisturbed and reconstituted Bothkenmar soft clay (after Burland, 1990). At large confining pressure soil converges to compression line for unstructured soil.

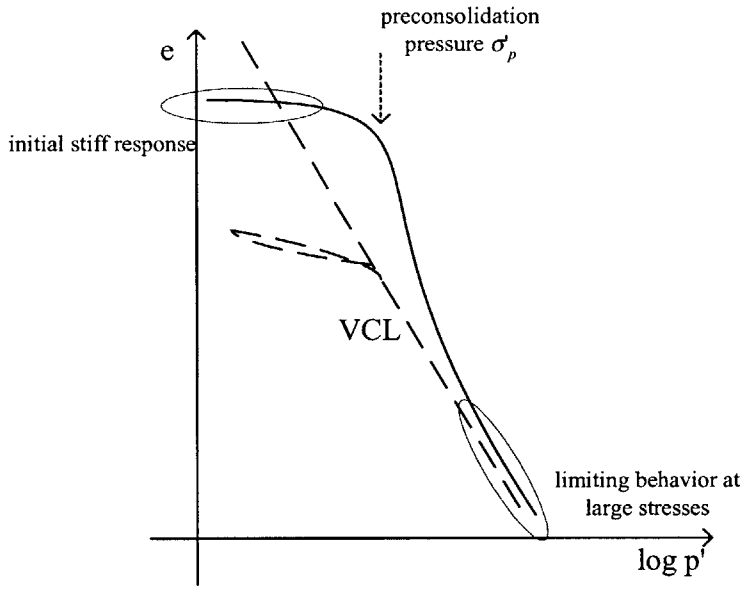

Figure 4. 4: Typical behavior of structured soils in 1-D compression curve. Note the *S*-shaped curve, the increase in preconsolidation pressure, and the limiting behavior at large stresses

Structured soils characteristically exhibit a very pronounced yield point associated with breakage of primary inter-particle bonds (Figure 4.4). The post-yield response can involve a large decrease in volume for a small increase in pressure*. After yield, structure is not removed immediately, but usually substantial post-yield strain is required. In that respect the yielding process is different from yield due to mechanical overconsolidation. The compressibility of the material beyond initial yield is usually high, but the slope of the post yield compression curve, actually depends on the rate of destructuration (via bond degradation). If bonding is exclusively at the inter-particle contacts then breakage can occur simultaneously at many of these contacts leading to an unstable or metastable condition (that is remedied by skeletal collapse due to the overpressure). If however bonding varies more widely within the skeleton, there is a more progressive degradation of the structure.

* In some cases softening behavior has been reported. In stress controlled tests this means localization of yielding (shear bands).

Many authors (e.g. Leroueil & Vaughan, 1990; Liu & Carter, 1997) assume that all structure can be removed at high confining pressures*, and subsequently the compression behavior of the structured soil converges to the VCL (e.g. see Figures 4.3, 4.4). However this is not always true, and in many cases the reconstituted soil can only obtained by remolding the material into a slurry or by crushing and recompacting the material.

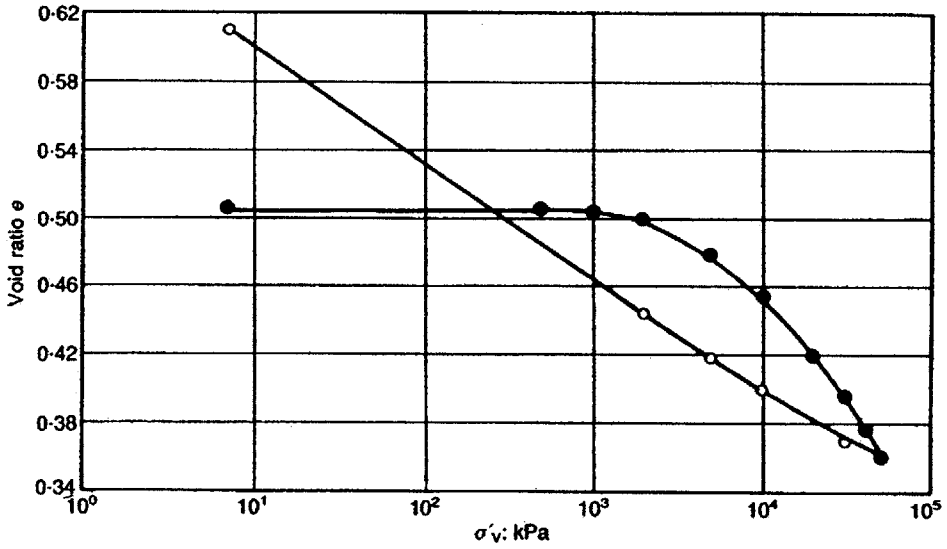

Figure 4. 5: Loss of structure on Culebra shale by compression (after Banks *et al.*, 1975)

Similar observations have been made (Leroueil & Vaughan, 1990; Kavvadas *et al.*, 1993b) in K_0 consolidation tests. In reconstituted soils, the effective stress path rapidly reaches a straight line corresponding to the K_0 value. On the contrary in structured soils the stress path initially overshoots the K_0-line (low K_0; high σ'_1/σ'_3 ratio), approaches the failure line and then gradually approaches the K_0-line for the remolded material, (see also Figure 4.6, 4.7). So the idealized behavior for structured soils (irrespective the source of structure) can be visualized in Figure 4.8.

* However, it is not clear if mechanical crushing can achieve the same disaggregation effects as agitation (blending) carried out in laboratory procedures (Zhang, 2001).

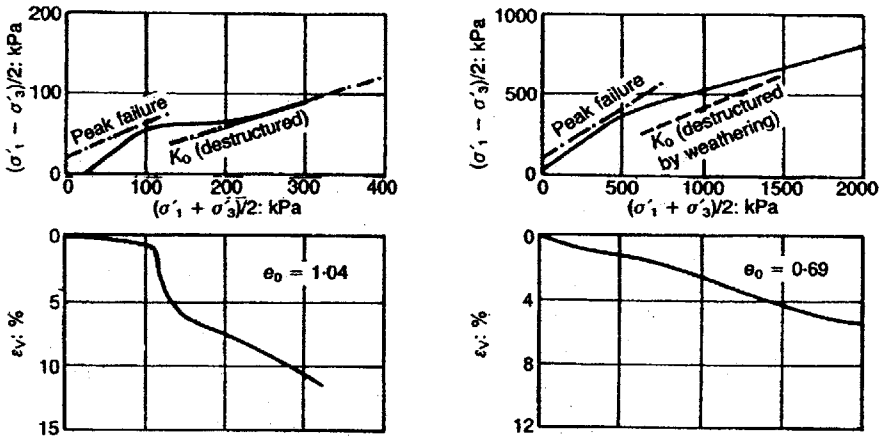

Figure 4. 6: One dimensional K_0 compression tests on different structured soils (after Leroueil & Vaughan, 1990)

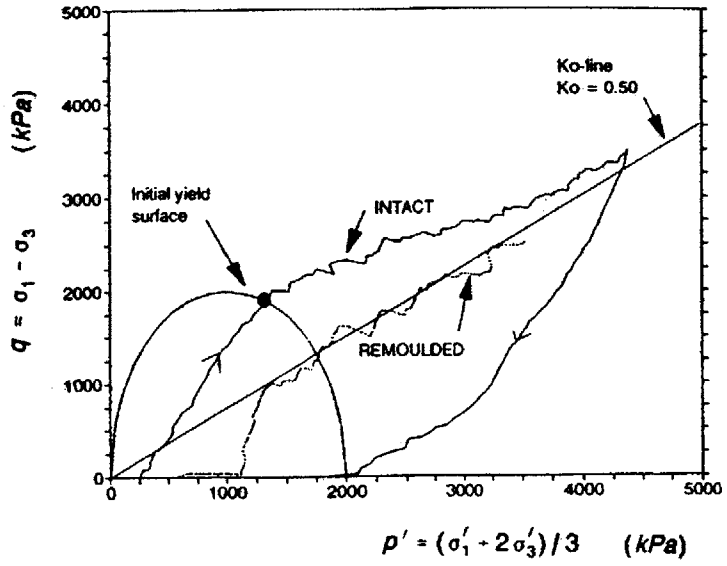

Figure 4. 7: K_0 consolidation test on Ptolemais lignite (after Kavvadas *et al.*, 1993b). Note the distinct behavior of the intact specimen

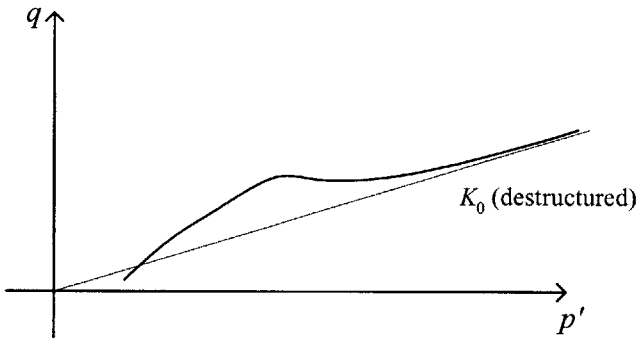

Figure 4. 8: Typical K_0 consolidation stress path. The stress paths ultimately approaches the K_0 line for unstructured soils

Structure has also great effect on the shear strength of soils since the presence of cementation bonds causes failure at higher stresses, since the bonds have to be broken before the soil reaches failure. It is concluded that cementation bonds contribute to the resistance of soil to shear (along with friction). The shear strength of a structured soil is therefore controlled primarily by structure and not by density, as is the case in unstructured soils.

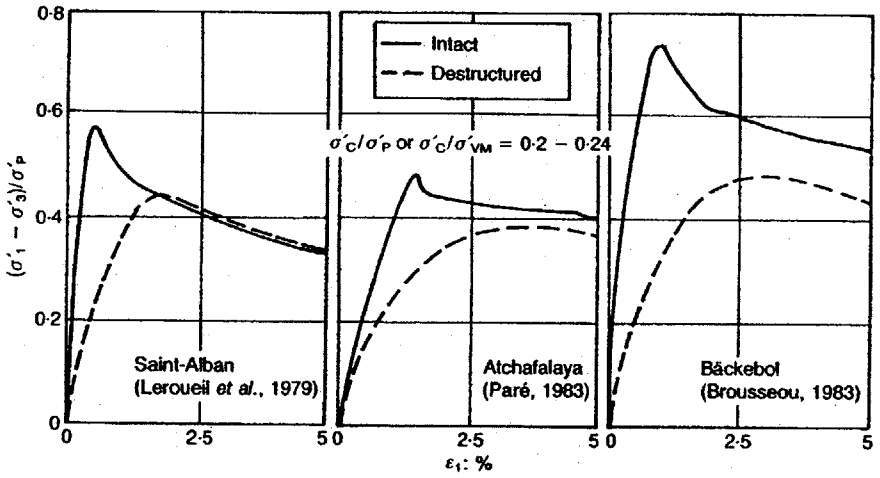

Figure 4. 9: Triaxial compression tests on intact and destructured natural clays (after Tavenas & Leroueil, 1985). Intact specimens exhibit increased shear strength.

Different points of initial yield define the region where possible states can exist and represents the bond strength envelope. As was discussed above, structure usually enlarges the initial yield in both compression and shear. An enlarged yield surface (compared to the unstructured state) is therefore anticipated. Usually this yield surface is substantially larger than the yield surface for the remolded material. Moreover, cementation induces real cohesion which may lead to extension of the yield surface to the negative p' axis (tensile stress). Kavvadas *et al.*(1993a,b) has argued that in structured soils where the bonds develop isotropically (this is usually the case in soft rocks) the yield surface is symmetric with respect to the isotropic axis. However, in natural clays the yield surface is often anisotropic and lies around the K_0 line.

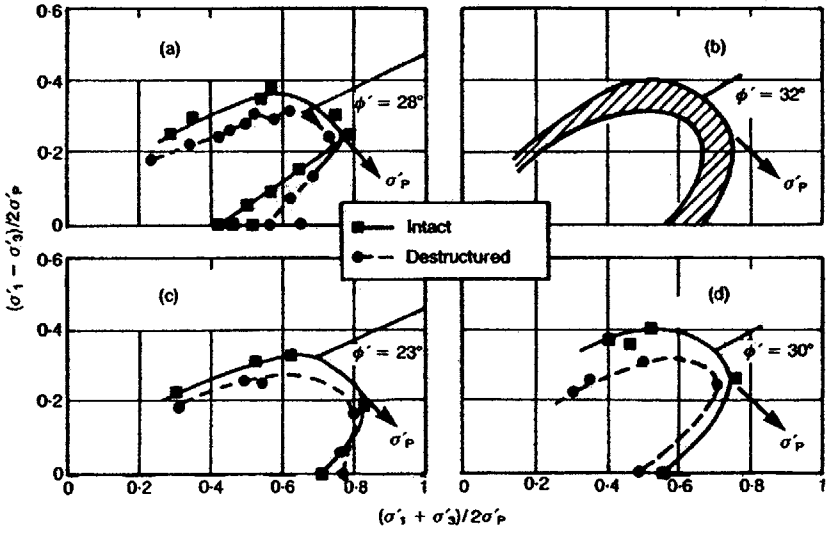

Figure 4. 10: Yield surfaces for intact and destructured soft soils (after Tavenas & Leroueil, 1985)

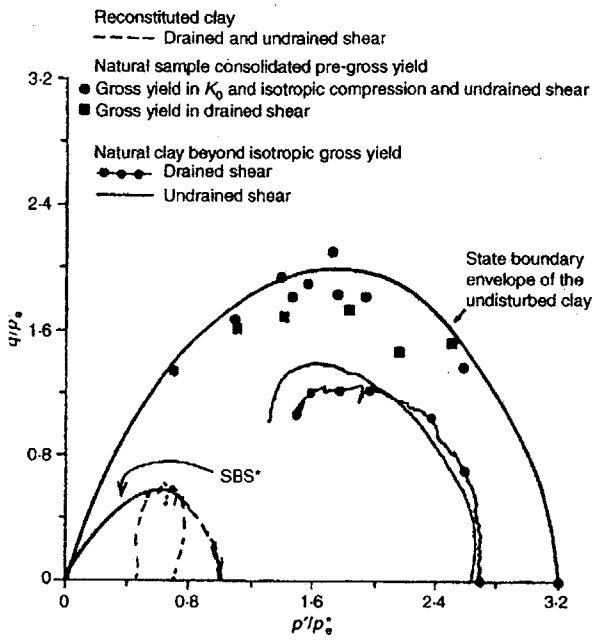

Figure 4. 11: State Boundary Surfaces for Pappadai clay, corresponding to structured and reconstituted state (SBS*) (after Cotecchia & Chandler, 1997).

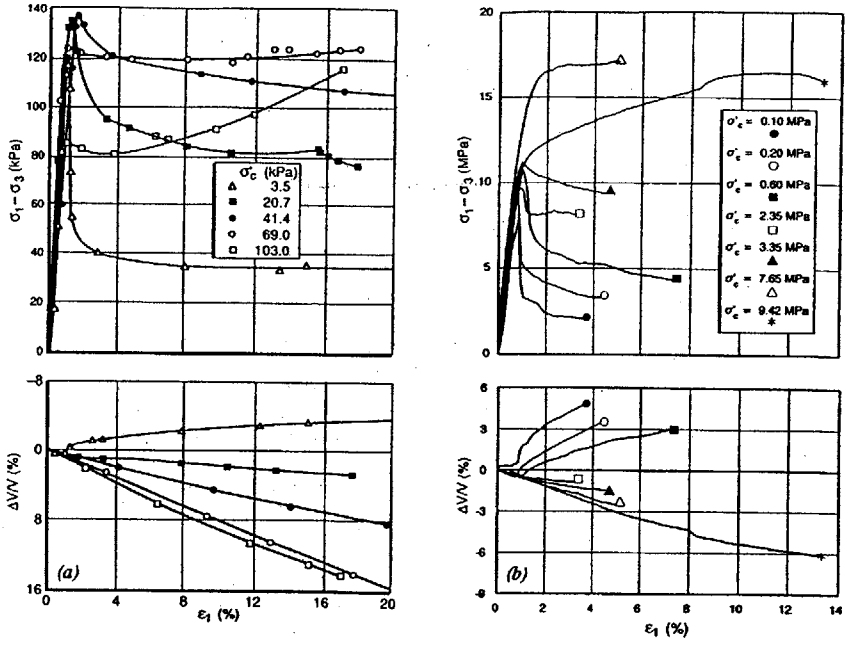

Figure 4. 12: Examples of CID tests on structured soils at different values of confining pressure (after Aversa *et al.*, 1993)

Another significant effect of soil structure is the behavior in drained shear. For unstructured soil it is known that the soil undergoes a transition from brittle/dilative to ductile/contractive behavior as the void ratio increases. It has been demonstrated by many researchers (e.g. Leroueil & Vaughan, 1990; Aversa *et al.*, 1993) that the same effects is observed in structured soils with increasing confining pressure (at constant void ratio). Representative experimental results are shown in Figures 4.12, 4.13. It should be also noted here that comparative test should be carried out with the same strain rate, since it is found experimentally that the rate of loading has a great effect on the response. Studies in strain localization field (e.g. Sulem & Vardoulakis, 1990) argue that this is due to strain rate dependence of localization.

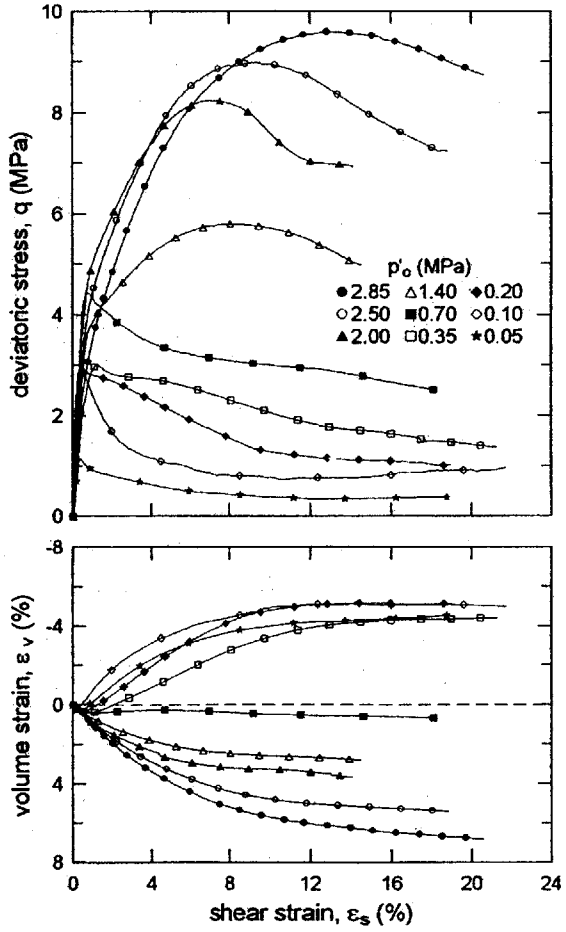

Figure 4. 13: Drained triaxial compression tests at increasing confining pressure for a pyroclastic rock. Stress-strain relationships (up), volumetric strain-shear strain relationships (bottom) (after Cecconi *et al.*, 1998).

4.1.2 Key features of structured soil behavior:

- The structured soil yields at a stress and void ratio which is an impossible state for the same constituent soil when fully destructured.
- The yield surface is larger than the fully remolded material yield surface, since cementation increases both the preconsolidation pressure and the shear strength and can impart real cohesion to the skeleton.
- Yield in compression or shear causes degradation of bonding. In case of full destructuration the enginering properties of the soil resemble the behavior of the intrinsic (constituent) resedimented soil.
- In shear tests, as the confining stress increases there is a transition from a brittle/dilatant behavior of the cemented soil to a ductile/compressive response typical of (unstructured) sands and clays at high confining pressures.

Detailed reviews of the effects of structure in a variety of natural and artificial soils, and weak rocks can be found in Burland (1990), Leroueil & Vaughan (1990), Kavvadas & Anagnostopoulos (1998), Cotecchia & Chandler (1997).

4.2 Structured and bonded soils in soil modeling

Most applications of the general framework of elastoplasticity and critical state soil mechanics, consider fully remolded or reconstituted soils, whose behavior depends on the stress history and the porosity of the material. In order to successfully model the behavior of natural soils, the key features for the effects of soil structure as described in the previous section should be taken into account.

Most existing formulations for structured soils (e.g. Lagoia & Nova, 1993; Adachi & Oka, 1993; Liu & Carter, 1999; Rouainia & Muir Wood, 2000; Kavvadas & Amorosi, 2000) reference their properties relative to the fully remolded state. The state of the soil is described by a parameter that quantifies the degree of bonding. Another common feature is that as straining continues bonding is gradually destroyed and the model converges to the reference (unstructured state) model.

A very appealing concept for modeling the behavior of structured soils is the Disturbed State Concept (DSC) (e.g. Desai, 1995). The degree of bonding is explicitly represented by a scalar that represents the fraction of the response according to the two extreme states (intact and fully remolded). For example, Liu *et al.* (1998) applied the DSC to model the compression behavior of structured soils. The formulation assumed linear behavior in the e-ln$p$' space for the fully destructured state and a disturbance function which depends on the confining pressure. The results reported are shown to reproduce the one-dimensional compression test with accuracy in several cases.

For the modeling the behavior of soils in more general stress paths the framework of strain hardening elastoplasticity seems most appropriate. Gens and Nova (1993) have proposed a set of principles for extending the framework of plasticity to account for soil structure. They assume that the initial yield surface is controlled primarily by bond strength, which is a direct measure of the structure.

Gens and Nova begin by considering an initial yield surface which has the same shape* as the one for the reference material, but is enlarged to account for the initial bond strength. Any shape of yield surface aligned to the isotropic axis could be used as a reference yield surface. The size of the surface is controlled by the bond strength in hydrostatic compression and tension, p'_{co}, p'_{t} respectively and the initial yield surface is enlarged in

* Cotecchia & Chandler (1997) provide experimental data favoring this assumption (see Figure 4. 11)

both directions(Figure 4.14). As loading proceeds the bonding degrades and the two yield surfaces converge.

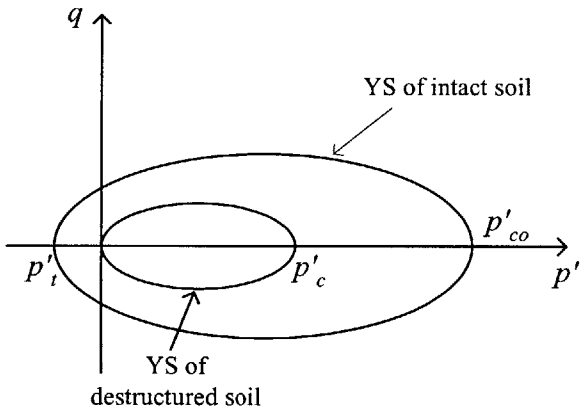

Figure 4. 14: Yield surface for the intact and the reference (reconstituted) material

The model should be able to capture the degradation of cementation bonds as straining continues. This can be achieved by introducing a measure of the degree of bonding that will be controlled by a damage type mechanism (i.e. bonding is related to the accumulated plastic strain). As a first approach, the unique bond strength measure can be used to control the different features of the structured soil (preconsolidation stress, tensile strength, elastic parameters), but this is by no means restrictive and further refinements should be pursued as more experimental data becomes available.

If b is the (scalar) measure indicating the amount of bonding, then ratios p'_{co} / p'_c and p'_t / p'_c should decrease monotonically with decreasing b and have limiting values of 1 and 0 respectively as b approaches zero. Two simple expressions obeying these principles are:

$$\frac{p'_{co}}{p'_c} = 1 + b \qquad (4\text{-}1)$$

$$\frac{p'_t}{p'_c} = \alpha\, b \tag{4-2}$$

Similarly, the destructuring behavior can be conveniently described by expressing b as an exponentially decaying bond strength with increasing accumulated plastic strains:

$$b(\varepsilon^p) = b_0 \exp(-a_0 \varepsilon^p),$$
$$\varepsilon^p = \int d\varepsilon^p \tag{4-3}$$

Such a law obeys intuition ($b \rightarrow 0$ as ε^p increases) and provides some flexibility through dimensionless parameters b_0 and a_0 (b_0 controls the initial magnitude of bonding in the initial state while the constant a_0 indicates the rate of destructuration).

The term, $d\varepsilon^p$, in eqn. 4-3 is a measure of the effective plastic strains. Two possible forms for $d\varepsilon^p$ are:

$$d\varepsilon^p = \sqrt{w(d\varepsilon^p_{vol})^2 + (1-w)(d\varepsilon^p_q)^2}$$
$$d\varepsilon^p = w\,|d\varepsilon^p{}_{vol}| + (1 - \mathrm{w})\,|d\varepsilon^p{}_q| \tag{4-4}$$

where w is a weight that can render the effective plastic strain fully volumetric (if $w = 1$), fully deviatoric ($w = 0$) or some weighted average. Note that in both forms the total plastic strain can only increase (irreversible damage).

For a destructured soil with yield surface $f(p', q, p_c) = 0$, the yield function for the structured soil is obtained through the transformation $p' \rightarrow p' + p_t$, and $p'_c \rightarrow p'_{co}$. So, the yield function for the structured soil will now be $f(p' + p_t, q, p_{co}) = 0$. If the elastic component of the soil is assumed to remain unaltered* by the change in degree of cementation the model is complete. The standard formulation for elastoplastic models

* Most existing formulations assume this, although physical reasoning suggest it is unrealistic. Chazallon & Hicher (1995) assume an elastic part with damage.

(see **Appendix A**) can be followed, with the addition of one extra hidden variable, the bond strength b, and its hardening rule.

As an example the extension for Modified Cam Clay (referred to as Structured Cam Clay) is presented in **Appendix C**. The effect of bonding are evident in the much different elasto-plastic modulus. The part of the elastoplastic modulus that is related to the bonding is always negative (softening) since the hardening parameter decreases monotonically.

4.2.1 Numerical implementation of SCC

The Structured Cam Clay was implemented in the MATLAB script *smodel*, which is suitable of running one-element tests of elasto-plastic models with critical state, using an adaptive explicit integration algorithm with error control over the step size (Abbo, 1997). This section illustrates the predictive capabilities of the SCC model through a series of representative simulations.

The analyses consider a structured clay whose normalized (i.e. unstructured) behavior corresponds to Boston Blue Clay (BBC). This soil is assumed to have the following values of relevant material parameters (Kavvadas, 1982).

Swelling ratio, κ	0.034
Compression ratio, λ	0.184
Critical State Line slope*, M	1.348
Poisson's ratio, ν	0.277
Initial void ratio, e_0	1.12

Table 4. 2: MCC Material parameters for resedimented/unstructured Boston Blue Clay

* CSL slope value calculated through relation with the friction angle in Triaxial Compression $\phi_{TC} = 33.4°$

Parametric analysis of representative tests where simulated using reasonable values for the parameters concerning soil structure. The parameter b_0 (which indicates the magnitude of preconsolidation pressure for structured soils compared to resedimented value (eqn. 4- 1) ranges b_0 = 0-3. The parameter a_0 which controls the destructuration rate (eqn. 4- 3) is expected to lie in range a_0 = 20-50. In this case, full destructuration ($b / b_0 <$ 0.01) occurs at approximately 10% plastic strain. The parameter controlling the type of destructuration (volumetric vs. deviatoric), namely w (eqn. 4- 4) was varied in the total possible range w = 0-1. For the tensile strength ratio α, a representative value $\alpha = 0.25$ was used in the analyses, since the behavior in the simulated tests is not expected to depend a lot on the tensile strength of the material. Finally in all following simulations p'_c = 100kPa is assumed. Note that since all parameters involved in SCC are dimensionless the output is in the same stress units as the input.

1. Isotropic compression tests:

In the first series of tests, a structured BBC is subjected to isotropic consolidation. In such tests the stress path lies on the isotropic axis ($q = 0$) throughout the test since such a path does not invoke shear strains. For structured soils it is well known that the only possible states lie on the Virgin Compression Line, which is usually assumed to be a straight line in semilog plot. The initial response is elastic for $p' \leq p'_{co}$.

Figures 4.17, 4.18, 4.19 show isotropic consolidation behavior for selected values of initial bond strength, b_0, and rate of destructuration, a_0, assuming fully volumetric effective plastic strain (w = 1 in eq.4- 4). It can be seen that the elastic domain is enlarged with increasing degree of bonding. For relatively large values of bonding, softening behavior is observed*. Such behavior is expected from the model since the magnitude of the always softening bond part of the elastoplastic modulus, is directly proportional to the

* In order to capture the observed strain softening when bond degree/destructuration rate is relatively high, strain controlled tests were simulated (as stress controlled tests would produce brittle collapse).

degree of bonding. The S-shaped curve observed in typical laboratory tests on sensitive clays can be duplicated here. The yielding point is very distinct in most cases. Moreover destructuring causes a transition of compression curve towards VCL, depending on value of a_0. Figure 4.18 shows the effect of rate of bond degradation for a selected value of initial bond strength, $b_0 = 0.5$.

The effects of the weight parameter, w, cannot be distinguished form those of a_0 in isotropic compression (Figure 4.19) (i.e. for isotropic consolidation tests the same response is obtained for constant product $a_0 w$ at a given b_0). For $w = 0$ (pure shear degradation) there is no bond degradation, which is not realistic.

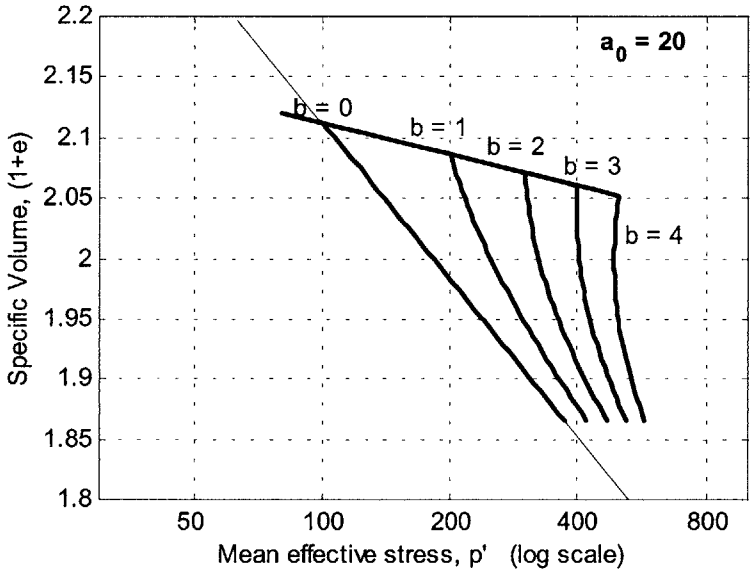

Figure 4. 15: Isotopic consolidation for varying degree of bonding and rate of destructuration $a_0 = 20$

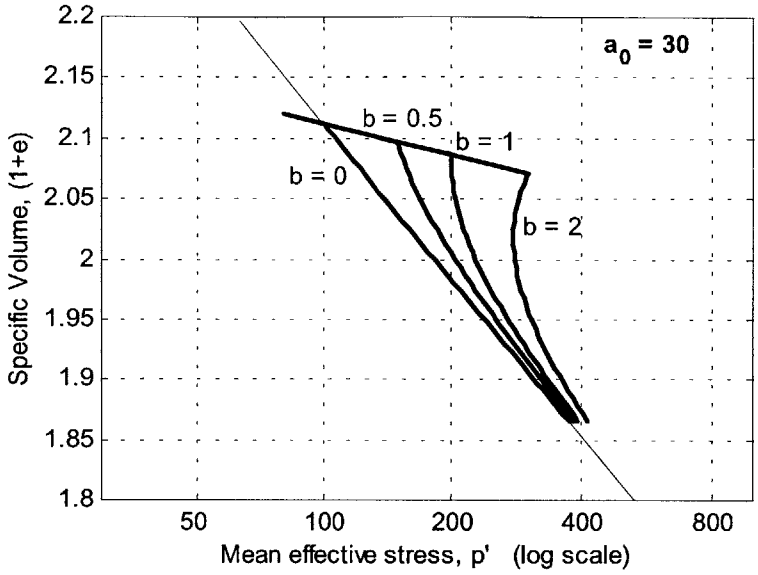

Figure 4. 16: Isotopic consolidation for varying degree of bonding and rate of destructuration $a_0 = 30$

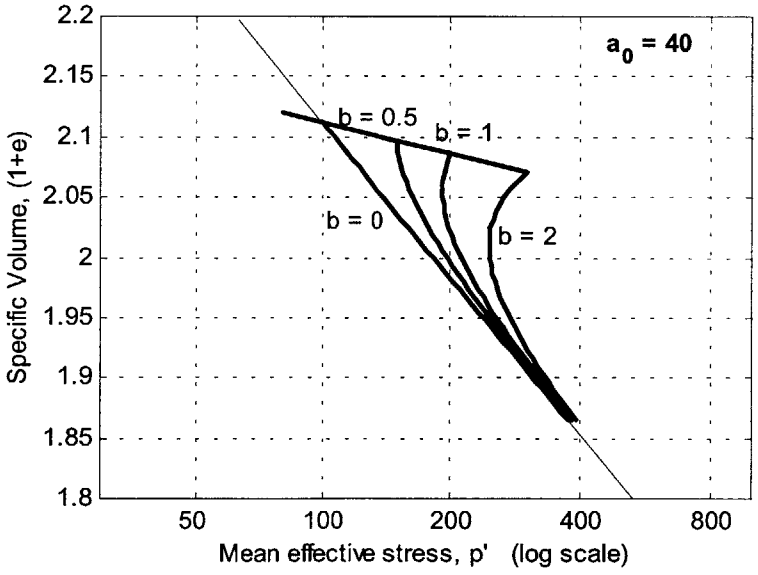

Figure 4. 17: Isotopic consolidation for varying degree of bonding and rate of destructuration $a_0 = 40$

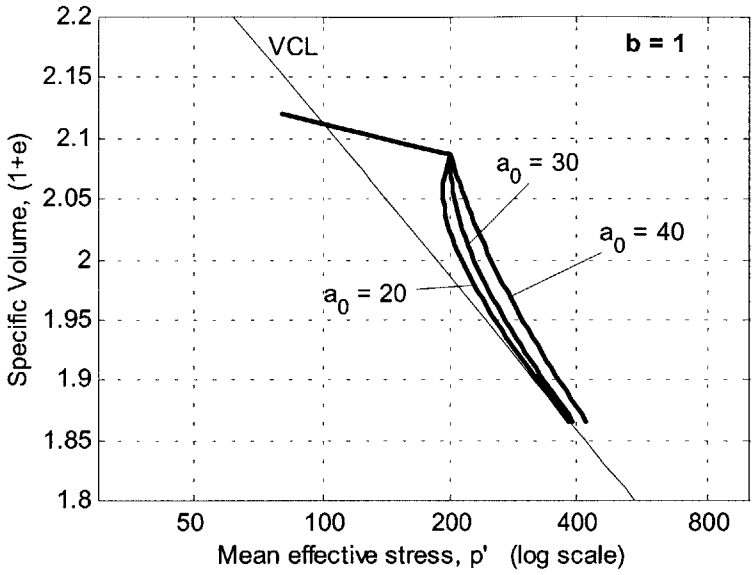

Figure 4. 18: Isotopic consolidation for varying rate of destructuration and degree of bonding $b = 1$

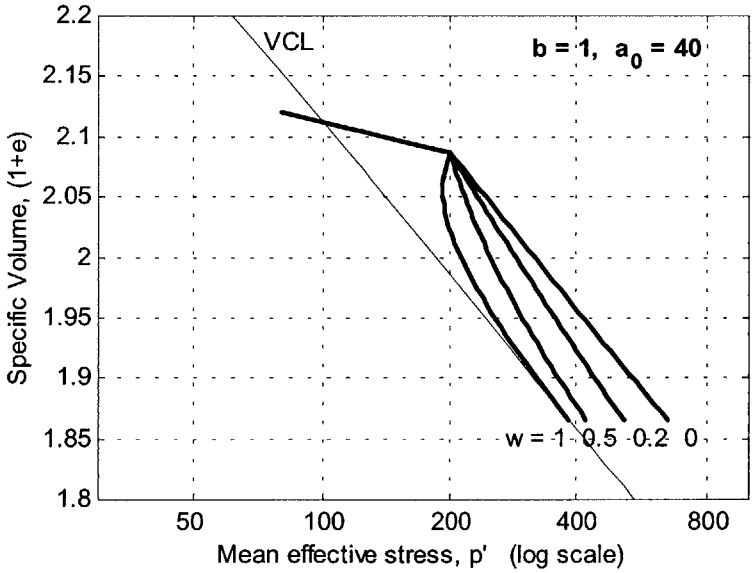

Figure 4. 19: Effect of type of destructuration for $b = 1$, $a_0 = 40$

2. K_0-consolidation tests:

A series of simulations were carried out for various degrees of bonding, a_0 = 30 and assuming pure volumetric degradation (w = 1). The model as expected from the previous series of simulations is capable of reproducing the S-shape behavior in v-p' graphs (Figure 4.20). Also the stress path has the shape of that observed in structured soils (e.g. Figure 4.8).

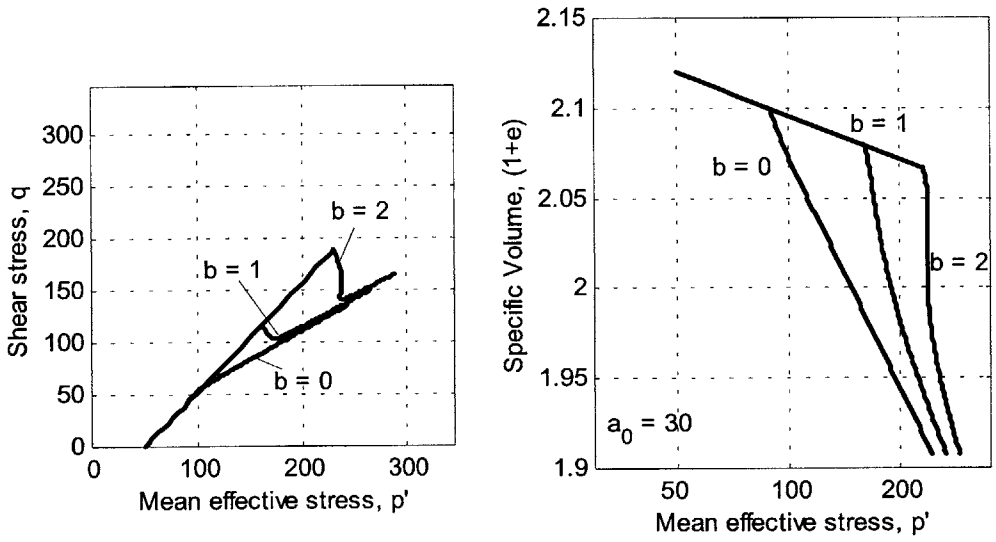

Figure 4. 20: K_0-consolidation tests for varying degree of bonding and a_0 = 30

3. Drained Triaxial Compression tests:

Shows a series of standard drained triaxial compression shear tests (CIDC) for samples at the same void ratio and degree of bonding (b = 1), but varying confining pressure. The selected parameters for this series of analyses are, a_0 = 40, w =0.5. As confining pressure increases the peak strength also increases and there is a reduction in the amount of contraction. For a wide range of (large) confining pressures the peak strength is followed by softening. This is due to the softening induced by the degradation of bond strength.

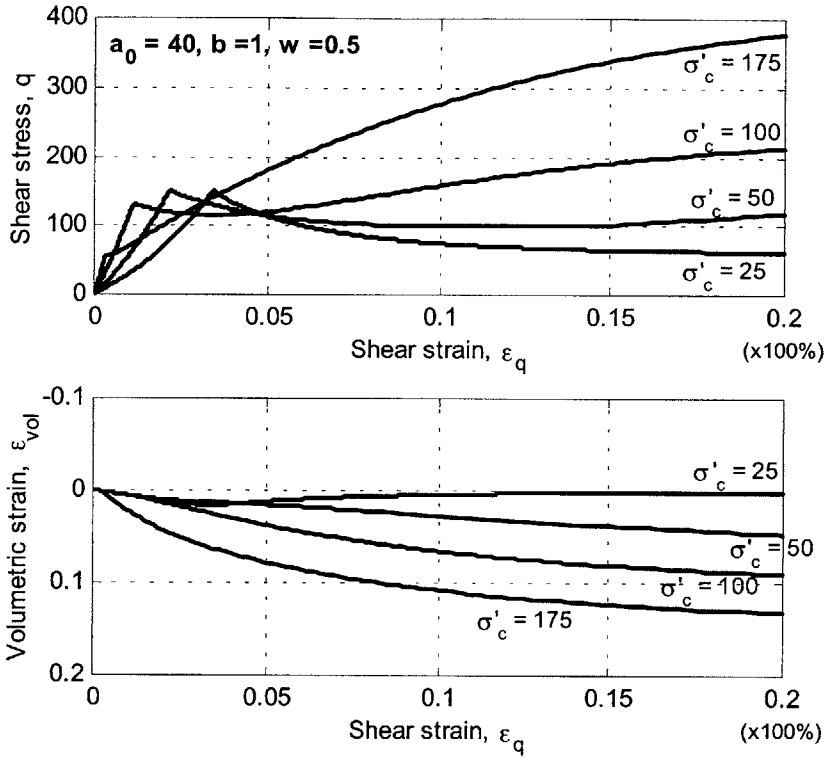

Figure 4. 21: Drained triaxial compression tests at the same void ratio and various confining pressures.

4. Undrained Triaxial Compression tests:

Figures 4.23, 4.24 present the results from simulations of undrained triaxial shear tests on structured soils at varying isotropic over-consolidation ratios (i.e. p'_{co} / p'_i, where p'_i is the initial mean effective stress). Figure 4.22 shows the same simulation for an unstructured soil (standard MCC) and is used as a reference plot. An analogous series of simulations were run for varying p'_i/p'_{co} ratio and two cases of structure. For the case of purely volumetric bond degradation (w = 1), the critical state is reached before structure is fully lost (Fig. 4.23). When distortional degradation is introduced (in the simulations w = 0.5, Fig. 4.24), critical state is only reached at the reference state (i.e. as shearing continues and the remaining bonding is lost). The undrained shear strength variation with initial confining pressure is shown in Figure 4.25.

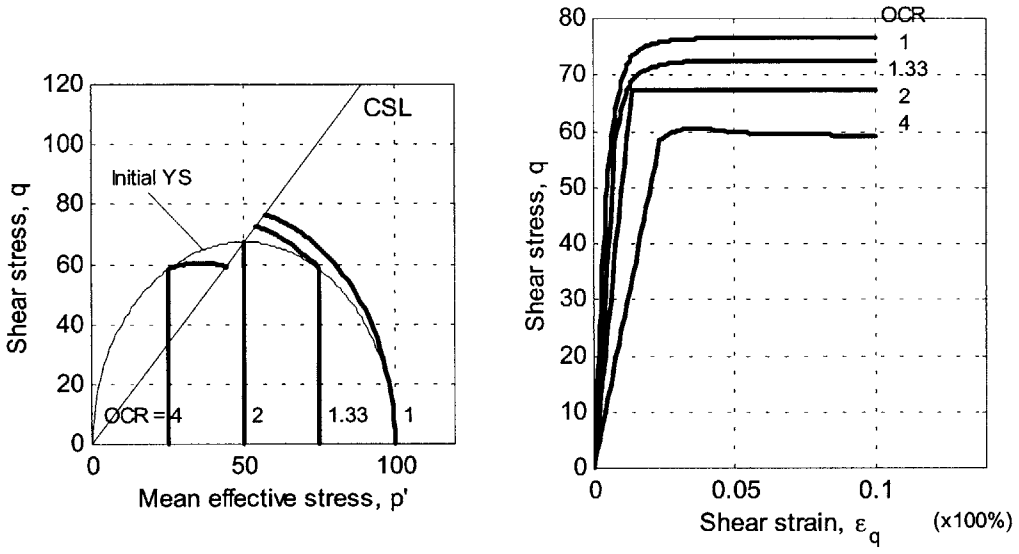

Figure 4. 22: Undrained shear tests for different over-consolidation ratios (unstructured soil)

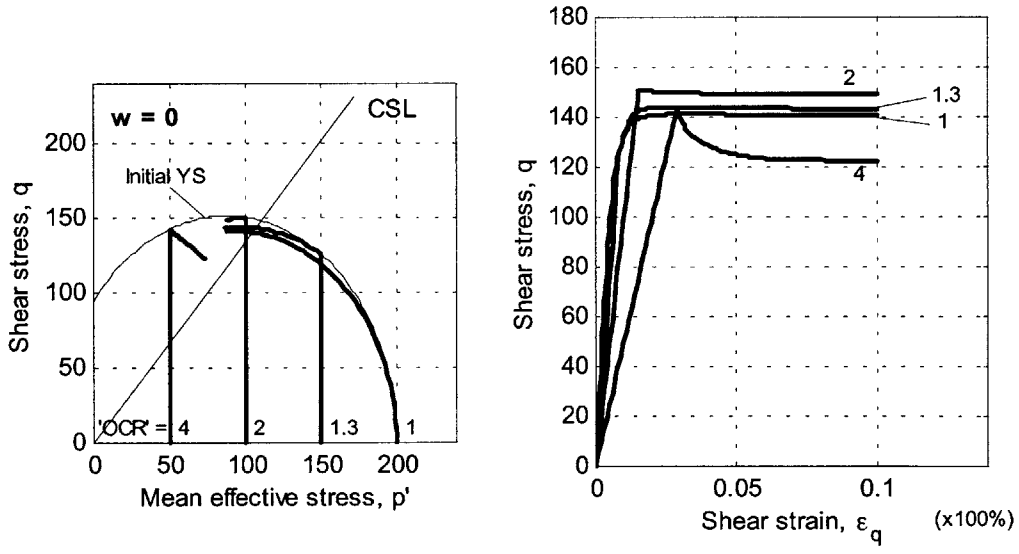

Figure 4. 23: Undrained shear tests of structured soil ($a_0 = 40$, $b = 1$, $w = 1$) at different equivalent over-consolidation ratios.

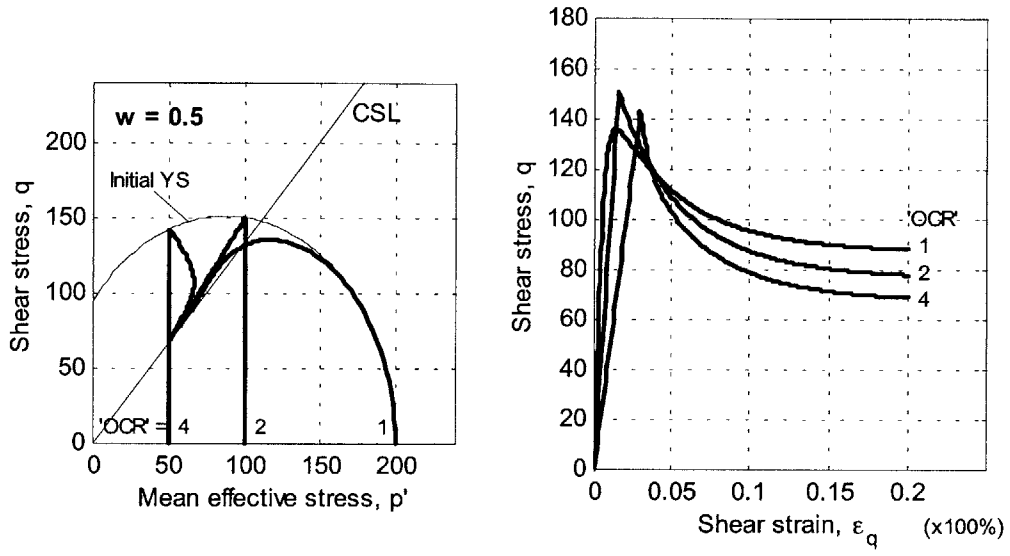

Figure 4. 24: Undrained shear tests of structured soil ($a_0 = 40$, $b = 1$, $w = 0.5$) at different equivalent over-consolidation ratios.

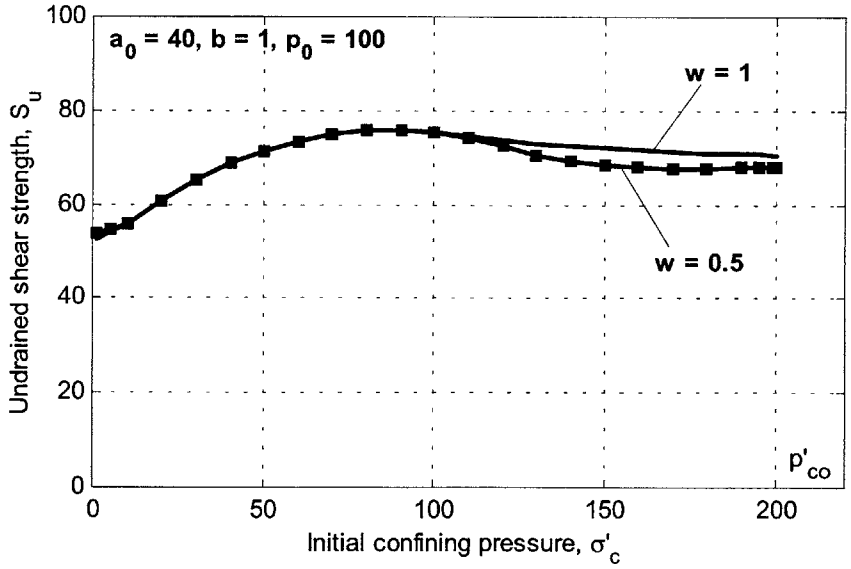

Figure 4. 25: Undrained shear strength for test run at different initial confining pressures.

The main features of the mechanical behavior of structured soils as outlined in section 4.1 are captured qualitatively by the SCC. The main advantage is that only a few parameters are introduced and that they possess physical meaning. Parameters a_0 b_0 control the rate of destructuration and the magnitude of bonding, respectively. Thus, at least in principle, these parameters can be evaluated by fitting experimental data from isotropic consolidation and/or oedometer tests. Note that destructuration depends also on parameter w which relates to the mechanism of debonding. The parameter w can be calibrated if consolidation data are available for at least two different stress ratios. Since it is known that in isotropic consolidation only volumetric plastic strains exist, the value of w can be obtained. The tensile strength is a well defined material parameter. However, its measurement even in cemented soils is a formidable task. Moreover laboratory data rarely involve stress paths in the region of negative or very small mean effective stress, therefore the exact value of the tensile strength is deemed for the moment not to be critical for the model's performance or calibration.

SCC should be viewed as a simple extension of a well known existing elasto-plastic model in order to capture the basic features of behavior of structured soils. The SCC model carries the inherent limitations of MCC (large elastic domain for high OCR, misprediction of K_0 etc. (Gens & Potts, 1988) and is restricted in the triaxial space where the guidelines used in its development were based. Moreover it does not distinguish between elasticity of structured and remolded soils, as the elastic part of the formulation does not reflect the degree of bonding. Another perhaps more important limitation is the assumed conservation of shape of the yield function. Important deviations from real behavior are expected when the ratio of strength of cementation bonds in shear and compression is different from that in uncemented soils. The model does not address localization of deformation issues, which are known to be important in Finite Element implementation of elasto-plastic models (e.g. Brinkgreve 1994). Finally the model is isotropic and does not take into account anisotropy, which could be important especially is structure is gradually destroyed.

4.2.2 Other elastoplastic models for structured soils

More refined approaches, (Muir Wood (1995), Rouainia & Muir Wood (1998, 2000), Kavvadas & Amorosi (1998, 2000)), include better modeling of irreversible behavior for stress paths inside the yield surface (using bounding surface plasticity). Their common feature is the introduction of an additional yield surface which bounds the elastic domain and is justified by experimental data in real soils which reveal a very small elastic domain. This inner yield surface can translate inside the (larger) bond strength envelope. Abrupt change in stiffness occurs when the bond strength envelope is reached.

It is noteworthy that although the sophistication they introduce (mainly to increase flexibility of reproducing experimental results), these model formulations follow the basic principles of the SCC model described above:

- The models have a reference yield surface of the same shape, which moreover will be the limiting yield surface of the material (when the bonds are destroyed via straining).
- They employ an exponential law of accumulated plastic strain as a measure for the degree of bonding.
- The elastic part of the model is the same irrespective of the presence of bonding.

Chapter 5: Summary of results and suggestions for further research

5.1 Summary and Conclusions

This thesis has illustrated the use of elasto-plasticity for modeling key aspects of the behavior of partially saturated and structured/cemented soils. Isolated aspects of soil behavior are taken into consideration, so as to keep the description simple. Simplicity was also the objective in choosing the form of the extensions on existing models and the parameters they introduced. Each development was presented as an extension of the well known Modified Cam Clay effective stress soil model. The primary goal has been to evaluate individual features of behavior through elemental test simulations.

It should be kept in mind that this thesis is only a primer to modeling the behavior of the complex structured soil from the Rio Piedras site. This research was done in order to demonstrate the capability of certain simple modifications to describe the trends of an assumed simplified behavior of real natural soils. The approach to the subject is however limited to modeling qualitatively behavior using flexible sets of parameters.

The most important results for the two soil models presented are summarized below.

5.1.1 Barcelona Basic Model

Partially saturated conditions can be described by two independent variables, namely net mean stress and matric suction. The MCC effective stress model is extended to the three dimensional *p-q-s* space as proposed by Alonso *et al.* (1990). Partially saturated soils

exhibit yield when loaded or when wetted at large confining pressures. Using path-independency of loading/wetting paths and observed changes in compression lines for different values of suction, a yield function associated with loading and collapse is constructed. Partially saturated soils also produce irreversible deformations upon drying over an existing limit of suction. Another yield mechanism (suction increase) is associated with drying (although lacking the observed hysteresis cycles in wetting and drying).

The behavior in shear was deduced indirectly by adopting the MCC yield surface and Critical State Line in triaxial space, and scaling to the apparent preconsolidation pressure and tensile strength (induced by suction). The BBM uses two hardening variables (equivalent preconsolidation pressure at saturation and previous maximum suction) that are assigned volumetric hardening rules. For the elastic part the BMM uses the pressure dependent non-linear elastic part of MCC for plastic deformation direction BBM assumes non-associated flow.

The key features on which BBM was constructed are simulated in single element tests of various loading conditions (loading and wetting, loading and drying, drying/wetting cycles, drained shear). It is concluded that the proposed extensions are capable of capturing qualitatively the desired features of behavior.

5.1.2 Structured Cam Clay

The proposed extensions following (Gens & Nova, 1993) were based on two principles: a) the effects of structure induce a degree of bonding regardless the specific origin of structure, b) the effects of structure can be described using the fully destructured soil as a reference state.

Based on the principles of elastoplasticity a scalar internal variable is introduced (degree of bonding) to account for the magnitude of cementation bonds. In the proposed extension both the shape of the yield function and the elastic component of the MCC were retained. The degree of bonding merely scales the yield surface to account for the initially large elastic domain to the presence of bonding.

Upon loading the cementation bonds in the soil gradually degrade and the soil approaches the final uncemented condition. Therefore the internal variable is controlled by a damage type mechanism and decays exponentially with accumulated plastic strain. As cementation is lost the yield surface converges to the reference yield surface.

The proposed extension requires three material parameters associated with the internal variable. The model is tested in representative stress paths in single element tests. It is concluded that the simple extension used, captures the features of behavior on which it was proposed.

5.2 Recommendations for further research

In order to develop a soil model capable of making reliable prediction of the mechanical behavior of special soils, a lot of effort has to be put in the directions of theoretical modeling and mathematical modeling as well.

The MCC which was used as basis has some known limitations, which are inherited -of course- to the extended models presented in Chapters 3 and 4. It is known to contain an unrealistically large elastic domain, especially in low confining pressures etc. (e.g. Gens & Potts, 1988). Moreover the model is fully isotropic while a large range of soils exhibit anisotropic behavior.

A more refined model for structured and/or unsaturated should be able to cope with the following:

- Most natural soils, both sand and clays, exhibit inherent and/or stress-induced anisotropy. Including anisotropy will require two considerations. First, the recoverable (elastic) component of the model should be replaced with an anisotropic elastic stress-strain law. Second and most important, is the ability to account for anisotropic behavior in yielding and hardening. This has been done successfully in many existing effective stress models for saturated soils (e.g. Hasiguchi (1977), MIT family of models (Kavvadas, 1982; Whittle, 1987; Pestana, 1994)), by introducing a variable (tensor) that explicitly controls the orientation of the yield surface in the stress (hyper-)space. It would be therefore helpful to use such a model as a basis for extension to structured and unsaturated domains.

- A more realistic behavior inside the yield surface is also required. This consists of two different aspects, namely the elastic component and irreversible deformations inside the yield surface. It should be noted however, that the elastic component of many elastoplastic models is not crucial for the model's performance, since the threshold for purely elastic deformations is very small (in the order of 10^{-3}) and upon yielding the plastic deformations are usually far larger in magnitude. Nevertheless, prediction of irreversible deformations inside the yield surface is essential when dealing with cyclic loading, since only then can pore pressure build-up be simulated. Many existing effective stress models (e.g. MIT-E3, MIT-S1) as well two models addressing structured soils employ bounding surface plasticity, (Model for Structured Soils, Kavvadas & Amorosi, 2000; Bubble model, Rouiania & Muir Wood, 2000).

- It is desirable for a model to predict reliably parameters that are often critical to design in geotechnical engineering. More specifically it is important to have reliable prediction of a) undrained shear strength which is associated with the bearing capacity of a soil formation, and b) K_0 value, which controls the initial state of stress. For instance the most widely used soil model, MCC, gives relatively poor prediction of key parameters (e.g. Gens & Potts, 1982, Brinkgreve, 1994; Potts & Zdravkovic, 1999).

- The analysis of boundary value problems using constitutive modeling is the ultimate goal, when developing a soil model. For such analyses to be successful the model should be able to represent accurately the 3-D stress state that usually arise in such problems. The extension of a model from triaxial stress space to more generalized stress space can be done in many ways depending on the choice for dependency from the Lode angle. It has been shown that the choice can be crucial (e.g. Potts & Zdravkovic, 1999) and is found that most soils compare well with models that have the form proposed by Matsuoka-Nakai (1974) or Lade & Duncan (1975) in the deviatoric plane.

It is concluded that a choice of a relatively sophisticated soil model as a reference model seems to be inevitable. A suitable candidate for the reference model is the latest MIT soil model (MIT-S1) which successfully covers most of the above considerations (Pestana, 1994).

In a more general sense, refinements in the constitutive models can only be introduced as experimental data become available. It should be noted here that most of the modeling effort is based on a clear conceptual understanding of specific aspects of soil behavior. For example, most observations for structured soils are derived from compression test data. Therefore, the modeling of structured soils relies heavily on the behavior in one-dimensional and triaxial compression tests. Most of the existing constitutive models are

calibrated using data from triaxial tests and their predictive capabilities are verified along other stress paths in triaxial space. To some degree this evaluation process stems from limitations in the sophistication of laboratory tests. It should be realized that all extensions made are based on features of behavior in triaxial space and therefore, expectations of model performance in more complex stress paths should be viewed with caution (Rudnicki, 2000, makes the same argument commenting on models for rocks).

For structured soils it seems that a (scalar) hardening variable with damage-type mechanism should be associated with different aspects of destructuration. Therefore a refined elastoplastic model for structured soils is expected to have hardening variable that control different modes of behavior. For example, the first choice is the apparent preconsolidation pressure that controls the yield stress and the magnitude of the yield function, as was exemplified in Chapter 4. However other refinements can follow, for example dependence of shear strength on degree of bonding (independent of the preconsolidation pressure), change in elastic parameters as destructuring occurs (this approached is followed by Chazallon & Hicher, 1995). It is obvious, that such a model can only be gradually constructed and possibly each version is likely to introduce new hardening variables and requiring more exclusive verification. One hidden problem of model complexity is that input parameters are rarely independent.

For refining the description of unsaturated soils behavior, progress seems to be invariably linked with advances in experimental techniques that control and measure suction. Soil models following the same principles can be developed, based on observations of tests that involve loading (i.e. changing in stresses) and wetting/drying (i.e. changes in suction). However the whole approach seems to be drastically different than normal elastoplastic models when changes in suction and loading are involved since there is likely to coupling between loading and wetting/drying (Josa *et al.* 1987).

For a successful modeling of the old alluvium of Hato Rey formation the above elements should be combined with dual structure component (e.g. Gens & Alonso, 1992). This will involve careful theoretical modeling in the microstructural level (e.g. Dormieux *et al.* 1995), and an effective means of coupling between the two levels.

Interestingly, Kavvadas (1998) extends the definition of structure to include partially saturated soils. In such case matric suction is visualized as a form of 'cementation' since it increases the preconsolidation pressure and induces apparent cohesion, while wetting is the equivalent destructuration process. Therefore modeling of partially saturated and structured could conceptually be done in conjunction, bridging the produced irreversible deformation into a single yielding mechanism.

As a general comment progress in soil modeling is primarily controlled by experimental data (quality and quantity) and theoretical patterns of behavior. There seems to be elegant, flexible models capable of matching different patterns of behavior and good enough computational schemes to calculate their response. However modeling of increasingly complex soil behavior should be attempted only after a solid theoretical foundation is verified by experimental results.

Appendix A: Incremental Linearized Plasticity

This appendix summarizes the basic formulation for incremental rate-independent elasto-plasticity. As the theory of plasticity is now very well established more details can be found in the references listed at the end of the chapter. This appendix introduces elasto-plasticity in a general six dimensional stress space, while subsequent model formulations (Appendix B) focus on a simplified two dimensional stress space ('triaxial space'). In the following application of elasto-plasticity to soils σ is assumed to be the effective stress tensor.

A.1 Single Yield function

For elasto-plastic materials the behavior depends on the relative position of the stress state relative to the *yield locus* $f(\sigma) = 0$ in the stress space and the *loading increment* $d\sigma$.

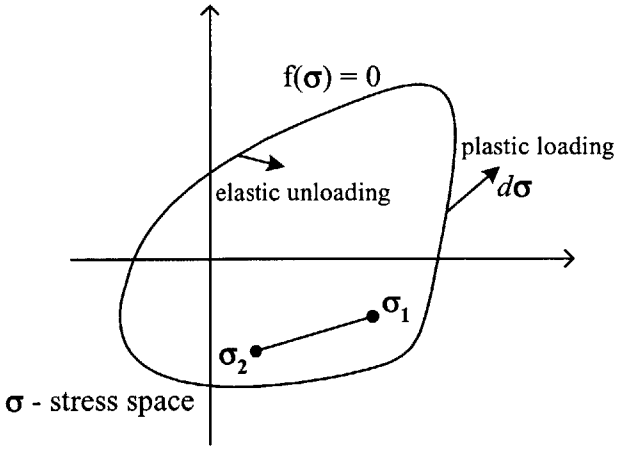

Figure A. 1: Yield function, loading scenarios and convexity

If the current stress state lies on the yield surface and the loading increments points outwards (see Figure A.1), then there is *plastic loading*. Elastic behavior occurs for all stress states inside the yield surface (i.e. $f(\boldsymbol{\sigma}) < 0$), while elastic unloading* occurs when the stress increment points inwards. Mathematically the loading criterion is expressed as:

$$\begin{aligned} &f(\boldsymbol{\sigma}) = 0 \ \wedge \ \partial f / \partial \boldsymbol{\sigma} : d\boldsymbol{\sigma} > 0, \quad \text{plastic loading} \\ &f(\boldsymbol{\sigma}) = 0 \ \wedge \ \partial f / \partial \boldsymbol{\sigma} : d\boldsymbol{\sigma} < 0, \quad \text{elastic unloading} \\ &f(\boldsymbol{\sigma}) = 0 \ \wedge \ \partial f / \partial \boldsymbol{\sigma} : d\boldsymbol{\sigma} = 0, \quad \text{neutral loading} \\ &f(\boldsymbol{\sigma}) < 0, \qquad \text{elastic behavior} \end{aligned} \tag{A- 1}$$

The yield function $f(\boldsymbol{\sigma})$ is a convex† function of the stress state (see Figure A.1) and bounds the elastic domain. The *consistency* criterion, expressed by $df = 0$, ensures that the stress state remains on the loading surface throughout the plastic loading. In the case of *ideal plasticity* the stresses cannot increase anymore ($d\boldsymbol{\sigma} = \mathbf{0}$), the strains become undetermined (in stress-driven tests) and the elastic domain remains constant. In *hardening* (or *softening*) plasticity the elastic domain expands (or shrinks) upon plastic loading. The size of the yield surface is controlled by a set of *internal* (*hardening*) *variables*, $\boldsymbol{\kappa}$‡ (Figure A.2).

---

* Neutral loading is possible for stress loading increments tangent to the yield locus

† The definition of convexity of a scalar function F is:
For $\mathbf{x}_1, \mathbf{x}_2 \in D(F)$ and $\forall \ \lambda \in [0,1]$ the following inequality holds
$F(\lambda \mathbf{x}_1 + (1-\lambda) \mathbf{x}_2) \leq \lambda F(\mathbf{x}_1) + (1-\lambda) F(\mathbf{x}_2)$.
Note: for functions F that are twice differentiable the convexity criterion equals $F''(x) \leq 0$

‡ The internal variables can be scalar (e.g. in isotropic hardening), a vector or a second-order tensor (e.g. in kinematic hardening)

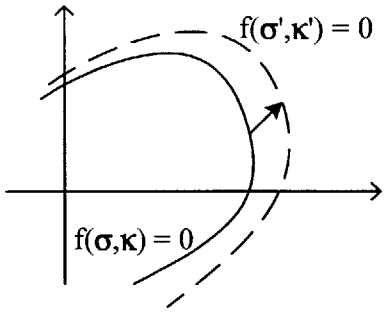

Figure A. 2: Hardening of the yield surface

The two basic assumptions of elastoplasticity are that a) the total strain can be decomposed in an *elastic* and a *plastic* part, i.e.

$$d\varepsilon = d\varepsilon^e + d\varepsilon^p \qquad \text{(A- 2)}$$

and b) the plastic strain direction depends on the stress state (and not the stress increment, as is the case in elasticity). In the simplest case the direction of plastic strain increments coincides with the *gradient of the yield function*:

$$d\varepsilon^p = d\lambda\,(\partial f/\partial\sigma) = d\lambda\, f_{,\sigma}{}^{*} \qquad \text{(A- 3)}$$

where $d\lambda$ is simply a scalar multiplier (*plastic multiplier*). This is called the *associated flow rule*[†]. In the more general case the plastic strain increment has the direction of the gradient of the *plastic potential* g (see Figure A.3):

$$d\varepsilon^p = d\lambda\,(\partial g/\partial\sigma) = d\lambda\, g_{,\sigma}{}^{\ddagger}. \qquad \text{(A- 4)}$$

---

* For brevity $\dfrac{\partial f}{\partial \mathbf{c}} = \dfrac{\partial f}{\partial c_{ij}} = f_{,\mathbf{c}}$

† Associate flow rule is theoretically expected in yielding of materials with crystallic structure, and moreover satisfies the conditions for uniqueness of solution.

‡ The explicit form of the plastic potential does not interest us as long as its gradients are known.

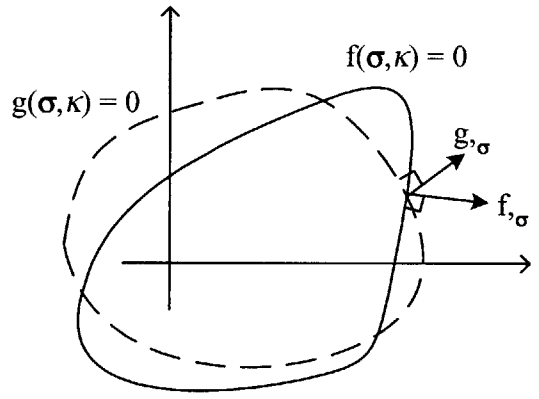

Figure A. 3: Gradient of the yield function and plastic potential

The magnitude of the plastic strains (i.e., the plastic multiplier) is determined using the consistency criterion:

$$df = \partial f/\partial \boldsymbol{\sigma} : d\boldsymbol{\sigma} + \partial f/\partial \boldsymbol{\kappa}\, d\boldsymbol{\kappa} = 0 \qquad \text{(A- 5)}$$

The consistency criterion ensures that the stress state lies at the yield surface at the end of the plastic loading.

The internal variables $\boldsymbol{\kappa}$ represent the loading history of the material and are function of the plastic strains, $\boldsymbol{\kappa} = \boldsymbol{\kappa}(\boldsymbol{\varepsilon}^p)$. At this point the assumption of incremental linearity is made and a scalar, *elasto-plastic modulus H*, is introduced through the relation:

$$d\lambda = \frac{1}{H}\frac{\partial f}{\partial \boldsymbol{\sigma}} : d\boldsymbol{\sigma} \qquad \text{(A- 6)}$$

So the plastic strain and the hardening variable increments depend linearly on the stress increment:

$$d\boldsymbol{\varepsilon}^p = \mathbf{E}^p(\boldsymbol{\sigma},\boldsymbol{\kappa}) : d\boldsymbol{\sigma}\,,$$
$$d\boldsymbol{\kappa} = \boldsymbol{L}(\boldsymbol{\sigma},\boldsymbol{\kappa}) : d\boldsymbol{\sigma} \qquad \text{(A- 7)}$$

It is obvious that a loading increment $\lambda d\boldsymbol{\sigma}$ would produce $\lambda d\boldsymbol{\varepsilon}^p$, $\lambda d\boldsymbol{\kappa}$.

Inserting relations A-3,4,6 into the consistency criterion (A-5), the elasto-plastic modulus is determined as:

$$d\lambda H = -\frac{\partial f}{\partial \kappa} d\kappa = -\frac{\partial f}{\partial \kappa}\frac{\partial \kappa}{\partial \varepsilon^p} d\varepsilon^p = -\frac{\partial f}{\partial \kappa}\frac{\partial \kappa}{\partial \varepsilon^p} d\lambda \frac{\partial g}{\partial \sigma}$$

$$\Rightarrow \qquad H = -\frac{\partial f}{\partial \kappa}\frac{\partial \kappa}{\partial \varepsilon^p}\frac{\partial g}{\partial \sigma} = -\frac{\partial f}{\partial \kappa_i}\frac{\partial \kappa_i}{\partial \varepsilon^p_{jk}}\frac{\partial g}{\partial \sigma_{jk}} \qquad \text{(A- 8)}$$

➢ For stress-driven tests (given loading increment $d\boldsymbol{\sigma}$) the plastic multiplier is

$$d\lambda = \frac{1}{H}\frac{\partial f}{\partial \boldsymbol{\sigma}} : d\boldsymbol{\sigma} \qquad \text{(A- 9)}$$

The strain increment is

$$d\boldsymbol{\varepsilon} = d\boldsymbol{\varepsilon}^e + d\boldsymbol{\varepsilon}^p = \mathbf{D}^{-1}\, d\boldsymbol{\sigma} + d\lambda\, g_{,\boldsymbol{\sigma}}\,, \qquad \text{(A- 10)}$$

where **D** is the fourth order *elasticity stiffness tensor*. The change in hardening parameters is:

$$d\boldsymbol{\kappa} = d\lambda\, \boldsymbol{\kappa}_{,\varepsilon^p}\, g_{,\boldsymbol{\sigma}} \qquad \text{(A- 11)}$$

It can be seen that in such case the *tangent elasto-plastic compliance tensor* is

$$\mathbf{D}^{-1}_{ep} = \mathbf{D}^{-1} + \frac{1}{H}\frac{\partial f}{\partial \boldsymbol{\sigma}} \otimes \frac{\partial g}{\partial \boldsymbol{\sigma}} \qquad \text{(A- 12)}$$

and that in ideal plasticity (or critical state) where $H = 0$ the plastic strain increment remains undetermined.

➢ In strain-controlled tests ($d\boldsymbol{\varepsilon}$ given) the stress increment can be expressed as follows

$$d\boldsymbol{\sigma} = \mathbf{D} : d\boldsymbol{\varepsilon}^{e} = \mathbf{D} : (d\boldsymbol{\varepsilon} - d\boldsymbol{\varepsilon}^{p}) = \mathbf{D} : (d\boldsymbol{\varepsilon} - d\lambda\, g_{,\sigma}) = \mathbf{D} : (d\boldsymbol{\varepsilon} - \frac{1}{H}(f_{,\sigma} : d\boldsymbol{\sigma})\, g_{,\sigma}) \quad \Rightarrow$$

$$H\, d\boldsymbol{\sigma} + f_{,\sigma} : \mathbf{D} : g_{,\sigma}\, d\boldsymbol{\sigma} = H\, \mathbf{D} : d\boldsymbol{\varepsilon} \quad \Rightarrow$$

$$d\boldsymbol{\sigma} = \frac{H\, \mathbf{D} : d\boldsymbol{\varepsilon}}{H + f_{,\sigma} : \mathbf{D} : g_{,\sigma}} \tag{A- 13}$$

It can be seen that the plastic multiplier and the *elasto-plastic tangent stiffness tensor** in this case are:

$$d\lambda = \frac{f_{,\sigma} : \mathbf{D} : d\boldsymbol{\varepsilon}}{H + f_{,\sigma} : \mathbf{D} : g_{,\sigma}} \tag{A- 14}$$

$$\mathbf{D}_{ep} = \mathbf{D} - \frac{\mathbf{D} : g_{,\sigma} \otimes f_{,\sigma} : \mathbf{D}}{H + f_{,\sigma} : \mathbf{D} : g_{,\sigma}} \tag{A- 15}$$

In case of ideal plasticity (or critical state) $H = 0 \Rightarrow d\boldsymbol{\sigma} = d\boldsymbol{\varepsilon}^{e} = \mathbf{0}$, $d\boldsymbol{\varepsilon}^{p} = d\boldsymbol{\varepsilon}$

A more detailed algorithm for the numerical integration of the incremental equations is presented found in Appendix D.

A.1.1 Plasticity with linear isotropic elasticity

In isotropic elasticity the stress and strain tensors can be decomposed in a *volumetric* and *deviatoric* part, through the standard linear/tensor algebra formulation

$$\mathbf{c} = \frac{1}{3} c\, \mathbf{1} + \mathrm{dev}(\mathbf{c}) \tag{A- 16}$$

* In non-associated flow the elastoplastic stiffness tensor is NOT symmetric

where $c = \mathrm{tr}(\mathbf{c}) = \mathbf{c} : \mathbf{c}$ and $\mathrm{dev}(\mathbf{c}) = \mathbf{c} - \frac{1}{3} c\,\mathbf{1}$ *

The stress and (infinitesimal) strain tensors can be written:

$$p = \frac{1}{3}\sigma, \qquad \mathbf{s} = \mathrm{dev}(\boldsymbol{\sigma})$$

$$\varepsilon_{vol} = \varepsilon, \qquad \mathbf{e} = \mathrm{dev}(\boldsymbol{\varepsilon})$$

and the decomposition of the stress and strain tensors is:

$$\boldsymbol{\sigma} = p\,\mathbf{1} + \mathbf{s} \tag{A- 17}$$

$$\boldsymbol{\varepsilon} = \frac{1}{3}\varepsilon_{vol}\,\mathbf{1} + \mathbf{e} \tag{A- 18}$$

The stress-strain relation in the elastic domain can be simplified as follows†

$$d\boldsymbol{\sigma} = \lambda\,\mathrm{tr}(d\boldsymbol{\varepsilon})\,\mathbf{1} + 2\mu\,d\boldsymbol{\varepsilon} = (\lambda + \frac{2}{3}\mu)\,d\varepsilon_{vol}\,\mathbf{1} + 2\mu\,d\mathbf{e} \quad \text{also} \quad d\boldsymbol{\sigma} = dp\,\mathbf{1} + d\mathbf{s}$$

therefore $dp = K\,d\varepsilon_{vol}$

$$d\mathbf{s} = 2G\,d\mathbf{e} \tag{A- 19}$$

Accordingly the gradient of the yield function and the plastic flow direction can be decomposed in volumetric and deviatoric components (see Appendix A.3)

$$\boldsymbol{Q} = \frac{1}{3}Q\,\mathbf{1} + \boldsymbol{Q}'$$

$$\boldsymbol{P} = \frac{1}{3}P\,\mathbf{1} + \boldsymbol{P}' \tag{A- 20}$$

where

* $\mathbf{1} = \delta_{ij}$ is the second order unit tensor

† λ, μ are *Lame's* constants, $G = \mu$ is the shear modulus and $K = \lambda + 2/3\,\mu$ is the bulk modulus

$$Q = \frac{\partial f}{\partial p} = f_{,p}\,, \qquad \boldsymbol{Q}' = \frac{\partial f}{\partial \mathbf{s}} = f_{,\mathbf{s}}$$
$$P = \frac{\partial g}{\partial p} = g_{,p}\,, \qquad \boldsymbol{P}' = \frac{\partial g}{\partial \mathbf{s}} = g_{,\mathbf{s}} \tag{A- 21}$$

The relations giving the plastic multiplier are significantly simplified, volumetric and deviatoric parts being separated, e.g.

$$d\lambda = \frac{Q K\, d\varepsilon_{vol} + 2G\,\boldsymbol{Q}' : d\mathbf{e}}{H + Q K P + 2G\,\boldsymbol{Q}' : \boldsymbol{P}'} \tag{A- 22}$$

A.2 Multiple yield surface elasto-plasticity

Many soil models presented in the literature have yield loci comprised of several yield functions (e.g. Lade, 1977; Prevost, 1978; Loret, 1989b).

So if there are n yield functions f_j, $j = 1{:}n$ the elastic domain (i.e. the yield surface) is defined as:

$$f(\boldsymbol{\sigma},\boldsymbol{\kappa}) = \max_j \{f_j(\boldsymbol{\sigma},\boldsymbol{\kappa})\} \le 0 \tag{A- 23}$$

Accordingly n loading criteria exist, one corresponding to each yield function. The vector $\boldsymbol{\kappa}$ contains all the hidden variables for the n yield functions.

For a stress state lying on the yield surface, three cases can be distinguished:

---

* Note: Usually only some components of the second order tensors are involved in calculations (e.g. in principal stress space only three components are non-zero). A useful transformation (described in Appendix A.4) substitutes the double contraction of tensors with scalar product of vectors. Therefore in simplified problem (which is usually the case) the dimension of the problem and the computations involved are reduced significantly.

Case 1:

$(f_i(\boldsymbol{\sigma}) = 0 \wedge f_{i,\boldsymbol{\sigma}} : d\boldsymbol{\sigma} > 0)$ AND

$(f_j(\boldsymbol{\sigma}) < 0$ OR $(f_j(\boldsymbol{\sigma}) = 0 \wedge f_{j,\boldsymbol{\sigma}} : d\boldsymbol{\sigma} \leq 0))$ $(j = 1{:}n, j \neq i)$

In this case only one yield surface is active; the plastic multiplier for the (unique) plastic strain increment is determined from the consistency condition of this yield function. This does not necessarily mean that only the active yield function hardens (or softens), since the hardening variables controlling the size of other yield functions may have hardening rules that depend on the total plastic strain. The formulation is exactly the same as in the previous section except that yield function f and plastic potential g are substituted by those of the active yield surface, namely f_i, g_i.

For instance, the plastic multiplier in a stress-controlled test would be given by

$$d\lambda = d\lambda_i = \frac{1}{H_i} \frac{\partial f_i}{\partial \boldsymbol{\sigma}} : d\boldsymbol{\sigma} \tag{A- 24}$$

while the plastic strain is

$$d\boldsymbol{\varepsilon}^p = d\boldsymbol{\varepsilon}_i^p = d\lambda_i \, g_{i,\boldsymbol{\sigma}} \tag{A- 25}$$

$$d\kappa_r = d\lambda_i \, L_{ri} \tag{A- 26}$$

Note that the yielding (and hardening) of just one mechanism does not necessarily mean that the rest of the yield functions remain stationary. This is the case only when independent mechanisms exist (this means that matrix **L** is diagonal). In the opposite case there is latent hardening of the inactive yield surfaces. Such case is referred to as dependent mechanisms, and one such example is when the hardening parameters depend on the total plastic strain.

Case 2:

$(f_i(\boldsymbol{\sigma}) = 0 \wedge f_{i,\boldsymbol{\sigma}} : d\boldsymbol{\sigma} > 0)$ AND $(i = a(k), k = 1{:}m, m > 1)$

$(f_j(\boldsymbol{\sigma}) < 0$ OR $(f_j(\boldsymbol{\sigma}) = 0 \wedge f_{j,\boldsymbol{\sigma}} : d\boldsymbol{\sigma} \leq 0))$ $(j = 1{:}n, j \neq i)$

In this case m (more than one) yield mechanisms are active. The theory of multi-mechanisms as described by Loret (1989b) supposes that the plastic strain increment consists of plastic strain contributed by each active yield surface. Therefore

$$d\boldsymbol{\varepsilon}^p = \sum_{k=1}^{m} d\lambda_{a(k)} \frac{\partial g_{a(k)}}{\partial \boldsymbol{\sigma}} = d\lambda_i \, g_{i,\boldsymbol{\sigma}} \quad * \qquad \text{(A- 27)}$$

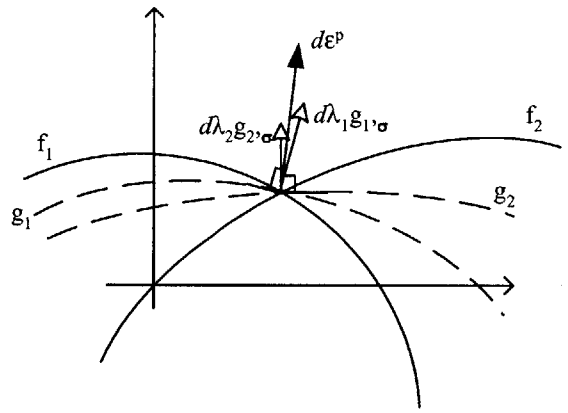

Figure A. 4: Plastic flow for multiple yielding mechanisms

There are m unknown plastic multipliers (scalars) to be determined, via the consistency criteria of the m active yield surfaces:

$$df_i = 0 \qquad \Rightarrow \qquad \partial f_i/\partial \boldsymbol{\sigma} : d\boldsymbol{\sigma} + \partial f_i/\partial \boldsymbol{\kappa}\, d\boldsymbol{\kappa} = 0 \qquad \text{(A- 28)}$$

Using the gradient of the i-th yield surface

$$f_{i,\boldsymbol{\sigma}} = \partial f_i/\partial \boldsymbol{\sigma} \qquad \text{(A- 29)}$$

and the hardening rules for the hardening parameters

* Summation over index i is implied. Note that i does not run from 1 to n, but assumes only specific values that correspond to the active yield surfaces.

$$d\kappa_r = L_{ri}\, d\lambda_i \qquad (r = 1{:}l \text{ number of hardening variables}) \qquad \text{(A- 30)}$$

the consistency criteria can be recast in the form

$$\begin{aligned} & f_{i,\sigma} : \mathbf{D} : (d\varepsilon - d\lambda_j\, g_{j,\sigma}) + \partial f_i/\partial \kappa_r\, L_{rj}\, d\lambda_j = 0 \qquad (i, j = a(k)) \\ \Rightarrow \quad & (f_{i,\sigma} : \mathbf{D} : g_{j,\sigma} + h_{ij})\, d\lambda_j = f_{i,\sigma} : \mathbf{D} : d\varepsilon \qquad \text{(A- 31)} \end{aligned}$$

where $h_{ij} = \partial f_i/\partial \kappa_r\, L_{rj}$ (generalized elasto-plastic moduli)

These represent m linear equation which can be solved for the unknown plastic multipliers*. More details on the existence and uniqueness of the solution of the equations (inversion of $f_{i,\sigma} : \mathbf{D} : g_{j,\sigma} + h_{ij}$) are given by Loret (1989b).

Case 3:

$$(f_j(\sigma) < 0 \text{ OR } (f_j(\sigma) = 0 \wedge f_{j,\sigma} : d\sigma \le 0)) \qquad (j = 1{:}n)$$

In this case only none of the yield surfaces is active and the increment corresponds to unloading (i.e. elastic behavior).

A.3 Decomposition in Volumetric and Deviatoric components

The gradient of the yield function is written with the help of the deviatoric decomposition†:

$$\boldsymbol{Q} = \frac{\partial f}{\partial \boldsymbol{\sigma}} = \frac{\partial f}{\partial p}\frac{\partial p}{\partial \boldsymbol{\sigma}} + \frac{\partial f}{\partial \mathbf{s}} : \frac{\partial \mathbf{s}}{\partial \boldsymbol{\sigma}} = \frac{1}{3}\frac{\partial f}{\partial p}\mathbf{1} + \frac{\partial f}{\partial \mathbf{s}} : \frac{\partial(\boldsymbol{\sigma} - p\mathbf{1})}{\partial \boldsymbol{\sigma}} = \frac{1}{3}\frac{\partial f}{\partial p}\mathbf{1} + \frac{\partial f}{\partial \mathbf{s}} : (\mathbf{I} - \mathbf{1}\otimes\mathbf{1}) = \frac{1}{3}\frac{\partial f}{\partial p}\mathbf{1} + \frac{\partial f}{\partial \mathbf{s}}$$

where the volumetric and deviatoric components of the yield surface gradient are written:

---

* In case of stress controlled tests the system of linear equation reads $h_{ij}\, d\lambda_j = f_{i,\sigma} : d\boldsymbol{\sigma}$

† $\mathbf{1}$, $\mathbf{I}$ are the second and fourth order unit tensors respectively

$$Q = \frac{\partial \mathrm{f}}{\partial p} = \mathrm{f}_{,p}\,, \qquad \boldsymbol{Q}' = \frac{\partial \mathrm{f}}{\partial \mathbf{s}} = \mathrm{f}_{,\mathbf{s}}$$

The gradient of the plastic potential can be similarly decomposed

$$P = \frac{\partial \mathrm{g}}{\partial p} = \mathrm{g}_{,p}\,, \qquad \boldsymbol{P}' = \frac{\partial \mathrm{g}}{\partial \mathbf{s}} = \mathrm{g}_{,\mathbf{s}}$$

Consequently all the tensorial operations are decomposed into volumetric and deviatoric components

- $d\boldsymbol{\varepsilon}^p = d\lambda\,\mathbf{P} \quad \Rightarrow \quad d\varepsilon_{vol} = d\lambda\,P$ and $d\mathbf{e} = d\lambda\,\mathbf{P}'$

- $$\frac{\partial \mathrm{f}}{\partial \boldsymbol{\sigma}} : d\boldsymbol{\sigma} = \frac{1}{3}\frac{\partial \mathrm{f}}{\partial p}\mathbf{1} : d\boldsymbol{\sigma} + \frac{\partial \mathrm{f}}{\partial \mathbf{s}} : d\boldsymbol{\sigma} = \frac{1}{3}\frac{\partial \mathrm{f}}{\partial p} 3\,dp + \frac{\partial \mathrm{f}}{\partial \mathbf{s}} : (d\mathbf{s} + \frac{1}{3}\,p\mathbf{1}) = \frac{\partial \mathrm{f}}{\partial p}dp + \frac{\partial \mathrm{f}}{\partial \mathbf{s}} : d\mathbf{s}$$

- $$d\lambda = \frac{\mathrm{f}_{,\boldsymbol{\sigma}} : \mathbf{D} : d\boldsymbol{\varepsilon}}{H + \mathrm{f}_{,\boldsymbol{\sigma}} : \mathbf{D} : \mathrm{g}_{,\boldsymbol{\sigma}}} = \frac{(\frac{1}{3}\mathrm{f}_{,p}\mathbf{1} + \mathrm{f}_{,\mathbf{s}}) : [(K - \frac{2}{3}\mu)\mathbf{1}\otimes\mathbf{1} + 2\mu\,\mathbf{I}] : (\frac{1}{3}\,d\varepsilon\,\mathbf{1} + d\mathbf{e})}{H + (\frac{1}{3}\mathrm{f}_{,p}\mathbf{1} + \mathrm{f}_{,\mathbf{s}}) : [(K - \frac{2}{3}\mu)\mathbf{1}\otimes\mathbf{1} + 2\mu\,\mathbf{I}] : (\frac{1}{3}\mathrm{g}_{,p}\mathbf{1} + \mathrm{g}_{,\mathbf{s}})}$$

which after some manipulation becomes

$$d\lambda = \frac{\mathrm{f}_{,p}\,K\,d\varepsilon_{vol} + 2\mu\,\mathrm{f}_{,\mathbf{s}} : d\mathbf{e}}{H + \mathrm{f}_{,p}\,K\,\mathrm{g}_{,p} + 2\mu\,\mathrm{f}_{,\mathbf{s}} : \mathrm{g}_{,\mathbf{s}}} = \frac{Q\,K\,d\varepsilon_{vol} + 2\mu\,\boldsymbol{Q}' : d\mathbf{e}}{H + Q\,K\,P + 2\mu\,\boldsymbol{Q}' : \boldsymbol{P}'} \qquad \text{(A- 32)}$$

A.3.1 Relations with triaxial stress space variables

Most published constitutive models for soils have been presented in a reduced triaxial stress space by introducing the variable

$$q = \sqrt{3J_2} = \sqrt{\tfrac{3}{2}\mathbf{s} : \mathbf{s}}\,, \qquad \text{(A- 33)}$$

where J_2 is the second invariant of the deviatoric stress tensor. This variable is a direct measure of deviation from the hydrostatic axis (equivalent shear stress). In analogous fashion, equivalent deviatoric strain increment can be defined as:

$$d\varepsilon_q = \sqrt{\tfrac{2}{3}\, d\mathbf{e} : d\mathbf{e}} \tag{A- 34}$$

Hence, the deviatoric stress-strain relations in the reduced triaxial space can be written:

$$dq^e = \sqrt{\tfrac{3}{2}\,\mathbf{s} : \mathbf{s}} = \sqrt{\tfrac{3}{2}(2\mu\, d\mathbf{e}) : (2\mu\, d\mathbf{e})} = 3\mu\sqrt{\tfrac{2}{3}\, d\mathbf{e} : d\mathbf{e}} = 3\ \mu\ d\varepsilon_q^{\,e} \tag{A- 35}$$

The expression for the loading criterion can be reduced to its triaxial space form as follows:

$$dq = \frac{\partial q}{\partial J_2}\frac{\partial J_2}{\partial \mathbf{s}} : d\mathbf{s} = \frac{3}{2\sqrt{3J_2}}\mathbf{s} : d\mathbf{s}$$

$$\Rightarrow \quad \frac{\partial \mathrm{f}}{\partial \boldsymbol{\sigma}} : d\boldsymbol{\sigma} = \frac{\partial \mathrm{f}}{\partial p}dp + \frac{\partial \mathrm{f}}{\partial \mathbf{s}} : d\mathbf{s} = \frac{\partial \mathrm{f}}{\partial p}dp + \frac{\partial \mathrm{f}}{\partial q}\frac{\partial q}{\partial J_2}\frac{\partial J_2}{\partial \mathbf{s}} : d\mathbf{s} = \frac{\partial \mathrm{f}}{\partial p}dp + \frac{\partial \mathrm{f}}{\partial q}\frac{3}{2\sqrt{3J_2}}\mathbf{s} : d\mathbf{s}$$

$$\Rightarrow \quad \frac{\partial \mathrm{f}}{\partial \boldsymbol{\sigma}} : d\boldsymbol{\sigma} = \frac{\partial \mathrm{f}}{\partial p}dp + \frac{\partial \mathrm{f}}{\partial q}dq \tag{A- 36}$$

The flow rule for the triaxial deviatoric strain is:

$$d\varepsilon_q = \sqrt{\tfrac{2}{3}\, d\mathbf{e} : d\mathbf{e}} = d\lambda\sqrt{\tfrac{2}{3}\,\mathbf{P}' : \mathbf{P}'} = d\lambda\, P_q \tag{A- 37}$$

A.4 Transformed variables

In order to implement the constitutive equations efficiently in a computer program it is convenient to transform efficiently, the deviatoric part of symmetric second order tensors into vectors, while the double contraction of tensors can be replaced by the dot product (following Kavvadas, 1982). The vectors are constructed in that way so that their length decreases when some components of the tensor are zero. Thus, this method exploits the reduced stress space of specific problems.

Let **a**, **b** be two symmetric second order tensors and dev(**a**), dev(**b**) their deviatoric counterparts.

The double contraction of dev(**a**) and dev(**b**) is:

$$\text{dev}(\mathbf{a}) : \text{dev}(\mathbf{b}) = \begin{bmatrix} a_x - \frac{a}{3} & a_{xy} & a_{xz} \\ a_{xy} & a_y - \frac{a}{3} & a_{yz} \\ a_{xz} & a_{yz} & a_z - \frac{a}{3} \end{bmatrix} : \begin{bmatrix} b_x - \frac{b}{3} & b_{xy} & b_{xz} \\ b_{xy} & b_y - \frac{b}{3} & b_{yz} \\ b_{xz} & b_{yz} & b_z - \frac{b}{3} \end{bmatrix} =$$

$$= (a_x - \frac{a}{3})(b_x - \frac{b}{3}) + (a_y - \frac{a}{3})(b_y - \frac{b}{3}) + (a_z - \frac{a}{3})(b_z - \frac{b}{3}) + 2a_{xy}b_{xy} + 2a_{xz}b_{xz} + 2a_{yz}b_{yz} =$$

$$= a_x b_x + a_y b_y + a_z b_z - \frac{ab}{3} + 2a_{xy}b_{xy} + 2a_{xz}b_{xz} + 2a_{yz}b_{yz} \qquad \text{(A- 38)}$$

If we transform the tensors according to the rule

$$\mathbf{c} = c_{ij} \rightarrow \boldsymbol{C} = [\frac{1}{\sqrt{6}}(2c_y - c_x - c_z),\ \frac{1}{\sqrt{2}}(c_z - c_x),\ \sqrt{2}c_{xy},\ \sqrt{2}c_{yz},\ \sqrt{2}c_{zx}]^T \qquad \text{(A- 39)}$$

Then the scalar product of the vectors $\boldsymbol{A}\cdot\boldsymbol{B}$ is (A- 40)

$$\frac{1}{6}(2a_y - a_x - a_z)(2b_y - b_x - b_z) + \frac{1}{2}(a_z - a_x)(b_z - b_x) + 2a_{xy}b_{xy} + 2a_{yz}b_{yz} + 2a_{zx}b_{zx} =$$

$$= \frac{2}{3}(a_x b_x + a_y b_y + a_z b_z) - \frac{1}{3}(a_x b_y + a_x b_z + a_y b_x + a_y b_z + a_z b_x + a_z b_y) + 2a_{xy}b_{xy} + 2a_{yz}b_{yz} + 2a_{zx}b_{zx}$$

By comparison of equations A-38 and A-40, it can be seen that

$$\text{dev}(\mathbf{a}) : \text{dev}(\mathbf{b}) = \boldsymbol{A}\cdot\boldsymbol{B} \qquad \text{(A- 41)}$$

It is also noted that

$$\text{dev}(\mathbf{c}) : \text{dev}(\mathbf{c}) = \boldsymbol{C}\cdot\boldsymbol{C} = 2J_{2,\mathbf{c}} \qquad \text{(A- 42)}$$

where $J_{2,\mathbf{c}}$ is the second invariant of the deviator of tensor **c**.

Stress (σ, **s**)	Strain (ε, **e**)	Yield Surface Gradient (Q, **Q'**)	Plastic Flow Direction (P, **P'**)
$\sigma = \frac{\sigma_x + \sigma_y + \sigma_z}{3}$	$\varepsilon = \varepsilon_x + \varepsilon_y + \varepsilon_z$	$Q = Q_x + Q_y + Q_z$	$P = P_x + P_y + P_z$
$S_1 = \frac{2\sigma_y - \sigma_x - \sigma_z}{\sqrt{6}}$	$E_1 = \frac{2\varepsilon_y - \varepsilon_x - \varepsilon_z}{\sqrt{6}}$	$Q_1 = \frac{2Q_y - Q_x - Q_z}{\sqrt{6}}$	$P_1 = \frac{2P_y - P_x - P_z}{\sqrt{6}}$
$S_2 = \frac{\sigma_z - \sigma_x}{\sqrt{2}}$	$E_2 = \frac{\varepsilon_z - \varepsilon_x}{\sqrt{2}}$	$Q_2 = \frac{Q_z - Q_x}{\sqrt{2}}$	$P_2 = \frac{P_z - P_x}{\sqrt{2}}$
$S_3 = \sqrt{2}\,\sigma_{xy}$	$E_3 = \sqrt{2}\,\varepsilon_{xy}$	$Q_3 = \sqrt{2}\,Q_{xy}$	$P_3 = \sqrt{2}\,P_{xy}$
$S_4 = \sqrt{2}\,\sigma_{yz}$	$E_4 = \sqrt{2}\,\varepsilon_{yz}$	$Q_4 = \sqrt{2}\,Q_{yz}$	$P_4 = \sqrt{2}\,P_{yz}$
$S_5 = \sqrt{2}\,\sigma_{zx}$	$E_5 = \sqrt{2}\,\varepsilon_{zx}$	$Q_5 = \sqrt{2}\,Q_{zx}$	$P_5 = \sqrt{2}\,P_{zx}$

Table A. 1: Transformed tensorial measures used (after Kavvadas, 1982)

In many practical problems some components of the stress deviator are zero:

- In *plane strain* problems $\sigma_{zx} = \sigma_{yz} = 0$ so only C_1, C_2, C_3 are non-zero
- In *triaxial* cell laboratory tests $\sigma_x = \sigma_y$ and all shear stresses are zero, so only C_1 is non-zero. Note that

$$S_1 = \sqrt{\frac{2}{3}}\,q \qquad \text{and} \qquad E_1 = \sqrt{\frac{3}{2}}\,\varepsilon_q \tag{A- 43}$$

Appendix B: Formulation of the Barcelona Basic Model (BBM) for unsaturated soils

This appendix contains the formulation for the Barcelona Basic Model (e.g. Alonso *et al.*, 1990), a rational extension of the Modified Cam Clay into the unsaturated soil mechanics domain. This Appendix describes the original formulation as presented by Alonso *et* al. (1990) using triaxial stress space variables.

The model uses three stress state variables, two hardening parameters and a total of nine material constants (with the addition of specific volume).
The stress state variables are defined as:

net mean stress $p = (\sigma_1 + 2\sigma_3)/3 - u_a$ (B- 1)

shear stress $q = \sigma_1 - \sigma_3$ (B- 2)

matric suction $s = u_a - u_w$ (B- 3)

where u_a, u_w are the pressures in the air and the water phases.

The hardening parameters are:

pre-consolidation stress for saturated conditions p_0^*

maximum past suction s_0

The yield function is expressed by the slope of the Critical State Line, M, (same as in MCC) and effective preconsolidation stress at different suction levels, which makes use of compression ratio at different suction levels $\lambda(s)$ and the reference stress p_c. The compression ratio at different suction levels is controlled by two parameters r and β, which control the limiting value (minimum) of compression ratio at high values of suction and the rate of evolution of $\lambda(s)$ respectively (see eqn. B.7 for details). Increases

in apparent cohesion are controlled by parameter, k. Hardening of the hidden variables p_0^*, s_0 requires $\lambda(0)$ and λ_s respectively (compression ratios in e-ln$p$ space, at saturation and for changes in suction). For modeling the elastic behavior the model requires three parameters, namely the swelling ratio in e-ln$p$ space κ, (constant) elastic shear modulus, G (these two are the same as in MCC) and swelling ratio associated with reversible changes in suction κ_s. The parameters β [$LM^{-1}T^2$], p_c [$L^{-1}MT^{-2}$], G [$L^{-1}MT^{-2}$] are dimensional and consistent units must be used in the BBM formulation.

B.1 Yield function

The Barcelona Basic Model has two independent yield surfaces (see Figure B.1):
The first yield function is an ellipse (in p-q stress space) enlarged according to the suction level (see Figure B.2). It crosses the $p = 0$ axis at $p = -p_s$ and $p = p_0$. In the limiting condition of full saturation (i.e. $s = 0$) it reduces to the familiar MCC yield surface. The hardening variable p_0^* is associated with the size of this yield function.

$$f_1(p, q, s, p_0^*) \equiv q^2 - M^2 (p + p_s)(p_0 - p) = 0 \tag{B- 4}$$

where

$$p_s = k\, s \tag{B- 5}$$

$$\frac{p_0}{p_c} = \left(\frac{p_o^*}{p_c} \right)^{\frac{\lambda(0)-\kappa}{\lambda(s)-\kappa}} \tag{B- 6}$$

$$\lambda(s) = \lambda(0)\left[(1-r)e^{-\beta s} + r\right] \tag{B- 7}$$

The second yield surface is merely a plane of constant suction, and is associated with hardening parameter s_0.

$$f_2(s, s_0) \equiv s - s_0 = 0 \tag{B- 8}$$

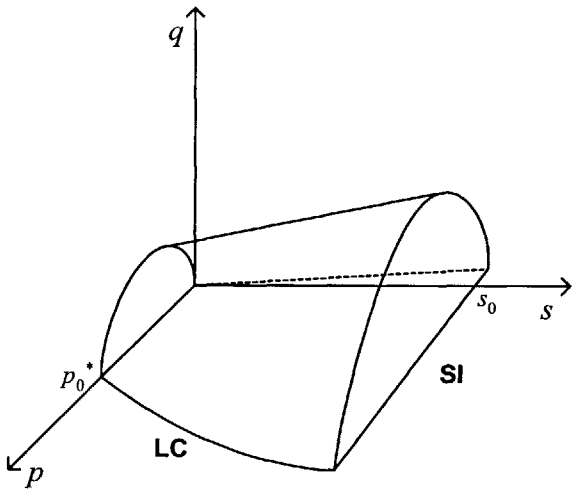

Figure B. 1: Yield surfaces in *p-q-s* space

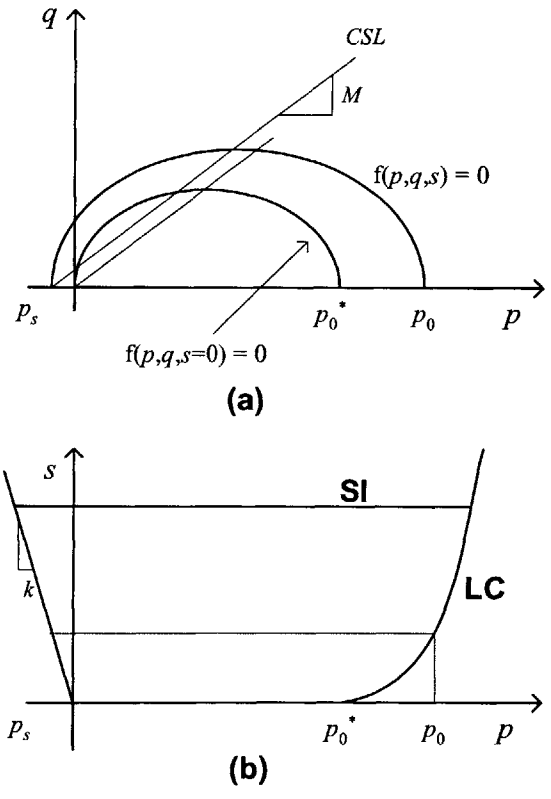

Figure B. 2: Projection of the 3-D yield surface on planes of a) constant suction, and b) on the zero deviatoric stress plane

The gradients of the yield functions with respect to the stress variables are:

For yield function f_1:

$$f_{1,p} = M^2(p - p_0 + p_s) \tag{B- 9}$$

$$f_{1,q} = 2\,q \tag{B- 10}$$

$$f_{1,s} = \frac{\partial f_1}{\partial s} = \frac{\partial f_1}{\partial p_s}\frac{\partial p_s}{\partial s} + \frac{\partial f_1}{\partial p_0}\frac{\partial p_0}{\partial s} = M^2(p - p_0) - M^2(p + p_s)\frac{\partial p_0}{\partial s} \tag{B- 11}$$

by introducing $\chi = \frac{\lambda(0) - \kappa}{\lambda(s) - \kappa}$, the last term can be written as (B- 12):

$$\frac{\partial p_0}{\partial s} = \frac{\partial p_0}{\partial \chi}\frac{\partial \chi}{\partial \lambda(s)}\frac{\partial \lambda(s)}{\partial s} = p_0 \ln\frac{p_0^*}{p_c}\frac{-(\lambda(0) - \kappa)}{(\lambda(s) - \kappa)^2}\lambda(0)(1 - r)(-\beta)e^{-\beta s} =$$

$$= p_0 \ln\frac{p_0^*}{p_c}\frac{\chi}{\lambda(s) - \kappa}(\lambda(s) - r\,\lambda(0))$$

For yield function f_2:

$$f_{2,p} = 0 \tag{B- 13}$$

$$f_{2,q} = 0 \tag{B- 14}$$

$$f_{2,s} = 1 \tag{B- 15}$$

The loading-unloading criterion (for stress states on the j-th yield surface) is

$$f_{j,p}\,dp + f_{j,q}\,dq + f_{j,s}\,ds \tag{B- 16}$$

B.2 Flow rule

In the original formulation (Alonso *et al.*, 1990) a non-associated flow is considered in order to counter effect the fact that Modified Cam Clay overpredicts K_0 values in one-

dimensional consolidation (following Ohmaki, 1982). The gradients of the plastic potential are:

For plastic potential g_1:

$$g_{1,p} = M^2(p - p_0 + p_s) \tag{B- 17}$$

$$g_{1,q} = 2\,q\,\alpha \tag{B- 18}$$

where $$\alpha = \frac{M(M-9)(M-3)}{9(6-M)} \frac{1}{1-\frac{\kappa}{\lambda(0)}} \tag{B- 19}$$

For plastic potential g_2:

$$g_{2,p} = 1 \tag{B- 20}$$

$$g_{2,q} = 0 \tag{B- 21}$$

B.3 Hardening rules

Both hidden variables harden according to volumetric hardening rules, that are triggered by the total volumetric plastic strain. The incremental form of these hardening rules are as follows:

For equivalent preconsolidation pressure at saturation:

$$dp_0^* = \frac{v}{\lambda(0)-\kappa} p_0^*\, d\varepsilon_{vol}^p \tag{B- 22}$$

For maximum suction:

$$ds_0 = \frac{v}{\lambda_s - \kappa_s}(s_0 + p_{at})\, d\varepsilon_{vol}^p \tag{B- 23}$$

where p_{at} is the atmospheric pressure.

Elastoplastic moduli:

The two yielding mechanisms are independent. Therefore there is no latent hardening (i.e. $L_{12} = L_{21} = 0$ in eqn. A-26)

The elasto-plastic moduli are defined through the following relations.

$$H_1 = h_{11} = -\frac{\partial \mathrm{f}_1}{\partial p_0^*}\frac{\partial p_0^*}{\partial \varepsilon_{vol}^p}\frac{\partial \mathrm{g}_1}{\partial p} = -\frac{\partial \mathrm{f}_1}{\partial p_0}\frac{\partial p_0}{\partial p_0^*}\frac{\partial p_0^*}{\partial \varepsilon_{vol}^p}\frac{\partial \mathrm{g}_1}{\partial p} \tag{B- 24}$$

since $\dfrac{\partial \mathrm{f}_1}{\partial p_0} = -M^2(p + p_s)$, $\dfrac{\partial p_0}{\partial p_0^*} = \dfrac{p_0}{p_0^*}\chi$ and $\dfrac{\partial p_0^*}{\partial \varepsilon_{vol}^p} = p_0^*\dfrac{v}{\lambda(0) - \kappa}$

we obtain the formula:

$$H_1 = M^4(p + p_s)\frac{p_0 v}{\lambda(s) - \kappa}(2p - p_0 + p_s) \tag{B- 25}$$

$$H_2 = h_{22} = -\frac{\partial \mathrm{f}_2}{\partial s_0}\frac{\partial s_0}{\partial \varepsilon_{vol}^p}\frac{\partial \mathrm{g}_2}{\partial p} = \frac{v(s + p_{at})}{\lambda_s - \kappa_s} \tag{B- 26}$$

The plastic multiplier(s) is obtained through the plastic consistency criteria (see section B.5)

B.4 Elastic behavior

Isotropic non-linear elasticity is used in the BBM. The tangent stiffness changes in proportion both the net mean pressure and the matric suction (for constant suction the MCC formulas are retrieved). This version also assumes a constant elastic shear modulus, G:

$$d\varepsilon_{vol}^{e} = \frac{\kappa}{v}\frac{dp}{p} + \frac{\kappa_s}{v}\frac{ds}{s+p_{at}} = \frac{dp}{K} + \frac{ds}{K_s} \tag{B- 27}$$

$$d\varepsilon_s^{e} = (1/3G)\, dq \tag{B- 28}$$

B.5 Calculation of plastic multiplier

Since the elastic deformations depend also on the suction increment, the computation of plastic multiplier must be modified from the original formulation found in Appendix A.1 in both stress and strain controlled tests. The elastic incremental equation reads

$$d\boldsymbol{\varepsilon}^{e} = \mathbf{D}^{-1}\, d\boldsymbol{\sigma}^{e} + \boldsymbol{A}\, ds \tag{B- 29}$$

where $\mathbf{D}$ is the fourth order elasticity tensor and $\boldsymbol{A}$ is a second order tensor which links the elastic deformations due to changes in suction:

$$d\varepsilon_{ij}^{s} = A_{ij}\, ds \tag{B- 30}$$

in our case $A_{ij} = \frac{1}{3K_s}\mathbf{1}$ (B- 31)

and B-29 simplifies to $d\varepsilon_{vol}^{s} = \frac{ds}{K_s}$ (B- 32)

The plastic multiplier is given by (the indexes of the yield function and the elastoplastic modulus are dropped for brevity, 1 or 2 implied)

$$d\lambda = \frac{1}{H}\left[\frac{\partial \mathrm{f}}{\partial \boldsymbol{\sigma}} : d\boldsymbol{\sigma} + \frac{\partial \mathrm{f}}{\partial s} : ds\right] \tag{B- 33}$$

Stress controlled tests

In stress controlled tests (dσ and ds known) the total strain increments are

$$d\boldsymbol{\varepsilon} = d\boldsymbol{\varepsilon}^e + d\boldsymbol{\varepsilon}^p = \mathbf{D}^{-1}\, d\boldsymbol{\sigma} + A\, ds + d\lambda\, \mathrm{g}_{,\boldsymbol{\sigma}} \tag{B- 34}$$

$$\Rightarrow \quad \begin{cases} d\varepsilon_{vol} = d\varepsilon^e_{vol} + d\varepsilon^p_{vol} = \dfrac{1}{K} dp + \dfrac{1}{K_s} ds + d\lambda \dfrac{\partial \mathrm{g}}{\partial p} \\ d\varepsilon_q = d\varepsilon^e_q + d\varepsilon^p_q = \dfrac{1}{3G} dq + d\lambda \dfrac{\partial \mathrm{g}}{\partial q} \end{cases}$$

Strain controlled tests

In 'strain controlled' tests $d\boldsymbol{\varepsilon}$ and ds are defined. The elastic equations are inverted

$$d\boldsymbol{\sigma}^e = \mathbf{D}\, d\boldsymbol{\varepsilon}^e - \mathbf{D}\, A\, ds \tag{B- 35}$$

Substituting the elastic strain tensor as the difference between the total and plastic strain tensors

$$d\boldsymbol{\sigma} = \mathbf{D}\, (d\boldsymbol{\varepsilon} - d\lambda\, \mathrm{g}_{,\boldsymbol{\sigma}}) - \mathbf{D}\, A\, ds$$

and introducing the plastic multiplier (B- 33)

$$d\boldsymbol{\sigma} = \mathbf{D}\, [d\boldsymbol{\varepsilon} - \frac{1}{H} (\mathrm{f}_{,\boldsymbol{\sigma}} : d\boldsymbol{\sigma} + \mathrm{f}_{,s}\, ds)\, \mathrm{g}_{,\boldsymbol{\sigma}}] - \mathbf{D} : A\, ds$$

we can solve for the stress increments.

$$d\boldsymbol{\sigma} = \frac{\mathbf{D} : d\boldsymbol{\varepsilon} - \dfrac{1}{H} \mathbf{D} : \mathrm{g}_{,\boldsymbol{\sigma}}\, \mathrm{f}_{,s}\, ds - \mathbf{D} : A\, ds}{1 + \dfrac{1}{H} \mathrm{f}_{,\boldsymbol{\sigma}} : \mathbf{D} : \mathrm{g}_{,\boldsymbol{\sigma}}} \tag{B- 36}$$

Therefore the plastic multiplier is

$$d\lambda = \frac{\mathrm{f}_{,\sigma} : \mathbf{D} : d\boldsymbol{\varepsilon} - \frac{1}{H}\mathrm{f}_{,\sigma} : \mathbf{D} : \mathrm{g}_{,\sigma}\, \mathrm{f}_{,s}\, ds - \mathrm{f}_{,\sigma} : \mathbf{D} : \boldsymbol{A}\, ds}{H + \mathrm{f}_{,\sigma} : \mathbf{D} : \mathrm{g}_{,\sigma}} + \frac{1}{H}\mathrm{f}_{,s}\, ds$$

$$\Rightarrow \qquad d\lambda = \frac{\mathrm{f}_{,\sigma} : \mathbf{D} : d\boldsymbol{\varepsilon} + (\mathrm{f}_{,s} - \mathrm{f}_{,\sigma} : \mathbf{D} : \boldsymbol{A})ds}{H + \mathrm{f}_{,\sigma} : \mathbf{D} : \mathrm{g}_{,\sigma}}$$

$$(^{*})\Rightarrow \quad d\lambda = \frac{K Q\, d\varepsilon_{vol} + 3G Q_q\, d\varepsilon_q + \left(\mathrm{f}_{,s} - Q\frac{K}{K_s}\right)ds}{H + K Q P + 3G Q_q P_q} \qquad \text{(B- 37)}$$

* $\mathbf{D} : \boldsymbol{A} = [(K - 2/3\ \mu)\ \mathbf{1}\otimes\mathbf{1} + 2\mu\ \mathbf{I})]: (1/3K_s)\ \mathbf{1} = K/K_s\ \mathbf{1}$

Appendix C: Formulation for the SCC model for structured soils

This appendix describes the formulation of an extended Modified Cam Clay effective stress model for structured soils following the proposals of Gens & Nova (1993). All stresses refer to effective stresses (the prime is dropped for brevity). This model is referred to as Structured Cam Clay (SCC).

The Modified Cam Clay needs four material parameters and one hardening parameter (plus void ratio). The yield function is defined by the slope of the Critical State Line M, and the preconsolidation stress p_0. Hardening of the hidden variable is controlled by λ (compression ratio in e-ln$p$ space). The elastic deformation (non-linear elastic) is controlled by κ (swelling ratio in e-ln$p$ space) and ν (Poisson's ratio). The SCC formulation introduces an additional four material parameters and one additional hardening variable. The hardening variable b, referred to as bond strength, is introduced to control the size of the yield surface (compared to the reference MCC surface), while parameters b_0, a_0 and w are associated with the hardening of variable b and control the magnitude, the rate and the type (i.e. volumetric, deviatoric) of bond degradation, respectively. The fourth additional parameter α links tensile strength with bond strength.

C.1 Yield function

The SCC model uses a single yield function $f(\boldsymbol{\sigma}, p_0, b) = 0$ with two hidden variables. (eq. C- 1):

$$f = q^2 - M^2 (p + p_t)(p_{co} - p) = \frac{3}{2}\mathbf{s} : \mathbf{s} - M^2 (p + \alpha\, b\, p_0)[(1 + b)\, p_0 - p]$$

In p-q stress space this equation represents an ellipse with aspect ratio M, oriented along the isotropic axis ($q = 0$). The yield surface intercepts the isotropic axis at $p = -p_t$ and $p = p_{co}$, corresponding to yield points in hydrostatic tension and compression respectively).

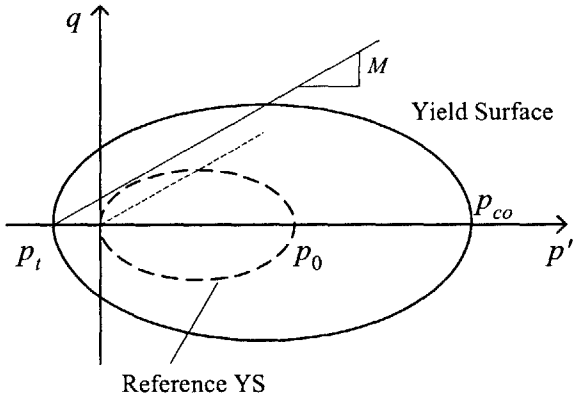

Figure C. 1: Yield function and reference yield surface for extension of MCC for structured soils

The reference yield surface is the familiar MCC ellipse of size p_0.

$$f_r = \frac{3}{2}\mathbf{s} : \mathbf{s} - M^2 p\,(p_0 - p) \qquad \text{(C- 2)}$$

Therefore, the size of the SCC yield surface is $p_t + p_{co} = (1 + \alpha + b)\,p_c$, (i.e. $[1 + \alpha + b]$ times greater than the reference yield locus).

The gradient of the yield locus is (volumetric and deviatoric components)

$$Q = \frac{\partial f}{\partial p} = M^2\,[\,2p + p_t - p_{co}\,] = M^2\,[\,2p + (\alpha\, b - b - 1)p_0\,] \qquad \text{(C- 3)}$$

$$\mathbf{Q}' = \frac{\partial f}{\partial \mathbf{s}} = 3\,\mathbf{s} \qquad \text{(C- 4)}$$

C.2 Flow rule

Associated plasticity is assumed (f = g), therefore the gradient of the plastic potential coincide with those of the yield function (relations C-3, C-4).

$$P = \frac{\partial g}{\partial p} = M^2 \left[2p + (\alpha b - b - 1) p_0 \right] \qquad \text{(C-3bis)}$$

$$\mathbf{P'} = \frac{\partial g}{\partial \mathbf{s}} = 3\,\mathbf{s} \qquad \text{(C-4bis)}$$

C.3 Hardening rules

The hardening rule for the preconsolidation pressure is the common volumetric hardening used in many models, including the original and modified Cam Clay. In its incremental form reads as

$$dp_0 = \frac{1+e_0}{\lambda - \kappa} p_0 \, d\varepsilon^p_{vol} = \frac{1+e_0}{\lambda - \kappa} p_0 \, P \, d\lambda \qquad \text{(C- 5)}$$

For the bond strength the hardening rule (in incremental form) [*] is

$$db = -a_0 \, b \, d\varepsilon^p = -a_0 \, b \, [w \, |d\varepsilon^p{}_{vol}| + (1 - w) \, |d\varepsilon^p{}_q|] \qquad \text{(C- 6)}$$

where w is a weight parameter that controls the type of destructuration ($w = 1$, volumetric destructuration; $w = 0$, deviatoric destructuration)

The elastoplastic modulus is computed as [†]

---

[*] Alternatively $d\varepsilon^p = [w \, (d\varepsilon^p{}_{vol})^2 + (1 - w) \, (d\varepsilon^p{}_q)^2]^{1/2}$ can be used as measure of the effective plastic strain

[†] It can be seen that $\frac{\partial b}{\partial \mathbf{e}^p} : \frac{\partial g}{\partial \mathbf{s}} = \frac{\partial b}{\partial \varepsilon^p_q} \frac{\partial \varepsilon^p_q}{\partial \mathbf{e}^p} : \mathbf{P'} = 1 \cdot \frac{2}{3\varepsilon^p_q} \mathbf{e}^p : \mathbf{P'} = \frac{2 d\lambda}{3\varepsilon^p_q} \mathbf{P'} : \mathbf{P'} = P_q = \frac{\partial g}{\partial q}$

$$H = -\frac{\partial f}{\partial p_0}\frac{\partial p_0}{\partial \varepsilon^p}\frac{\partial g}{\partial \sigma} - \frac{\partial f}{\partial b}\frac{\partial b}{\partial \varepsilon^p}\frac{\partial g}{\partial \sigma} = H_d + H_b \qquad \text{(C- 7)}$$

$$H_d = M^2\,[\alpha\, b\,(p_{co} - p) + (1 + b)(p + p_t)]\frac{1+e_0}{\lambda - \kappa}\,p_0\,P \qquad \text{(C- 8)}$$

$$H_b = M^2\,p_0\,[\alpha\,(p_{co} - p) + (p + p_t)]\,(-a_0\,b\,)\,[w\ \mathrm{sign}(d\varepsilon^p_{vol})\,P + (1-w)P_q] \qquad \text{(C- 9)}$$

It can be clearly seen that the elastoplastic modulus consists of two parts, namely a frictional and a bonding part. According to this formulation the effects are additive. Note also that the hardening behavior on the "wet" site and softening behavior on the "dry" side is no longer valid. The actual behavior (hardening/softening) depends largely on the degree of bonding (especially in the relatively intact states).

C.4 Elastic behavior

The elastic part for the SCC model remains the same as used in MCC. Isotropic behavior is assumed with the tangent elastic bulk modulus is chosen proportional to the mean stress. For the shear modulus, constant Poisson's ratio is assumed, while other simple choices* include constant shear modulus or shear modulus proportional to p_c.

$$dp = K_t\,d\varepsilon^e_{vol} = \frac{1+e_0}{\kappa}\,p\,d\varepsilon^e_{vol} \qquad \text{(C- 10)}$$

$$d\mathbf{s} = 2G\,d\mathbf{e}^e = \frac{3(1-2\nu)}{1+\nu}K_t\,d\mathbf{e}^e \qquad \text{(C- 11)}$$

* Assuming constant Poisson's ratio gives shear modulus G proportional to confining pressure p. This is not acceptable theoretically since it violates conservation of energy in closed cyclic loading (e.g. Muir Wood, 1990). Constant shear modulus implies variable Poisson's ratio, which in turn may achieve values outside the acceptable elastic limits. More refined approaches have been published in the literature: Borja and Tamagnini (1998) proposed a conservative hyperelastic formulation, while Pestana (1994) proposed formulas where both bulk and shear modulus are function of the mean stress, p and the equivalent deviatoric stress, q.

Appendix D: Algorithms for Numerical Implementation of Elasto-Plastic models

This appendix contains the algorithms for strain- and stress-driven single element tests, within the framework of hardening elasto-plasticity with single or multiple yield surfaces. The algorithm is implemented using MATLAB scripts. Note that tensors quantities were used in the theoretical development and vectors and matrices in the computer code.

General routines:

Function **MFYield.m** returns the value of the yield function for at a specific stress state and set of hardening parameters.

MdFdS.m and **MdgdS.m** return an array with the gradient of the yield surface and the plastic potential respectively at a specified stress state.

MElast.m returns the elasticity or the elastic compliance matrix.

The procedure of calculations has as follows:

For the integration of the (incremental) elasto-plastic constitutive equations, an *explicit* method is used. The imposed strain or stress path is divided into *subincrements*, for each of which the incremental equations are supposed to hold. This of course introduces numerical errors since the response is not linear and the equations hold at an infinitesimal level. The accuracy of such methods is invariably linked with the *size of substep*. For the strain controlled test an automatic sub-incrementization scheme (as described by Sloan, 1987) is used. This scheme automatically adjusts the size of the substep so that the error (assessed locally through a *second degree Euler* approximation) is below a prescribed level (*STOL*). For the stress-controlled tests direct substepping of the imposed stress increments is implemented.

D.1 Strain-controlled tests

Strain-controlled tests are useful since it provides the basis for the numerical implementation of the model in a displacement-based finite element program.

Input:	**Symbol**	**variable name**
Material parameters		param1, param2
Stress state	σ	strs
Hardening parameters	κ	hard
Strain increment	$d\varepsilon$	de
Yield status*		nsurf
Accuracy controllers		acc
Output:		
Updated stress state		strs
New yield status		nsurf
Updated hardening parameters		hard

Stress state inside Yield Surface:

If the stress state corresponds to points inside the yield surface then elastic deformations occur. The final stress state is computed by adding the (elastic) stress increments to the initial state. If the final state lies within the yield surface, step is completed. In cases where the strain increment causes the final stress state to lie outside the yield surface (impossible condition by definition), the fraction of the increment that causes the stress state to reach the yield surface must be computed. A *modified regula-falsi* iterative procedure is implemented to obtain the fraction of increment. The remaining strain increment, induces plastic loading and the procedure of the next section is followed (after updating the –tangential– elastic parameters).

* For the first step the yield status is determined by comparing the stress state with the yield surface $f(\sigma) < 0$ or $f(\sigma) = 0$

Stress state on Yield Surface:

For stress state on the yield surface, the loading criterion is implemented to determine whether (plastic) loading or (elastic) unloading occurs. For unloading the procedure of the previous section is followed. For plastic loading an explicit modified Euler algorithm with substepping is implemented. This algorithm achieves an error control in the calculated plastic stresses by automatically subincrementing the imposed strain increment (using a local error measure). After each subincrement the new stress state is then corrected to the yield surface (if necessary). The hardening parameter α and the yield status are updated and the loading step is completed.

The algorithm is described in more detail in Abbo (1997).

Algorithm for an elasto-plastic loading step (Strain-controlled)

---

1. Enter with $\boldsymbol{\sigma}$, κ, $d\boldsymbol{\varepsilon}$. The elastic stress increment is computed $d\boldsymbol{\sigma}_e = \mathbf{D}_e(\boldsymbol{\sigma})\, d\boldsymbol{\varepsilon}$

2. IF $| f(\boldsymbol{\sigma},\kappa) | < TOL^*$, loading-unloading criterion dFS = $\boldsymbol{Q}\, d\boldsymbol{\sigma}_e$ is implemented.
IF dFS > 0 then plastic loading occurs; GOTO step 5 with $d\boldsymbol{\sigma}_e$ and dFS.
IF dFS $\leq$ 0 then elastic unloading (or neutral loading) occurs.

3. Calculate the new stress state $\boldsymbol{\sigma}_1 = \boldsymbol{\sigma}_0 + d\boldsymbol{\sigma}_e$.
IF $f(\boldsymbol{\sigma}_1,\kappa_1) < -TOL$ then the whole stress increment lies within the yield surface[†] and a fully elastic step has occurred. Exit with $\boldsymbol{\sigma}_1$ as the new stress state, $\kappa_1 = \kappa_0$ and nsurf = 0.
IF $| f(\boldsymbol{\sigma}_1,\kappa_1) | \leq TOL$, exit with $\boldsymbol{\sigma}_1$, $\kappa_1 = \kappa_0$ and nsurf = 1.

---

* The mathematical condition f = 0 is substituted by abs(f)<*TOL* in the computer. Typical values used for *TOL* are 10^{-7} to 10^{-9}

† due to convexity

IF $f(\sigma_1,\kappa_1) > TOL$ there is transition from elastic to elasto-plastic behavior. Compute the portion a of $d\sigma_e$ that causes purely elastic deformation using a modified regula-falsi intersection scheme (**RIntsect.m**). Update stresses $\sigma_0 \leftarrow \sigma_0 + a\, d\sigma_e$,, nsurf and stress increment that causes plastic deformations $d\sigma_e \leftarrow (1-a)\, d\sigma_e$.

4. Set $T = 0$ and $\Delta T = 1$. LOOP steps 5 to 11, WHILE $T < 1$

5. Compute plastic stress increments $d\sigma$ and increments in hardening parameters $d\kappa$ for $(\sigma_1, \kappa_1, \Delta T\, d\sigma_e)$ and $(\sigma_2, \kappa_{12}, \Delta T\, d\sigma_e)$, where

$\sigma_1 = \sigma_T$, $\kappa_1 = \kappa_T$

$\sigma_2 = \sigma_T + d\sigma_1$, $\kappa_2 = \kappa_T + d\kappa_1$

The general procedure for calculating plastic strains $d\sigma$ and increments in hardening parameters $d\kappa$ for $(\sigma, \kappa, d\sigma_e)$ is (**MPlinc.m**)

Elasto-plastic modulus $H = -\dfrac{\partial f}{\partial \kappa} \boldsymbol{K}\boldsymbol{P}$, where $\boldsymbol{K} = \dfrac{\partial \kappa}{\partial \varepsilon_{ij}^{P}}$

Plastic multiplier $d\lambda = \dfrac{\mathrm{dFS}}{H + \boldsymbol{Q} \cdot \mathbf{D}_e(\sigma) \cdot \boldsymbol{P}}$

Plastic stress increments $d\sigma = d\sigma_e - d\lambda\, \mathbf{D}_e(\sigma)\, \boldsymbol{P}$

Hardening parameters increment $d\kappa = d\lambda\, \boldsymbol{K}\boldsymbol{P}$

6. Let

$$\bar{\sigma}_{T+\Delta T} = \sigma_T + \frac{1}{2}(d\sigma_1 + d\sigma_2)$$

$$\bar{\kappa}_{T+\Delta T} = \kappa_T + \frac{1}{2}(d\kappa_1 + d\kappa_2)$$

be the estimates of the for the stress and hardening parameters increments calculated by the Euler scheme

7. The relative error for the current substep is*

$$R_{T+\Delta T} = \max\left\{\frac{\left\|d\boldsymbol{\sigma}_2 - d\boldsymbol{\sigma}_1\right\|}{2\left\|\boldsymbol{\sigma}_{T+\Delta T}\right\|}, \frac{\left|d\kappa_2 - d\kappa_1\right|}{2\,\kappa_{T+\Delta T}}, EPS\right\}$$

where $\|\ .\ \|$ indicates the Euclidean norm, $|\ .\ |$ the absolute magnitude of a real number and *EPS* is the smaller number the computer recognizes.

8. IF $R_{T+\Delta T} > STOL$ then the substep has failed. Extrapolating the local error a (new) smaller increment of stresses causing plastic strain is chosen:

$$q = \max\left\{0.9\sqrt{STOL / R_{T+\Delta T}}, 0.1\right\}$$

$$\Delta T \leftarrow \max\{q\ \Delta T, \Delta T_{\min})$$

where ΔT is a minimum step size. Return to step 5.

9. The step is accepted and the stress are updated as

$$\boldsymbol{\sigma}_{T+\Delta T} = \overline{\boldsymbol{\sigma}}_{T+\Delta T}$$

$$\kappa_{T+\Delta T} = \overline{\kappa}_{T+\Delta T}$$

10. The new stress state is checked for drift from the yield surface

$|\ f(\boldsymbol{\sigma}_{T+\Delta T},\ \kappa_{T+\Delta T})\ | > TOL$, then correction schemes to the yield surface are implemented (**MAdj.m**).

11. The size of the next step is determined through

$$q = \min\left\{0.9\sqrt{STOL / R_{T+\Delta T}}, 1.1\right\}$$

$$\Delta T \leftarrow q\ \Delta T$$

$$T \leftarrow T + \Delta T$$

The next step size is limited by

$$\Delta T \leftarrow \max\{\Delta T, \Delta T_{\min}\}$$

$$\Delta T \leftarrow \min\{\Delta T, 1 - T\}$$

* Note that another suitable choice for the norm could be made. Also κ_2-κ_1 is not treated as a vector but rather the absolute value of each element is taken.

12. At end of increment $T = 1$, exit with new stress state σ_1 and hardening parameters κ_1.

The algorithm as given here is addresses single yield function effective stress plasticity models. Therefore slight modifications have to be made in order to include multi-mechanism models. The formulation found in sections A.2 can be used to calculate the plastic multipliers. It is thus straight forward to enter the algorithm with *nsurf* now as an array conveying the information about the active and non-active mechanisms, and carry out the calculation leading to the new stress state and hardening parameters. More details on the numerical implementation of multiple yielding mechanisms can be found in reference (Lade & Nelson, 1984).

However the existence of more than one mechanisms makes matters more complicated, since it is not guaranteed that the number of active mechanisms will remain the same throughout the plastic loading increment. It is obvious that the methodology applied here would fail, since it assumes that the state of each mechanism (active/inactive) remains the same throughout the loading step. Although it is easy to capture such a case when/if it occurs, the remedy is not that straightforward to apply. In such cases an implicit return scheme should be used, e.g. Borja & Lee (1990).

D.2 Stress-controlled tests

Stress controlled tests are useful for single point programs. For the numerical integration of the incremental equations a straightforward explicit integration scheme is used and the total imposed stress increment is divided into very small equal size substeps (recommended accuracy $\max(d\boldsymbol{\sigma}) = 0.001 \parallel \boldsymbol{\sigma} \parallel$).

Input:	**Symbol**	**variable name**
Material parameters		param1, param2
Stress state	σ	strs
Hardening parameters	κ	hard
Stress increment	$d\sigma$	ds
Yield status		nsurf
Accuracy controllers		acc
Output:		
Updated stress state		strs
Total strain increment		de
New yield status		nsurf
Updated hardening parameters		hard

Algorithm for an elasto-plastic loading step (Stress-controlled)

1. Enter with σ, κ, $d\sigma$.

2. IF $| f(\sigma,\kappa) | < TOL$, loading-unloading criterion $dFS = \boldsymbol{Q}\, d\sigma$ is implemented.
IF $dFS > 0$ then plastic loading occurs; GOTO step 4 with $d\sigma$.
IF $dFS \leq 0$ then elastic unloading (or neutral loading) occurs.

3. Calculate the new stress state $\sigma_1 = \sigma_0 + d\sigma$.
IF $f(\sigma_1,\kappa_1) < -TOL$ then the whole stress increment lies within the yield surface and a fully elastic step has occurred. Exit with σ_1 as the new stress state, $\kappa_1 = \kappa_0$, total strain increment $d\varepsilon = \mathbf{D}_e^{-1}\, d\sigma$ and nsurf = 0.
IF $| f(\sigma_1,\kappa_1) | \leq TOL$, exit with σ_1, $\kappa_1 = \kappa_0$, $d\varepsilon = \mathbf{D}_e^{-1}\, d\sigma$ and nsurf = 1.
IF $f(\sigma_1,\kappa_1) > TOL$ there is transition from elastic to elasto-plastic behavior. Compute the portion a of $d\sigma$ that causes purely elastic deformation using a modified regula-falsi intersection scheme (**RIntsect.m**). Update stresses $\sigma_0 \leftarrow \sigma_0$

+ $a\ d\sigma$, nsurf and stress increment that causes plastic deformations $d\sigma \leftarrow (1-a)$ $d\sigma$. Store elastic strains $d\varepsilon = \mathbf{D}_e^{-1}\ d\sigma$.

4. Calculate in turn:

Elasto-plastic modulus $H = -\frac{\partial f}{\partial \kappa} \boldsymbol{K}\boldsymbol{P}$, where $\boldsymbol{K} = \frac{\partial \kappa}{\partial \varepsilon_{ij}^{p}}$

Plastic multiplier $d\lambda = \frac{\mathrm{dFS}}{H}$

Plastic stress increments $d\varepsilon = \mathbf{D}_e^{-1}\ d\sigma_e + d\lambda\ \boldsymbol{P}$

Hardening parameters increment $d\kappa = d\lambda\ \boldsymbol{K}\boldsymbol{P}$

For multiple yield surface plasticity see comments in the end of the previous section (D.1).

D.3 Summary of modified regula-falsi method for determination of intersection with the yield surface

This procedure is followed when there is transition from purely elastic to elasto-plastic behavior. This occurs when:

1. At the beginning of the load increment the stress state lies inside the yield surface ($f(\sigma_0,\kappa_0) < 0$, i.e. σ_0 in the elastic region)*,

AND

2. at the end of the loading $f(\sigma + d\sigma,\kappa_0) > 0$), which would give a final stress state outside the yield function (that is by definition not possible).

Note: $d\sigma$ is the proposed elastic stress increment.

---

* Also for stress states on the yield surface and elastic unloading

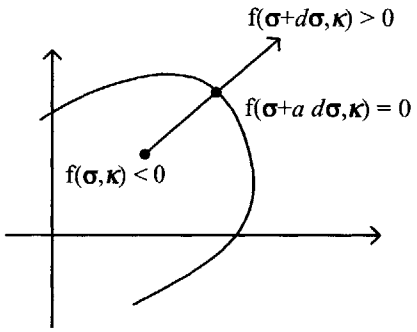

Figure D. 1: Transition from purely elastic to elastoplastic state

The fraction $a \in (0, 1)$ of the load increment that causes yield has to be specified. Due to the convexity of the yield function only one value of a exists so that $f(\boldsymbol{\sigma} + a\, d\boldsymbol{\sigma}) = 0$*. This can be specified analytically if the loading function has a simple form. However usually for the solution of the nonlinear equation a simple numerical procedure is implemented (bisection, Newton-Raphson, secant, regula-falsi etc.). In the present formulation the *modified regula-falsi method* will be used since it provides unconditional convergence and does not require the use of derivatives. Moreover it usually converges to acceptable accuracy results after 4-5 iterations.

Algorithm for location of the intersection point

---

1. Enter with initial stresses $\boldsymbol{\sigma}_0$ and hardening variables $\boldsymbol{\kappa}_0$, the stress increment $d\boldsymbol{\sigma}$ ($d\boldsymbol{\sigma}_e$ in the strain-driven tests), values a_0, a_1 bounding the intersection point and maximum number of iterations *NITS*.

---

* In the case of elastic unloading step there might occur $0 < f(\boldsymbol{\sigma}_0,\boldsymbol{\kappa}_0) < TOL$ and $f(\boldsymbol{\sigma}_0+d\boldsymbol{\sigma},\boldsymbol{\kappa}_0) > 0$, during which function f changes sign twice. This case is treated by determining values a_0 and a_1 so that $f(\boldsymbol{\sigma}_0+a_0 d\boldsymbol{\sigma},\boldsymbol{\kappa}_0) < -TOL$ **and** $f(\boldsymbol{\sigma}_0+a_1 d\boldsymbol{\sigma},\boldsymbol{\kappa}_0) > TOL$. See Abbo (1997) for details.

2. Set $F_s = f(\sigma_0, \kappa_0)$, $F_0 = f(\sigma_0 + a_0 d\sigma, \kappa_0)$ and $F_1 = f(\sigma_0 + a_1 d\sigma, \kappa_0)$

3. Execute steps 4 to 7 *NITS* times

4. Calculate $a = a_1 - (a_1 - a_0)\dfrac{F_1}{F_1 - F_0}$ and

$F_n = f(\sigma_0 + a\, d\sigma, \kappa_0)$

5. IF $F_n \leq TOL$ exit with a

6. IF $F_n \cdot F_0 < 0$ then

$a_1 = a, F_1 = F_n$

IF $F_n \cdot F_s > 0$ then $F_0 = \dfrac{F_0}{2}$

ELSE

$a_0 = a, F_0 = F_n$

IF $F_n \cdot F_s > 0$ then $F_1 = \dfrac{F_1}{2}$

7. Set $F_s = F_n$

8. Convergence not achieved, print error message and exit

D.4 Correction of the drift from the yield surface

At each increment the elastic modulus and the hardening parameters are assumed to remain constant (provided that the size of the step is small enough). This produces results that do not satisfy the governing equations exactly. As an example the new stress state and hardening parameters at the end of a plastic loading step may not satisfy the

consistency condition. Moreover it is known such error can accumulate causing a non-trivial drift from the yield function. When the stresses from a substep are detected to have deviated from the yield function, i.e. the value of the yield function is greater than a small threshold, a correction scheme must be implemented.

The correction scheme should produce a pair of corrected stresses and hardening parameters so that the value of the yield function is zero (or below some specified accuracy controller) and at the same time the total strain increment should remain the same*.

Let $\boldsymbol{\sigma}_0$, κ_0 be the uncorrected stresses and hardening parameters respectively. They are corrected according to the following formulas:

$$\boldsymbol{\sigma} = \boldsymbol{\sigma}_0 + d\boldsymbol{\sigma} = \boldsymbol{\sigma}_0 - d\lambda_c \, \mathbf{D}_e : \boldsymbol{P}_0 \qquad \text{(D- 1)}$$

$$\kappa = \kappa_0 + d\kappa = d\lambda_c \, \boldsymbol{K}_0 : \boldsymbol{P}_0 \qquad \text{(D- 2)}$$

(Note: plastic flow directions calculated at $\boldsymbol{\sigma}_0$, and $\boldsymbol{K}$ at $\boldsymbol{\sigma}_0$, κ_0)

The corrective plastic multiplier is calculated through Taylor series expansion of the yield function:

$$d\lambda_c = \frac{\mathrm{f}(\boldsymbol{\sigma}_0, \boldsymbol{\kappa}_0)}{H_0 + \boldsymbol{Q}_0 : \mathbf{D} : \boldsymbol{P}_0} \qquad \text{(D- 3)}$$

Although this correction scheme is both logically sound and provides accurate results, there are cases that the correction does not converge to the yield surface. In that case (usually indicated by new stress state that lies further form the yield surface than the

* Potts & Gens (1985) compare different algorithms for drift correction. Correction with consistent total strain increment apart from logically correct proved to be very accurate and is preferred to other techniques (e.g. constant mean stress or correction of plastic strains only at specified directions)

uncorrected one), an alternative (less precise but convergent) *normal* correction scheme can be used. In this approach *only* the stress is corrected through the relation:

$$\boldsymbol{\sigma} = \boldsymbol{\sigma}_0 + d\boldsymbol{\sigma} = \boldsymbol{\sigma}_0 - d\lambda_c \, \boldsymbol{Q}_0 \tag{D- 4}$$

$$d\lambda_c = \frac{\mathrm{f}(\boldsymbol{\sigma}_0, \boldsymbol{\kappa}_0)}{\boldsymbol{Q}_0 : \boldsymbol{Q}_0} \tag{D- 5}$$

The hardening parameters are not corrected and the total strain increment is not preserved.

Algorithm for correction of the drift from the yield surface

---

1. Enter with uncorrected stresses $\boldsymbol{\sigma}_0$ hardening variables $\boldsymbol{\kappa}_0$, and maximum number of iterations *NITS*

2. Execute steps 3 to 6 *NITS* times

3. Compute $d\lambda_c = \dfrac{\mathrm{f}(\boldsymbol{\sigma}_0, \boldsymbol{\kappa}_0)}{H_0 + \boldsymbol{Q}_0 \, \mathbf{D}_e \, \boldsymbol{P}_0}$

and correct

$\boldsymbol{\sigma} = \boldsymbol{\sigma}_0 - d\lambda_c \, \mathbf{D}_e \, \boldsymbol{P}_0$

$\boldsymbol{\kappa} = \boldsymbol{\kappa}_0 + d\lambda_c \, \boldsymbol{K}_0 \, \boldsymbol{P}_0$

4. IF $| \mathrm{f}(\boldsymbol{\sigma}, \boldsymbol{\kappa}) | >$ TOL then an alternative correction scheme is used.

$$d\lambda_c = \frac{\mathrm{f}(\boldsymbol{\sigma}_0, \boldsymbol{\kappa}_0)}{\boldsymbol{Q}_0 \, \boldsymbol{Q}_0}$$

$\boldsymbol{\sigma} = \boldsymbol{\sigma}_0 - d\lambda_c \, \boldsymbol{Q}_0$

$\boldsymbol{\kappa} = \boldsymbol{\kappa}_0$

5. IF $| f(\sigma,\kappa) | \leq$ TOL exit with corrected stress state σ and hardening parameters κ now lying on the yield surface.

6. Set $\sigma_0 = \sigma$ and $\kappa_0 = \kappa$

7. IF convergence is not achieved after *NITS* loops print error message and exit.

List of References

[Abbo 1997]
Abbo, A.J.(1997): *Finite Element Algorithms for Elastoplasticity and Consolidation*, Ph.D. Thesis, The University of Newcastle

[Adachi & Oka 1993]
Adachi, T.; Oka, F.(1993): An elasto-viscoplastic constitutive model for soft rock with strain softening, *Geotechnical Engineering of Hard Soils-Soft Rocks*, (eds. Anagnostopoulos, Schlosser, Kalteziotis, Frank), vol.1, pp.327-333

[Aitchison 1961]
Aitchison, G.D.(1961): Relation of moisture and effective stress functions in unsaturated soils, *Pore Pressure and Suction in Soils*, conf. British Nat. Soc. of Int. Soc. Soil Mech. Found. Eng. at Inst. Civil Eng., Butterworths, pp.47-52

[Aitchison *et al.* 1965]
Aitchison, G.D.; Russam, K.; Richards, B.G.(1965): *Moisture Equilibria and Moisture Changes in Soils Beneath Covered Areas*, A Symp.-in-print (ed. Aitchison), Butterworths, pp.1-21

[Aitchison & Woodburn 1969]
Aitchison, G.D.; Woodburn, J.A.(1969): Soil suction in foundation design, *Proc. 7th ICSMFE*, Mexico, vol.2, pp.1-8

[Alonso *et al.* 1987]
Alonso, E.E.; Gens, A.; Hight, D.W.(1987): Special problem soils, *Proc. 9th ECSMFE*, Dublin, vol.3, pp.1087-1146

[Alonso *et al.* 1990]
Alonso, E.E.; Gens, A.; Josa, A.(1990): A constitutive model for partially saturated soils, *Geotechnique*, vol.**40** (3), pp.405-430

[Alonso *et al.* 1994]
Alonso, E.E.; Gens, A.; Yuk Gehling, W.Y.(1994): Elastoplastic model for unsaturated expansive soils, *Proc. 3rd European Conf. On Numerical Methods in Geotechnical Engineering*, Manchester, pp.11-18

[Alonso *et al.* 1999]
Alonso, E.E.; Vaunat, J.; Gens, A.(1999): Modeling the mechanical behavior of expansive clays, *Engineering Geology*, vol.**54**, pp.173-183

[Anagnostopoulos *et al.* 1991]
Anagnostopoulos, A.G.; Kalteziotis, N.; Tsiambaos, G.K.; Kavvadas, M.(1991): Geotechnical properties of the Corinth Canal marls, *Geot. And Geol. Eng.*, vol.**9**, pp.1-26

[Aversa *et al.* 1993]
Aversa, S.; Evangelista, A.; Leroueil, S.; Picarelli, L.(1993): Some aspects of the mechanical behaviour of 'structured' soils and soft rocks, *Geotechnical Engineering of Hard Soils-Soft Rocks*, (eds. Anagnostopoulos, Schlosser, Kalteziotis, Frank), vol.1, pp.359-366

[Banks *et al.* 1975]
Banks, D.C.; Strohm, W.E.; De Angulo, M.; Lutton, R.J.(1975): Study of the clay-shale slopes along the Panama Canal, *Report No.3, Engineering analyses of slides and strength properties of clay shales along the Gaillard Cut*, Technical report S-70-9, US Army Engineers Waterways Experiment Station, Vicksburg, Miss.

[Barden *et al.* 1969]
Barden, L.; Madedor, A.O.; Sides, G.R.(1969): Volume change characteristics of unsaturated clays, *J. Soil Mech. Fnd Engng*, ASCE, vol.**95**, pp.33-51

[Bazant 1971]
Bazant, Z.P.(1971): Endochronic and classical theories of plasticity in finite element analysis, *Int. Conf. on Finite Elements in Nonlinear Solid and Structural Mechanics*, Geilo, vol.1, pp.1-15

[Biot 1941]
Biot, M.A.(1941): General theory of three dimensional consolidation, *Journal of Applied Physics*, vol.**12**, pp.155-164

[Bishop 1960]
Bishop, A.W.(1960): The principle of effective stress, *Norwegian Geotechnical Institute Publication No.32*, pp.1-5

[Blight 1983]
Blight, G.E.(1983): Aspects of the capillary model for unsaturated soils, *Proc. 7th Asian Conf. SMFE*, Haifa, vol.1, pp.3-7

[Borja & Lee 1990]
Borja, R.I.; Lee, S.R.(1990): Cam-Clay plasticity, part I: Implicit integration of elasto-plastic constitutive relations, *Comput. Methods Appl. Mech. Engrg.*, vol.**78**, pp.49-72

[Borja & Tamagnini 1998]
Borja, R.I.; Tamagnini, C.(1998): Cam-Clay plasticity, part III: Extension of the infinitesimal model to include finite strains, *Comput. Methods Appl. Mech. Engng.*, vol.**155**, pp.73-95

[Brinkgreve 1994]
Brinkgreve, R.B.J.(1994): *Geomaterial Models and Numerical Analysis of Softening*, Ph.D. Thesis, Technische Universiteit Delft,

[Burland 1990]
Burland, J.B.(1990): On the compressibility and shear strength of natural clays, *Geotechnique*, vol.**40** (3), pp.329-378

[Burland *et al.* 1996]
Burland, J.B.; Rampello, S.; Georgiannou, V.N.; Calabresi, G.(1996): A laboratory study of the strength of four stiff clays, *Geotechnique*, vol.**46** (3), pp.491-514

[Cecconi *et al.* 1998]
Cecconi, M.;Viggiani, G.; Rampello, S.(1998): An experimental investigation of the mechanical behaviour of a pyroclastic soft rock, *Geotechnics of Hard Soils-Soft Rocks*, (eds. Evangelista & Picarelli), vol.1, pp.473-480

[Chazallon & Hicher 1995]
Chazallon, C.; Hicher, P.Y.(1995): An elastoplastic model with damage for bonded geomaterials, *Numerical Models in Geomechanics - NUMOG V*, Davos (eds. Pande & Pietruszczak), pp.21-26

[Cheng & Dusseault 1997]:
Cheng, H.; Dusseault, M.B.(1997): A constitutive theory for progressively deteriorating geomaterials, *Computer Methods and Advances in Geomechanics*, Wuhan (ed. Yuan), vol.2, pp.863-868

[Cotecchia & Chandler 1997]
Cotecchia, F.; Chandler, R.J.(1997): The influence of structure on the pre-failure behaviour of a natural clay, *Geotechnique*, vol.**47**, pp.523-544

[Cotecchia & Chandler 2000]

Cotecchia, F.; Chandler, R.J.(2000): A general framework for the mechanical behaviour of clays, *Geotechnique*, vol.**50** (4), pp.431-447

[Coussy 1995]
Coussy, O.(1995): *Mechanics of Porous Continua*, John Wiley and Sons

[Croney & Coleman 1954]
Croney, D.; Coleman, J.D.(1954): Soil structure in relation to soil suction (pF), *J. Soil Sci.*, vol.5 (1), pp.75-84

[Croney *et al.* 1958]
Croney, D.; Coleman, J.D.; Black, W.P.M.(1958): Movement and distribution of water in soil in relation to highway design and performance, *Water and its Conduction in Soils*, Highway Res. Board, Special Report, Washington, DC, no.40, pp.226-252

[Dafalias & Herrman 1982]
Dafalias, Y.F.; Herrmann, L.R.(1982): Bounding surface formulation of soil plasticity, *Soil Mechanics-Transient and Cyclic Loads* (eds. Pande & Zienkiewicz, John Wiley and Sons, pp.253-282

[Dangla *et al.* 1997]
Dangla, P.; Malinsky, L.; Coussy, O.(1997): Plasticity and imbibition-drainage curves for unsaturated soils: a unified approach, *Numerical Models in Geomechanics - NUMOG VI*, Montreal (eds. Pietruszczak & Pande), pp.141-146

[Deere 1955]
Derre, D.U.(1955): *Engineering properties of the Pleistocene and recent sediments of the San Juan Bay area, Puerto Rico*, Ph.D. Thesis, University of Illinois, Urbana

[Delage *et al.* 1987]
Delage, P.; Suraj de Silva, G.P.R.; De Laure, E.(1987): *Proc. 9th ECSMFE*, Dublin, vol.1, pp.25-28

[Desai 1995]
Desai, C.S.(1995): Constitutive modelling using the disturbed state as microstructure self-adjustment concept, *Continuum Models for Materials with Microstructure*, (ed. Muhlhaus), pp.239-296

[Dormieux *et al.* 1995]
Dormieux, L.; Barboux, P.; Coussy, O.(1995): A macroscopic model of the swelling phenomenon of a saturated clay, *Eur. J. Mech., A/Solids*, vol.**14** (6), pp.981-1004

[Dudley 1970]
Dudley, J.H.(1970): Review of collapsing soils, *J.Soil Mech. Fdn Engng*, ASCE, vol.**96**, pp.925-947

[Elliot & Brown 1985]
Elliot, G.M.; Brown, E.T.(1985): Yield of a soft, high-porosity rock, *Geotechnique*, vol.**35**(4), pp.413-423

[Escario & Saez 1986]
Escario, V.; Saez, J.(1986): The shear strength of partially saturated soils, *Geotechnique*, vol.**36** (3), pp.453-456

[Finke *et al.* 1999]
Finke, K.A.; Mayne, P.W.; Klopp, R.A.(1999): Characteristic piezocone response in Piedmont residual soils, *ASCE GSP No.92, Behavioral Characteristics of Residual Soils*, pp.1-11

[Fredlund & Morgensten 1977]
Fredlund, D.G.; Morgensten, N.R.(1977): Stress state variables for unsaturated soils, *J. Geot. Eng. Div.*, ASCE, vol.**103**, pp.447-466

[Fredlund *et al.* 1978]
Fredlund, D.G.; Morgensten, N.R.; Widger, R.S.(1978): The shear strength of unsaturated soils, *Can. Geotech. Jnl.*, vol.**15** (3), pp.313-321

[Fredlund & Rahardjo 1993]
Fredlund, D.G. & Rahardjo, H.(1993): *Soil Mechanics for Unsaturated Soils*, Wiley-Interscience

[Geiser *et al.* 1997a]
Geiser, F.; Laloui, L.; Vulliet, L.; Desai, C.S.(1997): Disturbed state concept for partially saturated soils, *Numerical Models in Geomechanics - NUMOG VI*, Montreal (eds. Pietruszczak & Pande), pp.129-134

[Geiser *et al.* 1997b]
Geiser, F.; Laloui, L.; Vulliet, L.(1997): Constitutive modelling of unsaturated sandy silt, *Computer Methods and Advances in Geomechanics*, Wuhan (ed. Yuan), vol.**2**, pp.899-904

[Geiser *et al.* 1999]
Geiser, F.; Laloui, L.; Vulliet, L.(1999): Unsaturated soil modelling with special emphasis on undrained conditions, *Numerical Models in Geomechanics - NUMOG VII*, Graz (eds. Pande, Pietruszczak & Schweiger), pp.9-14

[Gens 1995]
Gens, A.(1995): Constitutive Laws, *Modern Issues in Non-Saturated Soils*, (eds. Gens, Jouanna, Schrefler), Springer-Verlag, pp.129-158 (*comment:* contains no less than 10 typing errors in formulation)

[Gens & Alonso 1992]
Gens, A.; Alonso, E.E.(1992): A framework for the behavior of unsaturated expansive clays, *Can. Geotech. J.*, vol.**29**, pp.1013-1032

[Gens *et al.* 1989]
Gens, A.; Alonso, E.E.; Josa, A.(1989): Elastoplastic modelling of partially saturated soils, *Numerical Models in Geomechanics - NUMOG III*, Niagara Falls (eds. Pietruszczak & Pande), pp.163-170

[Gens & Nova 1993]
Gens, A.; Nova, R.(1993): Conceptual bases for a constitutive model for bonded soils and weak rocks, *Geotechnical Engineering of Hard Soils-Soft Rocks*, (eds. Anagnostopoulos, Schlosser, Kalteziotis, Frank), vol.1, pp.485-494

[Gens & Potts 1982]
Gens, A.; Potts, D.M.(1982): A theoretical model for describing the behaviour of soils not obeying Rendulic's principle, *Proc. 1st Int. Symp. Numer. Mod. Geomech.*, Zurich, pp.24-32

[Gens & Potts 1988]
Gens, A.; Potts, D.M.(1988): Critical state models in computational geomechanics, *Eng. Comput.*, vol.**5** (3), pp.178-197

[Groen *et al.* 1995]
Groen, A.E.; de Borst, R.; van Eekelen, S.J.M.(1995): An elastoplastic model for clay: Formulation and algorithmic aspects, *Numerical Models in Geomechanics - NUMOG V*, Davos (eds. Pande & Pietruszczak), pp.27-32

[Hashiguchi 1977]
Hashiguchi, K.(1977): An expression of anisotropy in a plastic constitutive equation of soils, *Proc. 9th ICSMFE*, Tokyo, pp.302-305

[Hill 1950]

Hill, R.(1950): *The Mathematical Theory of Plasticity*, Oxford University Press

[Jardine *et al.* 1999]

Jardine, R.J.; Kuwano, J.; Zdravkovic, L.; Thornton, C.(1999): Some fundamental aspects of the pre-failure behavior of granular soils, *Pre-failure Deformation Characteristics of Geomaterials* (eds. Jamiolkowski, Lancellota, Lo Presti), vol.2, pp.208-236

[Jennings 1961]

Jennings, J.E.(1961): A revised effective stress law for use in the prediction of the behavior of unsaturated soils, *Pore Pressure and Suction in Soils*, conf. British Nat. Soc. of Int. Soc. Soil Mech. Found. Eng. at Inst. Civil Eng., Butterworths, pp.26-30

[Jimenez Salas *et al.* 1973]

Jimenez Salas, J.A.; Justo, J.L.; Romana, M.; Faraco, C.(1973): The collapse of gypseous silts and clays of low plasticity in arid and semiarid climates, *Proc. 8th ICSMFE*, Moscow, vol.2, pp.193-199

[Josa *et al.* 1987]

Josa, A.; Alonso, E.E.; Lloret, A.; Gens, A.(1987): Stress-strain behaviour of partially saturated soils, *Proc. 9th ECSMFE*, Dublin, vol.2, pp.561-564

[Justo *et al.* 1984]

Justo, J.L.; Delgado, A.; Ruiz, J.(1984): The influence of stress path in the collapse-swelling of soils at the laboratory, *Proc. 5th Int. Conf. Exp. Soils*, Adelaide, pp.67-71

[Kavvadas 1980]

Kavvadas, M.(1980): *Stress-Strain Models for Soils Based on Plasticity Theory*, MS Diploma Thesis, Massachusetts Institute of Technology

[Kavvadas 1982]

Kavvadas, M.(1982): *Non-linear consolidation around driven piles in clays*, ScD Thesis, Massachusetts Institute of Technology

[Kavvadas 1998]

Kavvadas, M.J.(1998): General report: Modeling the soil behaviour – Selection of soil parameters, *Geotechnics of Hard Soils-Soft Rocks*, (eds. Evangelista & Picarelli), vol.3, pp.1441-1481

[Kavvadas & Amorosi 2000]

Kavvadas, M.; Amorosi, A.(2000): A constitutive model for structured soils, *Geotechnique*, vol.**50** (3), pp.263-273

[Kavvadas & Anagnostopoulos 1998]

Kavvadas, M.J.; Anagnostopoulos, A.G.(1998): A framework for the mechanical behaviour of structured soils, *Geotechnics of Hard Soils-Soft Rocks*, (eds. Evangelista & Picarelli), vol.2, pp.591-601

[Kavvadas *et al.* 1993a]

Kavvadas, M.; Anagnostopoulos, A.; Kalteziotis, N.(1993): A framework for the mechanical behaviour of the cemented Corinth marl, *Geotechnical Engineering of Hard Soils-Soft Rocks*, (eds. Anagnostopoulos, Schlosser, Kalteziotis, Frank), vol.1, pp.577-583

[Kavvadas *et al.* 1993b]

Kavvadas, M.; Anagnostopoulos, A.; Leonardos, M.; Karras, B.(1993): Mechanical properties of the Ptolemais lignite, *Geotechnical Engineering of Hard Soils-Soft Rocks*, (eds. Anagnostopoulos, Schlosser, Kalteziotis, Frank), vol.1, pp.585-592

[Kaye 1959]

Kaye, C.A.(1959): Coastal geology of Puerto Rico, U.S. geological survey professional paper 317, United States government printing office, Washington

[Kelly *et al.* 1974]
Kelly, W.E.; Nacci, V.A.; Wang, M.C.; Demars, K.R.(1974): Carbonate cementation in deep-ocean sediments, *J. Geotech. Eng.*, ASCE, vol.**100**, pp.1449-1464

[Kohgo *et al.* 1991]
Kohgo, Y.; Nakano, M.; Miyazaki, T.(1991): Elastoplastic constitutive modelling for unsaturated soils, *Computer Methods and Advances in Geomechanics*, Cairns (eds. Beer, Booker & Carter), vol.**1**, pp.631-636

[Lade 1977]
Lade, P.V.: Elasto-Plastic stress-strain theory for cohesionless soil with curved yield surfaces, *Int. J. Solids Structures*, vol.**13**, pp.1019-1035

[Lade & Duncan 1975]
Lade, P.V.; Duncan, J.M.(1975): Elastoplastic stress-strain theory for cohesionless soil, *J. Geotech. Geoenviron. Eng.*, ASCE, vol.**101**, pp.1037-1053

[Lade & Nelson 1984]
Lade, P.V.; Nelson, R.B.(1984): Incrementalization procedure for elasto-plastic constitutive model with multiple, intersecting yield surfaces, *Int. J. Numer. Anal. Meth. Geomech.*, vol.**8**, pp.311-323

[Lagioia & Nova 1993]
Lagioia, R.; Nova, R.(1993): A constitutive model for soft rocks, *Geotechnical Engineering of Hard Soils-Soft Rocks*, (eds. Anagnostopoulos, Schlosser, Kalteziotis, Frank), vol.1, pp.625-632

[Lagioia & Nova 1995]
Lagioia, R.; Nova, R.(1995): An experimental and theoretical study of the behaviour of a calcarenite in triaxial compression, *Geotechnique*, vol.**45** (4), pp.633-648

[Leroueil & Vaughan 1990]
Leroueil, S.; Vaughan, P.R.(1990): The general and congruent effects of structure in natural soils and weak rocks, *Geotechnique*, vol.**40** (3), pp.467-488

[Li & Charlier 1995]
Li, X.L.; Charlier, R.(1995): A unified formulation of constitutive relations for saturated and partially saturated soils, *Numerical Models in Geomechanics - NUMOG V*, Davos (eds. Pande & Pietruszczak), pp.113-118

[Liu & Carter 1999]
Liu, M.D.; Carter, J.P.(1999): Virgin compression of structured soils, *Geotechnique*, vol.**49** (1), pp.43-57

[Liu *et al.* 1998]
Liu, M.D.; Carter, J.P.; Desai, C.S.; Xu, K.J.(1998): *Analysis of the compression of structured soils using the Disturbed State Concept*, Research Report No. R770, The University of Sydney

[Lloret & Alonso 1985]
Lloret, A.; Alonso, E.E.(1985): State surfaces for partially saturated soils, *Proc. 11th ICSMFE*, San Francisco, vol.2, pp.557-562

[Lo Presti 1994]
Lo Presti, D.C.F.(1994): General report: Measurement of shear deformation of geomaterials in the laboratory, *Pre-failure Deformation of Geomaterials* (eds Shibuya, Mitachi, Miura), vol.2, pp.1067-1088

[Loret 1989a]

Loret, B.(1989): An introduction to the classical theory of Elastoplasticity, *Geomaterials: Constitutive Equations and Modelling* (ed. Darve), Elsevier Applied Science, pp.149-186

[Loret 1989b]
Loret, B.(1989): Geomechanical applications of the theory of multimechanisms, *Geomaterials: Constitutive Equations and Modelling* (ed. Darve), Elsevier Applied Science, pp.187-211

[Maswoswe 1985]
Maswoswe, J.(1985): *Stress paths for a compacted soil during collapse due to wetting*, PhD Thesis, Imperial College, London

[Matsuoka & Nakai 1974]
Matsuoka, H.; Nakai, T.(1974): Stress-deformation and strength characteristics under three different principal stresses, *Proc. JSCE*, vol.**232**, pp.59-70

[Matyas & Radhakrishna 1968]
Matyas, E.L.; Radhakrishna, H.S.(1968): Volume change characteristics of partially saturated soils, *Geotechnique*, vol.**18** (4), pp.432-448

[McGown & Collins 1975]
McGown, A.; Collins, K.(1975): The microfabrics of some expansive and collapsing soils, *Proc. 5th Pan. Am. Conf. SMFE*, Buenos Aires, vol.1, pp.323-332

[Mitchell 1993]
Mitchell, J.K.(1993): *Fundamentals of Soil Behavior*, 2nd Edition, John Wiley & Sons, 437p.

[Mitchell & Solymar 1984]
Mitchell, J.K. & Solymar, Z.V.(1984): Time-dependent strength gain in freshly deposited or densified sand, *J. Geotech. Eng.*, ASCE, vol.**110**, pp.1559-1576

[Morgensten 1979]
Morgensten, N.R.(1979): Properties of compacted soils, contribution to Panel Discussion, Session IV, *Proc. 6th Pan-American Conf. Soils Mech. Found. Eng.*, Lima, vol.3, pp.349-354

[Morgensten & Balasubramanian 1980]
Morgensten, N.R.; Balasubramanian, B.(1980): Effect of pore fluid on the swelling of clay-shale, *Proc. 4th Int. Conf. on Exp. Soils*, Denver, vol.1, pp.190-205

[Muir Wood 1990]
Muir Wood, D.(1990): *Soil Behaviour and Critical State Soil Mechanics*, Cambridge University Press

[Muir Wood 1995]
Muir Wood, D.(1995): Kinematic hardening model for structured soil, *Numerical Models in Geomechanics - NUMOG V*, Davos (eds. Pande & Pietruszczak), pp.83-88

[Nelson & Miller 1992]
Nelson, J.D.; Miller, D.J.(1992): *Expansive Soils, Problems and Practice in Foundation and Pavement Engineering*, John Wiley & Sons

[Ohmaki 1982]
Ohmaki, S.(1982): Stress-strain behaviour of anisotropically, normally consolidated cohesive soil, *Proc. 1st Int. Symp. Num. Mod. Geomech.*, Zurich, pp.250-269

[Pandian *et al.*1993]
Pandian, N.S.; Nagaraj, T.S.; Sivakumar Babu, G.L.(1993): Tropical clays I: Index properties and microstructural aspects, *J. Geotech. Eng.*, ASCE, **119** (5), pp.826-839

[Pestana 1994]

Pestana-Nascimento, J.M.(1994): *A Unified Constitutive Model For Clays And Sands*, DS Diploma Thesis, Massachusetts Institute of Technology

[Pothier *et al.* 1997]
Pothier, C.; Robinet, J.C.; Jullien, A.(1997): A constitutive model for expansive and non expansive clays, *Numerical Models in Geomechanics - NUMOG VI*, Montreal (eds. Pietruszczak & Pande), pp.99-104

[Potts & Ganendra 1994]
Potts, D.M.; Ganendra, D.(1994): An evaluation of substepping and implicit stress point algorithms, *Comput. Methods Appl. Mech. Engrg.*, vol.**119**, pp.341-354

[Potts & Gens 1985]
Potts, D.M.; Gens, A.(1985): A crirtical assessment of methods of correcting the drift from the yield surface in elasto-plastic finite element analysis, *Int. J. Numer. Anal. Meth. Geomech.*, vol.**9**, pp.149-159

[Potts & Zdravkovic 1999]
Potts, D.; Zdravkovic, L.(1999): Some pitfalls when using Modified Cam Clay, *Proceedings from the European Cooperation in the field of Scientific and Technical research, Workshop on Soil-Structure interaction*, Thessaloniki

[Prager & Hodge 1951]
Prager, W.; Hodge, P.G.(1951): *Theory of Perfectly Plastic Solids*, Wiley

[Prevost 1978]
Prevost, J.H.(1978): Plasticity theory for soil stress-strain behavior, *J. Eng. Mech., ASCE*, vol.**104**, pp.1177-1194

[Richards *et al.* 1984]
Richards, B.G.; Peter, P.; Martin, R.(1984): The determination of volume change properties in expansive soils, *Proc. 5th Int. Conf. on Exp. Soils*, Adelaide, pp.179-186

[Roscoe & Burland 1968]
Roscoe, K.H.; Burland, J.B.(1968): On the generalised stress-strain behaviour of 'wet' clay, *Engineering Plasticity*, (eds. Heyman & Leckie), Cambridge University Press, pp.535-609

[Rouainia & Muir Wood 1998]
Rouainia, M.; Muir Wood, D.(1998): A kinematic hardening model for structured soil, *Geotechnics of Hard Soils-Soft Rocks*, (eds. Evangelista & Picarelli), vol.2, pp.817-824

[Rouainia & Muir Wood 2000]
Rouainia, M.; Muir Wood, D.(2000): A kinematic hardening constitutive model for natural clays with loss of structure, *Geotechnique*, vol.**50** (2), pp.153-164

[Rudnicki 2000]
Rudnicki, J.W.(2000): Geomechanics, *Int. J. Solids and Structures*, vol.**37**, pp.349-358

[Schofield & Wroth 1968]
Schofiled, A.N.; Wroth, C.P.(1968): *Critical State Soil Mechanics*, McGraw-Hill

[Sheng & Sloan 1999]
Sheng, D.; Sloan, S.W.(1999): *Load stepping schemes for critical state models*, Research Report No. 173.02.1999, The University of Newcastle

[Sheng *et al.* 1999]
Sheng, D.; Sloan, S.W.; Yu, H.S.(1999): *Aspects of finite element implementation of critical state models*, Research Report No. 176.02.1999, The University of Newcastle

[Sjoblom 2000]
Sjoblom, K.J.(2000): *The Mechanisms Involved During the Desaturation Process of a Porous Matrix*, Ph.D. Thesis, Massachusetts Institute of Technology

[Sloan 1987]
Sloan, S.W.(1987): Substepping schemes for the numerical integration of elastoplastic stress-strain relations, *International Journal for Numerical Methods in Engineering*, vol.**24**, pp.893-911

[Srinivasa Murthy *et al.* 1997]
Srinivasa Murthy, B.R.; Vatsala, A.; Sitharam, T.G.; Nagendra Prasad, K.(1997): Prediction of extension test results of soft cemented clays with a simple constitutive model, *Computer Methods and Advances in Geomechanics*, Wuhan (ed. Yuan), vol.2, pp.947-952

[Sulem & Vardoulakis 1990]
Sulem, J.; Vardoulakis, I.(1990): Bifurcation analysis of the triaxial test on rock specimens – A theoretical model for shape and size effects, *Acta Mechanica*, vol.**83**(3-4), pp.195-212

[Tavenas & Leroueil 1985]
Tavenas, F.; Leroueil, S.(1985): Discussion, *Proc. 11th ICSMFE*, San Francisco, vol.**5**, pp.2693-2694

[Tavenas & Leroueil 1990]
Tavenas, F.; Leroueil, S.(1990): Laboratory and in-situ stress-strain-time behaviour of soft clays, *Int. Symp. Geotech. Engng Soft Soils*, Mexico City, vol.2,

[Toll 1990]
Toll, D.G.(1990): A framework for unsaturated soil behaviour, *Geotechnique*, vol.**40** (1), pp.31-44

[Townsend 1985]
Townsend, F.C.(1985): Geotechnical characteristics of residual soils, *J. Geotech. Eng.*, ASCE, **111** (1), pp.77-94

[TRS 1997]
TRS (1997): *Tropical Residual Soils*, A Geological Society Engineering Group Working Party Report (ed. Fookes), P.G., London Geological Society

[Ulm 2000]
Ulm, F.J.(2000): Class notes (Mechanics of Material Systems)

[Vargas 1953]
Vargas, M.(1953): Some engineering properties of residual clay soils occurring in southern Brazil, *Proc 3rd ICSMFE*, Zurich, vol.1, pp259-268

[Vaughan 1988]
Vaughan, P.R.(1988): Characterizing the mechanical properties of in-situ residual soil, *Proc. Second Int. Conf. Geomech. Tropical Soils*, Singapore, vol.2, pp.469-487

[Vaughan *et al.* 1988]
Vaughan, P.R.; Maccarini, M.; Mokhtar, S.M.(1988): Indexing the engineering properties of residual soil, *Q. J. Eng. Geol.*, **21**, pp.69-84

[WCC 1998]
WCC (1998): Supplement site investigation reports for Tren Urbano section7, submitted by Woodward-Clyde Consultants to GMAEC

[Wesley 1999]
Wesley, L.D.(1999): Some lessons learned from the geotechnical engineering in volcanic soils, *Proc. Intl. Symp. On Problematic Soils (IS-TOHOKU'98)*, Balkema, vol.2, pp.851-863

[Wheeler 1996]

Wheeler, S.J.(1996): Inclusion of specific water volume within an elastoplastic model for unsaturated soil, *Can. Geotech. J.*, vol.**33**, pp.42-57

[Wheeler & Sivakumar 1995]
Wheeler, S.J.; Sivakumar, V.(1995): An elasto-plastic critical state framework for unsaturated soil, *Geotechnique*, vol.**45** (1), pp.35-53

[Whittle 1987]
Whittle, A.J.(1987): *A constitutive model for overconsolidated clays with application to the cyclic loading of friction piles*, DS Diploma Thesis, Massachusetts Institute of Technology

[Whittle 2000]
Whittle, A.J.(2000): Class notes (Theoretical Soil Mechanics)

[Yong *et al.* 1971]
Yong, R.N.; Japp, R.D.; How, G.(1971): Shear strength of partially saturated soils, *Proc. 4th Asian Reg. SMFE*, Bangkok, vol.2 (12), pp.183-187

[Yong & Warkentin 1966]
Yong, R.N.; Warkentin, B.P.(1966): *Introduction to soil behavior*, MacMillan

[Zhang 2001]
Zhang, G.(2001): *Characterization of an alluvial residual soil in San Juan, Puerto Rico*, Ph.D. Thesis, Massachusetts Institute of Technology

[Zhang 2001]
Zhang, G.(2001): Personal communication.